Medical University of South Carolina

MEDICA

MUSC Theses and Dissertations

2015

Modulation of GILT and PAX3 by Ganoderic Acid DM Enhances Radiation and Chemoimmunotherapy of Melanoma

Jessica D. Hathaway-Schrader
Medical University of South Carolina

Follow this and additional works at: https://medica-musc.researchcommons.org/theses

Recommended Citation

Hathaway-Schrader, Jessica D., "Modulation of GILT and PAX3 by Ganoderic Acid DM Enhances Radiation and Chemoimmunotherapy of Melanoma" (2015). *MUSC Theses and Dissertations*. 456.
https://medica-musc.researchcommons.org/theses/456

This Dissertation is brought to you for free and open access by MEDICA. It has been accepted for inclusion in MUSC Theses and Dissertations by an authorized administrator of MEDICA. For more information, please contact medica@musc.edu.

Modulation of GILT and PAX3 by Ganoderic acid DM Enhances Radiation and Chemoimmunotherapy of Melanoma

By

Jessica D. Hathaway-Schrader

A dissertation submitted to the faculty of the Medical University of South Carolina in partial fulfillment of the requirements for the degree of Doctor of Philosophy in the College of Graduate Studies.

Department of Microbiology and Immunology, 2015

Approved by: _____

A. Haque, Chair of Advisory Committee

_____

L. Kasman

_____

N. Sutkowski

_____

S. Tomlinson

_____

C. Paulos

_____

C. Vasu

_____

S. Reddy

Abstract

An abstract of a dissertation

Abstract

Melanoma is an aggressive skin cancer that plagues Western populations. Current treatments such as surgery, chemotherapy, and high-dose radiation have had some success, but often fail in treating late stage metastatic melanoma. Immunotherapies have been successful in treating a small percentage of late stage patients, but these treatments do not provide a long-lasting response to effectively clear the tumor. Therefore, current studies have been investigating whether combining common treatments with immunotherapies would provide the necessary boost to further improve tumor killing. An optimum presentation of HLA class II proteins is essential for the activation of CD4+ T cells, which provide a sustained killing of malignant tumors by activating cytotoxic CD8+ T cells. Our laboratory has recently shown that the induction of Gamma-Interferon-inducible Lysosomal Thiol reductase (GILT) in melanoma favors HLA class II antigen processing and CD4+ T cells recognition of tumors. The present study examined the role of GILT in generating a greater pool of reduced and functional epitopes for HLA class II-mediated presentation and recognition of CD4+ T cells. This study also investigated the mechanisms by which GILT expression negatively regulates a tumorigenic molecule, paired box 3 (PAX3), in melanoma cells; and how regulation of PAX3 leads to melanoma cell sensitization to radiation and chemoimmunotherapy. Additionally, this study tested a chemotherapeutic agent (GA-DM), which induced apoptosis in a p53-dependent pathway and altered GILT, PAX3, and HLA class II molecules in melanoma cells *in vitro*. Interestingly, the combination of radiation and GA-DM treatment *in vivo* in the B16 melanoma mouse model displayed increased survival

and decreased tumor volume among treatment groups. Based upon the results of this study, the combination treatment of radiation and GA-DM could be utilized to eliminate melanoma cells while boosting immune responses in the host. Understanding the molecular mechanisms of GILT-mediated downregulation of PAX3 as well as the radiation and GA-DM treatment death pathway could lead to a new target for devising novel chemoimmunotherapeutics for late stage metastatic melanoma.

Table of Contents

List of Tables

List of Figures

List of Abbreviations

Gamma Interferon-inducible lysosomal Thiol reductase (GILT)
Paired box 3(PAX3)
Ganoderic acid DM (GA-DM)
Cyclin-dependent kinase 2NA (CDK2NA)
Human double minute-2 (HDM2)
Cyclin-dependent kinase (CDK4)
Melanocortin-1 receptor (MC1R)
Microphthalmia-associated transcription factor (MITF)
B-Raf proto-oncogene, serine/threonine kinase (BRAF)
Adoptive cell therapy (ACT)
Tumor-infiltrating lymphocytes (TIL)
Cytotoxic T lymphocyte-associated antigen (CTLA-4)
Programmed death 1 (PD-1)
Extracellular matrix (ECM)
Vascular endothelial growth factor (VEG-F)
Nuclear factor- κB (NF-κB)
Protein kinase C (PKC)
Transforming growth factor-1 (TGF-1)
Metalloproteinases (MMPs)
Endoplasmic reticulum (ER)
Invariant chain (Ii)
Class II-associated Ii peptide (CLIP)
Antigen (Ag)
Antigen-presenting cells (APCs)
Class II transactivator (CIITA)
Signal transducers and activators of transcription 1 (STAT1)
T cell receptor (TcR)
Sry-like HMG box 10 (SOX10)
Tyrosine related protein-1 (Trp-1)
Tyrosinase (Tyr)
Dopachrome (Dct)
Death domain associated protein (Daxx)
Promyelocytic leukemia protein (PML)
Transforming growth factor beta (TGF-β)
Jun N-terminal kinase (JNK)
Activating protein 1 (AP-1)
Pro-opiomelanocortin (POMC)
Melanocyte stimulating hormone (MSH)
Adenylate cyclase (AC)
Cyclic adenosine monophosphate (cAMP)
cAMP response element binding transcription factor (CREB)
Bcl-2-like protein 4 (Bax)

Apoptotic protease activating factor 1 (Apaf-1)
Mouse double minute 2 homolog (MDM2)
Interferon (IFN)

Acknowledgments

I would like to thank first and foremost my mentor Dr. Azizul Haque for all of his help and guidance throughout my time here at MUSC. I would like to thank my fellow lab members, past and present, for all of their support and contributions to my research. I would like to thank my graduate committee: Drs. Kasman, Tomlinson, Paulos, Vasu, Reddy, and Sutkowski for their counsel and support into helping me become a better scientist. I would like to thank my husband Jake, my family, and friends for their everlasting support as I pursue my goals.

Chapter 1: Background and Review of Relevant Literature

Melanoma Origin and Progression

Melanoma is one of the fastest growing cancers in the world, with an incidence increasing more quickly than any other cancer (except lung cancer in women) [1]. It was responsible for an estimated 76,000 cases of skin cancer in 2014 [2]. It accounts for about 9,700 of 13,000 skin cancer-related deaths each year [1]. Many cases are underreported, and incidence rates may be higher than what is projected.

Melanoma is a cancer that arises from melanocytes, which are the normal pigment-producing cells in the skin [3]. These cells are derived from the neural crest during embryonic development [4]. Neural crest precursor cells then undergo melanocyte migration, survival, and differentiation, in the presence of β-catenin [5]. These processes rely heavily on the Wnt signaling pathway, c-KIT receptor tyrosine kinase, and transcription factors like PAX3 and MITF [6, 7]. These and other pathways can be modified and possibly reactivated after the transformation from melanocyte to melanoma [8-10].

In normal adult skin, melanocytes are found at the junction of the dermis and epidermis, just superficial to the basement membrane [3]. Melanocytes exist primarily as individual cells within the epidermis, but instead of forming interactions with each other, melanocytes form heterotypic interactions with nearby keratinocytes, the predominant cell type in the skin [3]. Melanocytes within the epidermis acquire some epithelial traits, such as the formation of adherens junctions to neighboring keratinocytes [11].

Progression from normal melanocytes into melanoma has multiple steps.

Melanoma is thought to arise in one of two ways: (1) with no visible precursor lesion or (2) in association with a benign melanocytic proliferation called a nevus (or mole) [11]. In the progression model of melanoma, the primary step is the formation of the nevus, where proliferation and aggregation of melanocytes to form nests at the epidermal/dermal junction or within the dermis [12]. Next, the nevus progresses to melanoma in situ, which is confined to the epidermal/dermal junction. Melanomas that do not develop from a precursor lesion may be first detected in this stage [13]. The following step in the progression model is where invasive melanoma cells grow into the dermis where they interact with multiple cell types and have access to vasculature [3]. The final step is metastatic disease, where malignant cells have traveled from the primary site and established disease at distant sites in the body. The most common sites of metastases in malignant melanoma are lymph nodes, lungs, liver, and brain [12, 13]. Metastases have also been found in the GI tract as well as bone [3].

Risk Factors

Major risk factors for developing melanoma include early childhood sun exposure, fair hair and complexion, tanning bed use, high amounts of common melanocytic nevi, immunosuppression, and a family history [14]. There are multiple genetic loci that have been identified in melanoma risk, such as CDKN2A, CDK4, MC1R, MITF, BRAF, and many others. Mutations in BRAF have been found in about 40-70% of melanomas, while CDK4 has been identified in about 10% [15, 16].

Cyclin-dependent kinase N2A (CDK2NA) expression has been found in both

melanoma and dysplastic nevi [17]. The CDKN2A gene encodes the $p16^{INK4a}$ and $p14^{ARF}$ proteins, which are both tumor suppressors with important roles in the cell cycle and apoptosis regulation [17]. $P16^{INK4a}$ binds to CDK4 and CDK6, thus inhibiting both proteins. $P14^{ARF}$ binds to human double minute-2 (HDM2) protein to promote its degradation [18]. Since HDM2 in turn ubiquitinates and condemns p53 to degradation, the total effect of $p14^{ARF}$ loss is a destabilization of p53 [18, 19]. Therefore, CDKN2A removes both the RB and p53 pathways through the loss of $p16^{INK4a}$ and $p14^{ARF}$, respectively [20].

As stated previously, cyclin-dependent kinase 4 (CDK4) mutations have been found in roughly 10% of melanomas [16]. CDK4 is a cell cycle checkpoint protein, and a mutation would lead to cell cycle progression. Mutations occur at a conserved arginine residue, such as Arg 24, which negates the interaction with $p16^{INK4a}$ [17]. As shown in a mouse model expressing mutated R24C within CDK4, there was a significant increase in potential to acquire melanoma, which supports the notion of human melanomas having enhanced and/or mutated CDK4 [21].

Another molecule found to be commonly mutated in families with a melanoma background is the melanocortin-1 receptor (MC1R). MC1R regulates constitutive and facultative pigmentation and has emerged as one of the leading moderate-risk loci for melanoma susceptibility [22]. MC1R is a G-protein-coupled receptor that activates adenylate cyclase in response to α-MSH binding [23, 24]. Increases in cyclic AMP upregulates microphthalmia-associated transcription factor (MITF), which induces the transcription of the pigment synthesis genes [23]. MITF, in turn, has mutant variants of

its own, such as the germline variant E318K [17]. However, the prevalence of the MITF (E318K) alteration is significantly lower (<1%) in the general Caucasian population compared to MC1R variants [25].

Although there are other genetic loci associated with melanoma, B-Raf proto-oncogene, serine, threonine kinase (BRAF) mutations are the most prevalent somatic genetic events in human cutaneous melanoma [26]. Mutations in BRAF have been found in about 40-70% of melanomas [27], where they are frequently detected in the tumors occurring in the skin not chronically damaged by the sun [28]. More than 50 mutations with the BRAF gene have been identified, but roughly 90% of these mutations are single-base transitions at position 1799, leading to the substitution of glutamic acid for valine at codon 600 ($Braf^{V600E}$) [29]. Interestingly, this mutation is not sufficient for malignant transformation of melanocytes on its own, and it is an early oncogenic event found also at high frequency in benign nevi [30, 31].

Melanoma Staging and Treatment

When a malignant transformation occurs, there are hallmark changes in the physical makeup of the melanoma tumor. These physical changes include asymmetry, border irregularity, variation in color, an increase in diameter greater than 6 mm, and enlargement of the lesion. Upon detection of melanoma, proper staging is required in shaping patient treatment options. Greater than 90% of early stage, localized melanoma is cured with excision of the tumor. However, survival is halved when the tumor is diagnosed after lymph node involvement and less than 20% when it has reached

metastatic disease [32]. Classification of melanoma is based on the TNM system, which is indicative of tumor size, nearby lymph nodes, and sites of metastasis. Early stage tumors (Stage 0, I, & II) are measured by Breslow's depth to determine excision margins [32]. When melanomas have invaded nearby lymph nodes to distant sites of the body accompanied by elevated LDH levels in the blood, it is classified as stage IV, and generally, the prognosis is grim.

Among patients with stage IV metastatic melanoma, the median survival is about 8 months (+/- 2 months), and only about 15% of patients survive more than 5 years from diagnosis [33]. Until recently, there were few treatments available for advanced melanoma. These treatments include chemotherapy, high-dose radiation, IL-2 administration, and immunotherapies ipilimumab, vemurafenib, and pembrolizumab.

Chemotherapy is an accepted therapy for stage IV metastatic melanoma, and dacarbazine is the most widely used single chemotherapeutic agent for later stages [34-36]. Current studies have shown response rates for dacarbazine at 5-12% [37, 38]. Most responses are transient, and only 1-2% of patients achieve a durable long-term response to chemotherapy [39]. However, chemotherapy is one of the most common treatments for late stage patients due to cost effectiveness.

Radiation therapy is a mainstay of treatment for many malignancies where direct killing of tumor cells by radiation therapy is due to irreversible DNA damage, which leads to the induction of cellular senescence, mitotic catastrophe, necrosis, and/or apoptosis. [40]. For many years, melanoma was considered highly radio-resistant [41]. However, this was proven untrue through many studies starting as early as 1913 by

Simpson et al. (reviewed in [42]). The use of local radiotherapy only to the primary site versus treating the local site and the lymphatic regions for cutaneous melanoma is a function of stratifying patients into low risk versus high risk for regional recurrence based on particular clinical and biological indicators. In later stages of melanoma, patients can receive roughly four fractions of 8Gy at weekly intervals, or 20 fractions of 2.5Gy each, administered daily five days per week for multiple weeks [43]. This regimen of treatment may vary due to the location of the tumor. For example, primary mucosal melanomas of the head and neck region have a ~30% 5-year survival rate [44]. In a retrospective study, patients received 50-70Gy overall [44]. It has also been shown that adjuvant radiotherapy can decrease the incidence of regional lymph node recurrence in patients with positive regional nodes in their initial surgical specimen. However, there was no evidence of any improvement in relapse-free or overall survival [45]. These treatments can be toxic to patients and lead to immune adverse events as well as higher susceptibility of other cancers later in life.

High-dose recombinant IL-2 received FDA approval for metastatic melanoma treatment in 1998 [36]. During phase II trials, a response rate of ~16% was observed using a single agent therapy. Only about 5% of patients experienced long-term, complete responses with IL-2. The IL-2 antitumor activity is dependent on its ability to modulate immune responses in the host, increasing both T and natural killer cell-mediated activities [33]. However, it has been shown that this therapy has not improved the overall survival in the patient population [36]. Also, IL-2 treatments produce severe toxicity as well as immune adverse events in patients. These events include hypotension, vascular leak

syndrome, and cardiac dysrhythmias [33]. Therefore, it was proven that IL-2 administration did not reach its potential in activating an anti-tumor immune response.

The transfer of tumor-specific T cells (ACT) has shown some promise. The most developed approach is based on the ex vivo selection of highly reactive, tumor-infiltrating lymphocytes (TIL), their activation and expansion before reinfusion into the patient [46]. These patients generate high response rates, but patients must be lymphodepleted to eliminate competition for endogenous serum cytokines [47]. This approach is both labor-intensive and costly, where it may take several weeks for cell culture to acquire enough cell numbers needed for an optimum response. Also, patients must be able to withstand the intensity of ACT, which includes total body irradiation and IL-2.

Because of the poor results from the IL-2 clinical trials as well as other adjuvant therapies (i.e. IFN-α, whole cell, and dendritic vaccines), different immunotherapies were developed in order to combat metastatic melanoma. In 2011, ipilimumab and vermurafenib received FDA approval to treat late stage melanomas.

Ipilimumab is a monoclonal antibody that targets cytotoxic T lymphocyte-associated antigen (CTLA-4), which is a co-inhibitory molecule that functions in regulating T cell activation [48]. In phases II and III clinical trials, ipilimumab demonstrated improved overall survival versus gp100 peptide vaccine and dacarbazine, independently [48]. However, during phase III trials, the response rate, complete response and partial response was only 10-15%, and the disease control rate was about 30% [48]. While ipilimumab is capable of inducing a long-term response in a minority of patients, the low response rate and small improvement in median survival limits its

effectiveness.

Vemurafenib is a selective inhibitor of Braf, a serine-threonine-specific protein kinase. [29]. It binds to the nucleotide-binding pocket of $Braf^{V600E}$ with higher affinity than ATP and renders the kinase unable to phosphorylate downstream targets [33]. This inhibition leads to cyclin D1 suppression, induction of cell cycle inhibitor p27, and eventually cell-cycle arrest [49]. During phase III trials with untreated patients with the $Braf^{V600E}$ mutation, overall survival at 6 months was 84% compared to 64% of patients treated with dacarbazine, while the response rates were 48% and 5%, respectively [50].

In September 2014, the FDA also approved the drug pembrolizumab for late stage melanoma as well. Pembrolizumab is a highly selective antibody against programmed death 1 (PD-1), where early clinical trials have shown high tumor response rates and long duration of effect in previously treated advanced melanoma [51]. Due to the new approval for this drug, long-term effects and effectiveness of this drug have not be further assessed.

Treatments such as ipilimumab and vemurafenib have shown profound initial responses in subgroups of patients, but the effect is short-lived. Drug resistance frequently appears after 6-9 months of therapy due to the development of different mechanisms of acquired tumor drug resistance that leads to the recovery of MAPK signaling or activation of alternative signaling pathways [33, 52]. This acquired resistance in unresectable/metastatic melanoma patients has become an increasing setback. A possible solution to acquired resistance is developing combination-targeted therapies. Current studies include combining chemotherapy/radiation with ipilimumab

and/or vermurafenib as well as other immunotherapy strategies [33, 36, 41, 53].

Biochemotherapy, such as cisplatin, vinblastine, and dacarbazine combined with IFN-α +/- IL-2, increases response rate, but has not been shown to significantly improve survival compared with chemotherapy alone in randomized phase II and II trials [34, 54]. Until today, biochemotherapy has not demonstrated significant clinical benefit in adjuvant trials nor in randomized prospective studies in the metastatic setting, but it is associated with additive toxicity [36]. Therefore, biochemotherapy regimens cannot be regarded as standard clinical practice and should be further evaluated in clinical trials [36].

On the other hand, bioradiotherapy strategies look to combine radiation therapy with immunotherapy. Such studies involved examining immunotherapies interferon-α2b, IL-2, ipilimumab, and ACT [33, 36, 46, 55-57]. In each of these studies, data suggests that these treatments may interact and lead to increased therapeutic effects, adverse events, or both. Interestingly, a retrospective analysis of 29 patients who received ipilimumab with radiation, there was no significant increase in adverse effects related to immunotherapy [56]. However, at the highest doses of administered radiation therapy, an increase in radiation therapy-related adverse events was noted. Importantly, in these studies, high doses of radiation are being administered to these patients. A 66 year-old patient received ipilimumab after recurrent, metastatic melanoma. The patient received 27Gy in 3 fractions after metastasis to the right internal mammary lymph node was detected. After three months after radiotherapy, the tumor had decreased in size from 1.5x1.6cm to 1.2x0.7cm [53]. Given the immunologic effects of radiation therapy, there

are ongoing investigations into radiation therapy and immunotherapy in the treatment of patients with melanoma [53]. Currently, there are two Phase I trials examining ipilimumab with different types of radiation therapy, three Phase I/II trials, and four Phase II trials comparing bioradiotherapy to ipilimumab alone. Therefore, a better understanding of the mechanisms underlying bioradiotherapies is essential in optimizing the key goal of killing malignant cells while boosting immune responses.

Inflammation and Angiogenesis in Melanoma

At the cellular level, melanoma tumors differentially express cytokines, chemokines, and soluble molecules responsible for immunosuppression and tumor proliferation. Inflammation is a part of the host's response to either internal or external environmental stimuli [58]. Melanoma cells have a strong cytokine-secreting ability and complex cell signaling networks [59]. This cytokine-secreting ability may also have an impact on melanoma invasion and detection. Inflammatory cytokines like IL-6, IL-12, IL-17, and IL-23 have been observed in melanoma [60-62]. Patients with elevated levels of IL-6 were more likely to have elevated TNFα, which allowed them to be susceptible to relapse and toxicity [63]. IL-6 has been correlated with STAT3 activation, a transcription factor involved in the regulation of the immune system, inflammation, cell survival, and cell proliferation [64]. When IL-6 is induced by IL-17, this, in turn, can stimulate the upregulation of STAT3 [61]. There have been many conflicting reports on the study of IL-6; when in early stages, IL-6 can be beneficial to tumor clearance. However, as the disease worsens, IL-6 can actually aid in the tumor progression. Also, an up-regulation of IL-6, IL-8, and IL-1β cytokines were observed in fibroblasts that were

co-cultured with highly invasive melanoma cell lines BLM and MV3 [65]. Melanoma-associated fibroblasts dominate the surrounding tissue around the tumor which suggests that the tumor microenvironment plays an essential role in invasion and metastasis. Another cytokine, IL-10, has been known to have immune suppressive properties. In one study, IL-10 mRNA was compared between melanoma tumors and metastasis with normal tissue [66]. Four out of five melanoma biopsies detected IL-10 mRNA, whereas the normal tissues did not express detectable levels of IL-10 [66]. Also, patients with advanced melanoma have a high percentage of CD4+ $CD25^{High}Foxp3^{+}$, IL-10-producing T regulatory lymphocytes [67]. The secretion of these cytokines may have the ability to create a microenvironment that leads to toxicity and invasion.

Along with inflammation at the tumor site, angiogenesis, the process of new formation of blood vessels from preexisting ones, may also enhance the cancer's ability to metastasize. Melanoma angiogenesis has been linked with poor prognosis, patient survival, ulceration, and an increased rate of relapse [68]. While malignant melanoma progresses, metastatic cells have to exit the primary tumor site by loosening cell to cell contact, adhering to and degrading extracellular matrix (ECM), migrating through the subendothelial basement membrane of local post-capillary veins and lymphatic vessels, and intravasating [69]. Secretion of the angiogenic molecule vascular endothelial growth factor (VEG-F) by melanoma cells has been correlated to the transition from the radial to the vertical growth phase [70]. VEG-F regulates the permeability of the endothelial barrier where it plays a vital role in tumor angiogenesis and is associated with most advanced stage melanomas [71, 72]. It also has been demonstrated that the upregulation

of VEG-F expression in metastatic melanoma is linked with an increase in the number of tumor-infiltrating inflammatory cells expressing VEG-F [73]. It may inhibit cytotoxic immune responses, promote tumor cell proliferation, and facilitate vascular dissemination of melanoma cells [69].

Another angiogenic factor that has been observed in melanoma is IL-8 [65, 74]. IL-8 expression is scarcely found in normal epidermis and benign melanocytic lesions [73]. IL-8 as well as IL-6 can act as circulating tumor cell attractants, which can accelerate tumor growth, angiogenesis, and recruitment of other chemo-attractant molecules [60]. IL-8 can promote nuclear translocation of STAT3 and β-catenin, without transcriptional activity [75]. IL-8 signaling has also been shown to increase the transcription of nuclear factor-κB (NF-κB) in melanoma, which may be increased through protein kinase C (PKC) activity [76]. Along with NF- κB, STAT3, and β-catenin, IL-8 indirectly upregulates the activity of AP-1 and mTOR, which are both implicated in cell proliferation, invasion, and cell survival [77]. VEG-F is linked with IL-8 signaling through its activation by the GPCR of the IL-8 receptor. It has also been demonstrated that transforming growth factor-1 (TGF-1) has the ability to enhance IL-8 expression in human melanoma cells and promote angiogenesis in multiple xenograft models [78].

Other angiogenic factors involved in melanoma include, but are not limited to, the matrix metalloproteinases (MMPs). MMPs are a large group of secreted proteinases that are involved in normal physiological and pathologic processes such as embryogenesis, wound healing, angiogenesis, tissue remodeling, tumor invasion, and metastasis [79]**.** Within this family of proteins, MMP-2, MMP-9, MMP-13, and MMP-14 have been

observed in melanoma and are used as biomarkers for staging [80, 81]. MMP-2 and MMP-9 degrade connective tissue and basement membrane collagen and are believed to play an important role in skin and uveal melanoma progression [79, 82]. The expression and activation of both enzymes have been correlated to the invasive and metastatic phenotypes of the tumors [73]. More so, MMP-2 expression contributes to metastatic spread and low survival rates [83]. MMP-9 has been found during the radial growth phase, but not the vertical phase, which suggests that MMP-9 is utilized during early events in melanoma progression [84]. An upregulation of these proteins may create a microenvironment that promotes melanoma invasion, metastasis, and evasion of the immune system. These inflammatory cytokines and angiogenic factors can play a vital role in the aggressiveness of melanoma, and they may also aid in the immune evasion of these cells. Understanding the regulation of melanoma cells by the immune system may help in the targeting of inflammatory and angiogenic molecules, thus shifting the tumor microenvironment to an anti-tumor state.

Melanoma and the Immune System

Melanoma is characterized as one of the most immunogenic tumors due to the presence of tumor-infiltrating lymphocytes in resected melanoma, some regressions, and clinical responses to immune activation [48]. The multiple ways that melanoma alters the immune system locally, at the site of the tumor, and systemically makes the disease difficult to treat, but ideal for the study of immunomodulation [85]. Immunomodulation, the alteration of the immune system or its function, is exploited in multiple forms by

melanoma tumors from changes in the cellular and sub-cellular makeup of the tumor to changes in the tumor microenvironment that suppress localized and systemic attempts at disease reduction. Therefore, many studies investigated mechanisms leading to tumor immune evasion.

Establishing a permanent immunological memory is an ideal strategy for current immunotherapies while providing an immune attack upon malignancies. Long-lasting immune responses and protection against melanoma is mainly dependent upon the activation of CD8+ and CD4+ T cells via the HLA class I and II pathways [86]. The HLA class II pathway is a critical component of the immune system as they present both self and foreign peptides to CD4+ T cells [87]. Through this pathway, a robust and lasting immune response can be generated as well as the establishment of effective immune memory [88]. HLA class II alpha/beta heterodimers are synthesized within the endoplasmic reticulum (ER) of cells and form a complex with the glycoprotein invariant chain (Ii) [89-91]. In the endolysosomal compartments, acidic proteases such as cathepsins S and L begin to degrade Ii into smaller intermediate peptides, leaving the class II-associated Ii peptide (CLIP) in the class II binding groove [92-95]. Simultaneously, processing of antigens (Ags) is occurring by acidic cathepsins B and D [92, 96, 97]. These acidic proteases unfold, cut, and splice both exogenous and endogenous Ags into smaller peptides. The non-classical class II molecule, HLA-DM, chaperones the removal of CLIP from the peptide binding groove and catalyzes the loading of high affinity peptides, leading to a stable HLA class II-peptide complex [88, 98, 99]. This complex is then transported to the cell surface for CD4+ T cell recognition.

Recent studies have shown that melanoma cells can constitutively express class I and class II proteins [100]. It has previously been reported that melanoma cells expressing HLA class II molecules cannot process cysteinylated peptides, leading to immune evasion [101, 102].

Melanoma cells lack an enzyme that is required for proper Ag processing and presentation to CD4+ T cells. Spontaneous cysteinylation of peptides and antigens occurs to interrupt HLA class II presentation [103]. This cysteinylation occurs through the formation disulfide bonds between cysteine residues or when cysteine residues bind to free-floating cysteine in the cytosol [101]. Gamma Interferon-inducible Lysosomal Thiol reductase (GILT), is an enzyme that can restore T cell recognition of cysteinylated melanoma tumor antigens [101]. GILT is abundantly expressed in professional antigen presenting cells (APCs), but is absent or very low in melanoma [104]. Within APCs, GILT is found in its proforms in early endosomes while its mature form is found in multivesicular late endosomes and multilaminar lysosomes [105, 106]. GILT is synthesized as a precursor and targeted via the mannose-6 phosphate receptor to the endolytic pathway where N- and C-terminal propeptides are removed to generate the mature form at 30 kDa [107]. GILT is active at a low pH and catalyzes the breaking of disulfide bonds, allowing Ags to unfold, which allows antigens and peptides to be further processed by acidic cathepsins as shown in Figure 1.1.

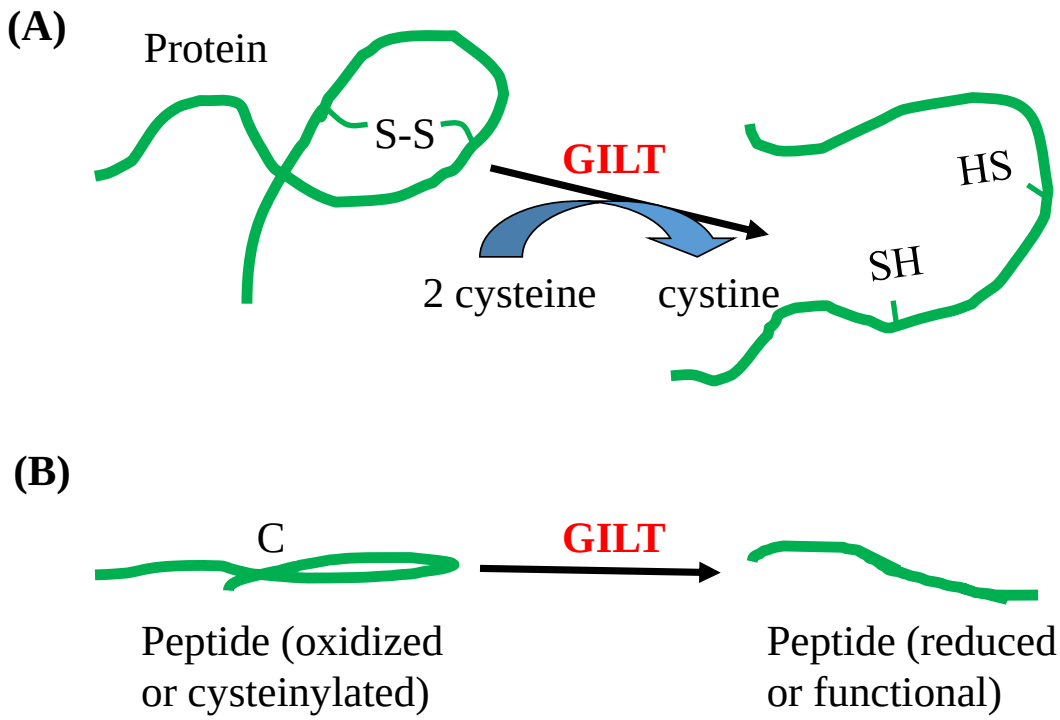

Figure 1.1 The role of GILT in the breaking of disulfide bonds. (A) GILT is active at low pH and catalyzes the breaking of disulfide bonds, making Ags/peptides unfold and can be further processed by acidic cathepsins. (B) Cysteine-containing processed peptides may become susceptible to disulfide bond formation with free-floating cystine in the cytosol, allowing the peptide to become oxidized (non-functional). Again, in the presence of GILT, the bond is broken, the peptide is reduced or functional, and can be efficiently loaded onto HLA class II molecules.

It has studied that GILT can be induced in melanoma by treatment with IFN-γ [97]. We have previously shown that GILT expression in melanoma cells increased HLA-DM molecules, favoring epitope loading onto class II molecules [97]. We also reported that GILT can upregulate active forms of cysteinyl cathepsins B and S as well as aspartyl cathepsin D [97]. Further investigation led to the finding that GILT colocalizes with cathepsins B and D in the endosomal/lysosomal compartments, leading to increased Ag processing and presentation [97].

Previous studies suggest that GILT is necessary for processing of post-translationally modified/oxidized epitopes for HLA class II-mediated presentation [108]. We have previously shown that GILT is regulated by signal transducers and activators of transcription 1 (STAT1) and not by the previously believed class II transactivator (CIITA), which is imperative for the activation of HLA class II gene loci [109]. GILT expression has been shown to enhance processing of Ags and peptides and CD4+ T cell recognition [101, 108]. An alteration in the expression of tumor Ags or disturbance in HLA class II presentation may be the reason why tumors cells evade immunogenic ablation [110-112]. Thus, the restoration of the HLA class II-peptide presentation pathway in melanoma may help tumor cells promote immunological destruction [86]. However, the mechanism that GILT utilizes in class II Ag presentation has yet to be clearly defined.

Significance

Melanoma is the 5th most common cancer in the United States [1]. Improved treatment options are necessary to combat this disease. Immunotherapies have had some success at fighting this disease at the earliest stages, but fail with aggressive, metastatic melanoma. Also, most of these treatments can be extremely toxic and harmful to patients. Alternative treatments must be sought out to fight this deadly disease. As previously stated, the insertion of GILT is vital for proper HLA class II antigen processing and presentation in melanoma [101, 108]. Current treatments for metastatic melanoma include surgery, chemotherapy, high-dose radiation, and some

immunotherapies. However, these treatments appear futile once the tumor has metastasized beyond localized lymph nodes. This stresses the need for improved disease targeting as well as new possibilities for combining treatments. Three parts of this study intend to investigate how GILT expression generates a greater pool of antigenic peptides for HLA class II-mediated presentation by human melanoma cells, how GILT negatively regulates the tumorigenic molecule PAX3 in human melanoma cells, and the modulation of GILT and PAX3 enhances radiation and chemoimmunotherapy of melanoma. Thus, current therapies may be optimized in combination with targeting PAX3 to enhance melanoma cell death.

Chapter 2: GILT expression generates a greater pool of reduced peptides for HLA class II-mediated presentation by human melanoma cells.

Introduction

As previously mentioned, melanoma is one of the most rapidly growing cancers plaguing western populations [1, 2]. To fill the gap in treatment options, immunotherapy has been tried in multiple forms over the past decade. Of these, autologous T cell transfer, interferon therapy, whole cell cancer vaccines, and antibody therapy (e.g., Ipilimumab and pembrolizumab) have had some success, yet an effective immunotherapy remains elusive. One of the main failures associated with melanoma immunotherapy is an incomplete stimulation of both CD4+ and CD8+ T cells [113-115], leading to incomplete tumor clearance and no gaining of effective immunological memory. This chapter looks to dissect novel Ag processing reactions in melanoma that could be exploited in both loaded dendritic cell and melanoma whole cell vaccine strategies.

The most widely known melanoma Ags are MART-1, NY-ESO-1, gp100, and tyrosinase [116-122]. These Ags have been shown to elicit both cytotoxic CD8+ and helper CD4+ T cell responses [123]. It is believed that cancer cells are mainly eliminated as a result of stimulation of by both natural killer and CD8+ T cells [124]. While cytotoxic CD8+ T cells are able to destroy melanoma cells [125-127], their interaction with tumor cells and killing efficiency are greatly supported in combination by CD4+ helper T cells [113]. One of the immune evasion mechanisms could be the oxidation of Ags/peptides that leads to posttranslational modification, masking tumor cells from T cell-induced cell death. Melanoma Ags MART-1, NY-ESO-1, gp100, and tyrosinase all

contain multiple epitope sequences specific for class II binding, many of which contain cysteine residues, which may also perturb CD4+ T cell recognition of melanoma cells [116, 120, 121, 128]. However, it remains unknown whether the expression of GILT in melanoma cells could enhance processing of these cysteinylated Ags/peptides to produce a greater pool of functional epitopes for delivery to CD4+ T cells via the HLA class II pathway.

In the previous chapter, it was stated that GILT is abundantly expressed in APCs, but is absent or very low in melanoma as well as other tumors [129]. GILT expression can be induced in melanoma and other tumor cells by treatment with IFN-γ [130]. GILT is active at low pH and catalyzes the breaking of disulfide bonds, making Ags/peptides susceptible to degradation by acidic cathepsins. Recent evidence suggests that GILT plays a role in the processing of post-translationally modified epitopes for HLA class II-mediated presentation to T cells [108]. The HLA class II pathway is a critical component of the immune system as it is responsible for presenting both self and foreign peptides to CD4+ T cells [87]. Once peptides are loaded onto HLA class II molecules, the T cell receptor (TcR) interacts with the HLA class II-peptide complex, and members of the B7 family (CD80/CD86) interact with CD28 molecules on the T cell surface [131, 132]. Through this pathway, a robust and lasting immune response can be generated as well as the establishment of effective immune memory [88].

An alteration in the expression of tumor Ags or disturbance in the HLA presentation pathway may be the reason why tumor cells evade immunogenic ablation [110-112]. Thus, the restoration of the HLA class II peptide presentation pathway in

melanoma may help tumor cells to promote immune-mediated destruction [86]. However, a complete understanding of GILT's involvement within the class II pathway has yet to be determined, and may contribute to the regulation of other factors, such as costimulatory molecules and intracellular proteases. Cathepsins B, D, S and L are lysosomal proteases found in professional APCs as well as in tumors [133-136]. Modulation of cathepsin expression and activity could likely lead to differential Ag processing and altered peptide repertoire in GILT-positive melanoma cells.

Hypothesis

I tested the hypothesis that GILT expression enhances cathepsin expression and activity in melanoma cells, leading to a greater generation of antigenic peptides for HLA class II-mediated presentation and CD4+ T cell recognition of melanoma.

Research Strategy

Experiment 1: Generated GILT-expressing melanoma cell lines.

Experiment 2: Tested HLA class II components (HLA-DR, HLA-DM, Ii, etc.) for protein expression in GILT +/- human melanoma cell lines.

Experiment 3: Examined costimulatory molecules (CD80, CD86) in GILT +/- human melanoma cell lines.

Experiment 4: Investigated aspartyl and cysteinyl cathepsin expression and activity in GILT +/- human melanoma cell lines.

Experiment 5: Analyzed peptide generation from supernatants collected from

GILT +/- human melanoma cell lines.

Materials & Methods

Cell lines

Human melanoma cell lines DM-331(University of Virginia) and HT-144 were grown in complete RPMI-1640 (Invitrogen, Grand Island, NY) medium containing 10% fetal bovine serum (FBS) (HyClone, Logan, UT), 50 U/ml penicillin, 50 µg/ml streptomycin (Mediatech Inc., Manassas, VA), and enriched with 1% L-glutamate (Mediatech) [109]. The human melanoma cell line J3 was cultured in complete IMDM media containing 10% bovine growth serum (BGS) (HyClone), 50 U/ml penicillin, 50 µg/ml streptomycin (Mediatech), and enriched with 1% L-glutamate (Mediatech) [101]. A human B-lymphoblastic cell line Frev (Dr. Janice Blum, University of Indiana) was also used as a positive control for GILT expression to test melanoma cell lines. Frev cells were cultured in suspension in complete IMDM media (CellGro) containing 10% BGS (HyClone), 50 U/ml penicillin, 50 µg/ml streptomycin (Mediatech), and enriched with 1% L-glutamate (Mediatech). The T cell hybridoma cell line 2.18a, specific for $\kappa_{188\text{-}203}$ peptide, was cultured in complete RPMI-1640 with 10% FBS, 50 U/ml penicillin, 50 µg/ml streptomycin, 1% L-glutamate, and 50µM β-mercaptoethanol (β-ME) [101, 137].

Table 2.1 Cell lines utilized for chapter 2.		
Melanoma Cell Line	**Conditions/Treatments**	**Reason for use**
J3.DR4	+/- GILT	Retrovirally transduced to express DR4, to determine role of GILT in Ag processing and presentation
DM-331	+/- GILT	Constitutive expression of DR4, to determine the role of GILT in Ag processing and presentation

DNA transfection assays

The human melanoma J3 cells were transduced using retroviral vectors for constitutive expression of HLA-DR4 (DRB1*0401) with linked drug selection markers for puromycin and histidinol resistance [101]. Surface HLA-DR4 complex expression on cells were confirmed by flow cytometric analysis using the DR4-specific mAb, 359-F10 [138]. Human melanoma cell lines DM-331 and HT-144, which constitutively express HLA-DR4 molecules on the cell surface, and J3.DR4 were transfected with a plasmid encoded with GILT cDNA and a puromycin drug resistance gene or a vector-encoded plasmid with the same puromycin drug resistance gene using a lipofectamine transfection reagent (Sigma-Aldrich, St. Louis, MO). All melanoma cell lines were first grown in 100mm tissue culture plates, incubated at 37ºC with 5% CO_2 until each plate reached 70-80% growth confluence. Cell growth media was then aspirated and each plate was washed twice with DPBS (HyClone). Cells were then removed from the culture plate using Trypsin EDTA (Invitrogen), collected and counted. Cell volumes were adjusted to $1x10^6$ cells per ml. Next, 1ml of cells were added to each well of a 6 well tissue culture late (Corning Incorporated). Each cell line was allowed time to adhere before

transfection began, under non-supplemented RPMI culture conditions. During which time a DNA lipofectamine complex was made. The DNA/lipofectamine complex consisted of 5 µg/µl of cDNA, either vector or GILT extracted plasmid cDNA, in 22 µl of lipofectamine reagent brought to a final volume of 600 µl in serum free RPMI media. This mixture was incubated for 30 minutes prior to being added to the cells. After the incubation time, 2.4 ml of serum free RPMI was added to the DNA/lipofectamine complex mixture and 1 ml of the mixture was added to each well of the 6 well culture plate containing the melanoma cells, 3 wells received the vector cDNA complex, and 3 wells received the GILT cDNA complex. These cells were then incubated under normal cell culture conditions for 24 hours then transfected cells were selected and expanded based upon encoded drug resistance to puromycin dihydrochloride (Sigma-Aldrich, St. Louis, MO). GILT expression was then assessed through western blot analysis.

Preparation of cell lysates

Transfected cells were grown to 80% confluence on 100mm plates, and then removed from the culture plate using Trypsin EDTA (Invitrogen), and collected in 15ml conical tubes. Cells were washed twice with HBSS (HyClone) and frozen at -80^{o}C for 24 hours. These pellets were next lysed in a complete lysis buffer composed of 10mM Tris, pH 7.5, 150 mM NaCl, 1% Triton X-100, 100 µM tosyl-Lys-chloromethyl ketone, and 200 µM PMSF on ice. Lysates were centrifuged at 2000 rpm for 5 minutes at 4^{o}C to remove cell nuclei and major cell debris. The supernatant from this was then transferred to a new centrifuge tube and re-centrifuged at 10,000 rpm for 8.5 minutes to ensure that

only protein was collected. The protein concentration within these cell lysates was determined using an albumin standard (Thermo Scientific) and all cell lysates were stored at -20^{o}C until future use in western blot analysis.

Protein determination

Cell lysates were assessed for protein concentration using a 2.0 mg/ml Bovine Serum Albumin standard (Thermo Scientific). Control albumin was diluted at limiting concentration values of 1, 0.8, 0.6, 0.4, 0.2, and 0µg/µl and loaded into an EIA medium binding 96 well plate (Corning Incorporated) in triplicate. Cell lysates were then added to test wells containing 20 µl of DDH_2O in triplicate. All wells then had 25 µl of BioRad working solution A (20 µl of BioRad DC Protein Assay reagent S in 1ml of BioRad DC Protein Assay reagent A) followed by the addition of 200 µl of BioRad DC Protein Assay reagent B, and allowed this to incubate at room temperature for 15 minutes. Plates were read at 630 nm using a BioTek ELx800 absorbance reader (BioTek). A line of best fit was determined based on the BSA standard, the equation of which was used to determine the amount of protein in µg/µl of each test sample.

Western blotting and densitometry

Once protein levels were quantified following cell lysate and protein determination, equal amounts of protein from vector and GILT matched cell lines were subjected to the reduced and boiled technique. All samples that were reduced had 1.5 µl of DTT reducing agent added to the sample protein with a standard amount of loading

buffer (NuPage Sample Buffer). All samples that were boiled after appropriate amounts of protein sample, loading buffer, and complete lysis buffer (to equilibrate reaction volumes) have been added, were heated on a heat block at 70^{o}C for 10 minutes. After these steps concluded, the samples were loaded onto NuPAGE 4-12% Bis-Tris gels (Invitrogen) and run at 200 volts for 50 minutes. Bis-Tris gels containing protein were then transferred to nitrocellulose membranes (Osmonics) employing a transfer chamber subjected to 30 volts for one hour. Nitrocellulose membranes were then removed and blocked in a solution of 5% milk in Tris-Buffered Saline and Tween 20 (TBS-T) overnight at 4^{o}C. After incubation, the nitrocellulose membranes were probed with protein specific mAbs. A β-actin antibody (Santa Cruz) was used as an equal protein loading control. Probed nitrocellulose membranes were next assessed using autoradiography film, following incubation with 3ml of Luminata Crescendo Western HRP Substrate (Millipore Corporation, Billerica, MA) for 3 minutes. Autoradiography films were scanned using a Canon MP250 scanner/printer and analyzed using a BioRad Geldoc XRS photocenter, where densitometric software enabled for the quantification of protein densities, based against respective actin controls.

Ags, peptides, and antibodies

The whole Igκ was purchased from Sigma-Aldrich. The human IgG immunodominant peptide $\kappa_{188\text{-}203}$ (sequence KHKVYACEVTHQGLSS) was produced by Fmoc technology and Applied Biosystems Synthesizer [103, 137]. Peptide purity (>99%) and sequence were analyzed by reverse phase HPLC purification and mass spectroscopy.

Nitrocellulose membranes were subjected to probing with various antibodies. The antibodies used were human GILT, HLA-DM, CD80, CD86, Cat B, Cat D, Cat S, Cat L, and β-actin (Santa Cruz Biotechnology Inc., Santa Cruz, CA). HLA-DR (L243) and Ii (Pin 1.1) were obtained from Dr. Janice Blum, Indiana University School of Medicine, Indianapolis, IN. Nitrocellulose membranes were incubated for 2-3 hours, rolling, at room temperature with a given antibody at a predetermined concentration (as per manufacturer standard) in a solution of 2.5% milk in TBS-T. Following incubation time, blots were washed for 30 minutes in TBS-T before being probed with the horseradish peroxidase secondary antibodies conjugated for anti-mouse (Pierce, Rockford, IL), anti-rabbit or anti-goat (Santa Cruz) for one hour. Finally, blots were washed again in TBS-T for 30 minutes then subjected to Luminata Crescendo Western HRP Substrate (Millipore Corporation, Billerica, MA) and assessed as described in western blot methods.

Confocal microscopy

J3.DR4.vec and J3.DR4.GILT cells were grown to 80% confluence to then be transferred to a 6 well plate with one coverslip (sterilized in 70% ethanol) with 5.0×10^5 cells in each well. After the cells had adhered for 24 hours, cells were washed with 1ml paraformaldehyde at room temperature for 20 minutes. Cells were then washed with 1ml of PBS/0.01% Triton-X/0.01% Glycine at room temperature for 15 minutes on the shaker twice. Next 500 µl of 5% BSA/PBS was added to each well and incubated at room temperature for 10 minutes. Coverslips were transferred to a labeled slide. 100 µl of 5% normal serum (50 µl/1ml 1% BSA/PBS) was added to each slide and incubated for 10

minutes at room temperature followed by 50 µl of primary antibody diluted in 1% BSA/PBS added directly over the coverslip and incubated for 1 hour. Slides were washed in 1% BSA/PBS (200µl per slide) on the shaker for 10 minutes twice. Next, 50-100 µl of 5% normal serum was added to each slide and incubated at room temperature for 10 minutes. Slides were dried using a paper towel and 50 µl of secondary antibody was added and incubated in the dark at room temperature for 1 hour. All steps following were performed in the dark at room temperature. Secondary antibody was removed and 200 µl of 1% BSA/PBS was added for 10 minutes on the shaker twice. Liquid was removed and 200 µl of PBS was added, placed on the shaker for 5 minutes twice. 60 µl of DAPI stain was added to the slides for 10 minutes at 1:5000 dilution in 1% BSA/PBS. Liquid was removed, and slides were washed twice with PBS for 10 minutes each. A new set of slides were labeled and 20 µl of Fluoromount-G mounting media was added to each slide. Old slides were completely dried, and the coverslips were transferred to new slides and incubated for 1 hour. Slides were dried and nail polish was added to the outer edges of the coverslip and left overnight. Images were taken the following day using a Leica TCS SP2 AOBS, 63 water immersion objective using 405 and 543 lasers. Images with each staining were taken using the overlay to assess the positioning of the protein in question.

Flow cytometry

J3.DR4.vec, J3.DR4.GILT, DM-331.vec, and DM-331.GILT cells were cultured and washed with staining buffer (PBS+1% heat-inactivated BGS) (Hyclone), and

resuspended in a binding buffer (cat. No. 556454, BD Bioscience: 0.1 M HEPES (pH 7.4), 1.4 M NaCl2, and 25 mM CaCl2). Next, $5x10^5$ cells were stained and incubated with 2µl of primary antibody for 1 hour at 4ºC with anti-DR, anti-CD80, and anti-CD86 (Santa Cruz). Cells were then washed with isotonic phosphate-buffered saline with 5%fetal calf serum 4 times. Cells were then incubated with 1ul of fluorescence labeled secondary antibodies for 1 hour. Cells underwent additional wash steps with isotonic phosphate-buffered saline with 5% fetal calf serum 4 times. Cells were then fixed with 2% paraformaldehyde. Samples were then analyzed on a FACScan using CellQuest software (BD Bioscience, Mountain View, CA) for cell surface expression of class II, CD80/CD86 molecules with NN4 and other appropriate isotype controls [97, 139, 140]. Data presented is representative of three independent experiments.

Cathepsin Bioassay

Cathepsin B, S, L, and D activity assay kits were purchased from BioVision, Inc. (BioVision). Cathepsin B, S, L, and D activity was measured in human melanoma cells J3.DR4.vec, J3.DR4.GILT, DM-331.vec, and DM-331.GILT. Cells were collected in cell line appropriate media by centrifugation at $1x10^6$ml, where cells were lysed in 50ul of chilled CB Cell Lysis Buffer (BioVision). Cells were incubated with CB Cell Lysis Buffer for 10 minutes, centrifuged at 10,000rpm for 5 minutes, and supernatants were transferred to a new tube. 50ul of cell lysate was added in triplicate to a 96-well plate. 50ul of CB Reaction Buffer (BioVision) was added to each sample, and 2ul of the 10mM CB Substrate Ac-RR-AFC (200uM final concentration (BioVision) was added. The CB

Inhibitor provided in the bioassay was used as a negative control. Plates were incubated at 37^{o}C for 1-2 hours. Plates were read at 400nm excitation filter and 505nm emission filter using a BioTek ELx800 reader (BioTek). Experiments were performed in triplicates and repeated at least three times. Results and standard deviations for a single representative experiment were shown.

Liquid chromatography-mass spectroscopy (LC-MS)

J3.DR4.vec and J3.DR4.GILT were cultured, fed with IgG κ for 24 hours. Supernatant was then collected, and the κI peptide KHKVYACEVTHQGLSS was analyzed by capillary liquid chromatography using an Applied Biosystems 140D solvent delivery system. Samples were applied directly to 300μM diameter fused silica capillaries packed with Vydac C18 resin and separated with gradients of buffer A (2% acetonitrile and 98% H2O containing 0.2% isopropanol, 0.1% acetic acid and 0.001% trifluoroacetic acid) and buffer B (95% acetonitrile and 5% H2O containing 0.2% isopropanol, 0.1% acetic acid, and 0.001% trifluoroacetic acid). Peptide was eluted at a flow rate of 7μl/minute directly into the electrospray ionization source of a Finnigan LCQ mass spectrometer. Nitrogen was used as the sheath gas with a pressure of 35 psi with no auxiliary gas. Electrospray ionization was conducted with a spray voltage of 4.8 kV, a capillary voltage of 26V, and a capillary temperature of 200^{o}C. Spectra were scanned over an *m/z* range of 200-2000. Base peak ions were trapped using the quadruple ion trap and further analyzed with a high resolution scan (zoom-scan) using an isolation width of 3 *m/z* and collision-induced dissociation scans with a collision energy of 40.0.

Sample Preparation for LC MS/MS

Cell elutions were reduced with DTT and alkylated with 55mM iodoacetamide. The protein was digested with 100ng of trypsin (Sigma, proteomics grade) overnight at 37^{o}C. The digested sample was then desalted using a C18 ziptip (Milipore) following the manufacturer's protocol. The eluent was dried down, and peptides were resuspended in 5μL of mobile phase A (98% water, 2% acetonitrile, 0.1% formic acid) and transferred to an auto sampler vial for LC-MS/MS analysis.

LC MS/MS Analysis-LTQ XL

Trypsin-digested samples were analyzed via liquid chromatography (LC)-electrospray ionization (ESI)-tandem mass spectrometry (MS/MS) on a linear ion trap mass spectrometer (LTQ, Thermo) coupled to a Dionex U3000 nano LC system. A 25cm 75micron C-18 reversed phase LC column (packed in house, with Waters ODS C18, 5u) was utilized with a 120 minute gradient from 2%acetonitrile, 0.2% formic acid to 50% acetonitrile, 0.2% formic acid. Data Dependent Analysis was utilized on the LTQ to perform MS/MS on the 10 most intense ions in each MS spectra with a minimum ion count of 1000.

Database Searching and Quantitation

The raw data were searched with Proteome Discoverer 1.4. The Human IPI v3.72 database was used. Static modification of carbomidomethyl on cysteines and variable

modifications of methionine oxidation and the oxidation, di-oxidation, tri-oxidation, and cysteinylation of cysteines were included. Protein identifications must have 2 unique peptides with an Xcorr vs. charge state > 1.5, 2.0, 2.5 for +1, +2, and +3 ions, a good match for at least 4 consecutive y or b ion series from the MS/MS spectra to be considered a positive identification. Peptides identified from the above analysis that were detected in both the oxidized and reduced states were analyzed further for changes in oxidation with treatment by GILT. Xcalibur (Thermo) was used to display the extracted ion chromatograph (XIC) and integrate the area of the peak. Peak areas were used to calculate the percent oxidation by dividing the summed areas for all forms of a given peptide in its oxidized form by the summed areas for all forms of the peptide (both reduced and oxidized) to calculate the percent oxidation. Areas from peptides with miscleavages and those detected in multiple charge states were included in the areas. A comparison of the percent oxidation between GILT-positive and GILT-negative samples was then performed.

HLA class II Ag presentation assays

J3.DR4.vec, J3.DR4.GILT, DM-331.vec, and DM-331.GILT ($5x10^5$ cells/ml) were cultured at 37ºC in culture media in a 96-well plate (cat#3595, Corning Incorporated). Whole Igκ Ag (10μM) was added to the appropriate wells and incubated overnight. Cells were then washed and co-cultured with the $\kappa_{188-203}$ peptide specific T cell hybridoma (2.18a) for 24 hours. Following incubation, the plates were stored at -80ºC until tested for IL-2 production. Cells +/- GILT were also incubated with whole

IgGκ overnight at 37°C. Supernatants were collected by centrifugation, filtered with a 0.45 μM filter and incubated with J3.DR4.vec and DM-331.vec cells overnight. Supernatants obtained from GILT-expressing cells were also incubated in the presence of oxidized cysteine (290 μM), which were incubated with cells that were then fixed in 1% paraformaldehyde, washed and co-cultured with the $\kappa_{188\text{-}203}$ peptide specific T cell hybridoma (2.18a) for 24 hours. T cell production of IL-2 was measured by enzyme-linked immunosorbent assay (ELISA) according to the manufacturer's instructions (R&D Systems, Minneapolis, MN, USA) [101]. Anti-IL-2 was purchased from Sigma-Aldrich. All assays were repeated at least three times.

Statistical Analysis

Data from each experimental group were subjected to statistical analysis. ANOVA with post-hoc tests, Repeated Measures ANOVA with post-hoc tests, or Student's *t*-tests were used, as appropriate. Two-sided tests were used in all cases and *P* values <0.05 were considered statistically significant.

Results

GILT expression influences Ii and HLA-DM protein expression in human melanoma cells.

Studies performed in our laboratory and by others have shown that unlike many other cancers, melanoma cells express detectable levels of HLA class II Ag-presenting molecules [97]. Although having Ag presentation machinery, melanoma cells inefficiently process and present Ags to CD4+ T cells, resulting in their immune

avoidance. The reductive cleavage of protein Ags/peptides in acidic endolysosomal compartments is also required before antigenic components of the class II pathway, such as Ii and HLA-DM, can regulate epitope/peptide loading into the HLA class II binding groove [88, 98, 99]. Ii regulates HLA class II presentation while HLA-DM affects peptide loading onto class II molecules and presentation of stable class II-peptide complexes to T cells [92]. While melanoma cells express both Ii and HLA-DM, what remains unknown is the impact that enhanced processing of Ags by GILT will have on the T cell recognition of melanoma cells. To examine GILT's effect, it was first required to express GILT in multiple human melanoma cell lines as melanoma tumors lack or express low levels of GILT protein. Using vector/GILT cDNA and a lipofectamine transfection reagent [97], we successfully generated melanoma cell lines J3.vec, J3.GILT, DM-331.vec, and DM-331.GILT. Steady state GILT expression in transfected cells was confirmed by western blot analysis, seen in Figure 2.1.

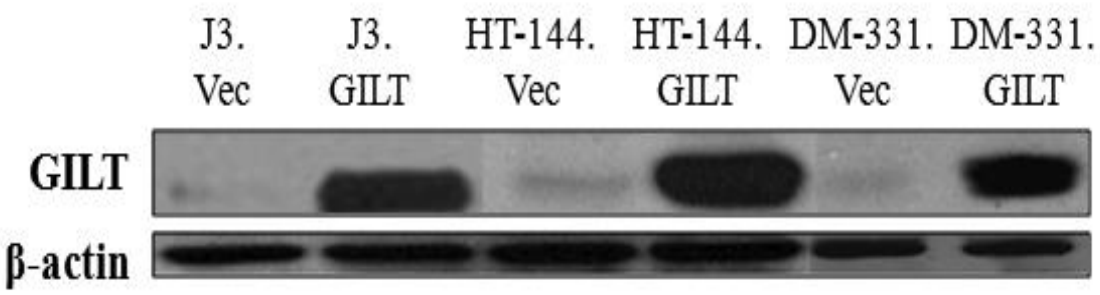

Figure 2.1. GILT insertion in human melanoma cells. Melanoma cells J3.DR4, HT-144, and DM-331 were cultured and transfected with GILT cDNA or empty vector using lipofectamine transfection assay. Cells were then cultured, lysed, and subjected to western blot analysis to test for GILT expression. Cell lines J3.DR4.GILT, HT-144.GILT, and DM-331.GILT show high levels of GILT protein while vector cell lines did not.

J3.vec and J3.GILT cells were further transfected with HLA-DR to generate J3.DR4.vec

and J3.DR4.GILT as described in the Materials and Methods section of this chapter. Following transfection, I first examined the expression of class II proteins by western blot analysis and flow cytometry. Expression of GILT in melanoma cells did not significantly alter intracellular class II proteins as determined by Figure 2.2. I next examined GILT's effect on Ii and HLA-DM protein expression by western blot analysis. GILT expression slightly upregulated Ii and DM proteins in two different melanoma cell lines (Figure 2.2), which may influence the loading of Ag peptides into the class II binding groove, an important step in Ag presentation and T cell recognition.

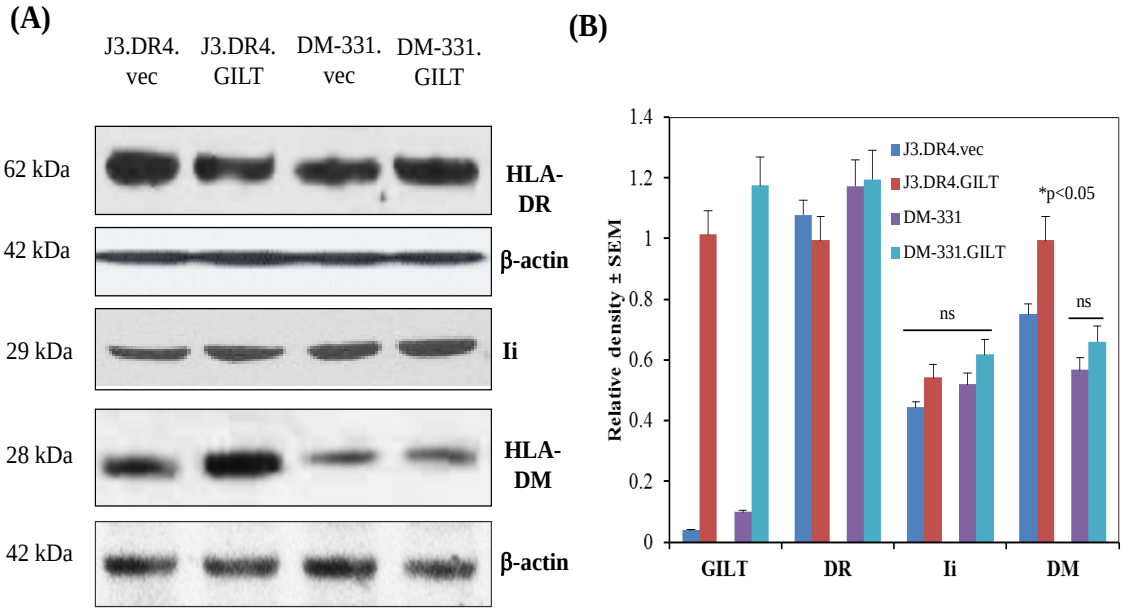

Figure 2.2 GILT insertion influences the expression of components involved in the class II pathway in human melanoma cells. (A) Western blot analysis of whole cell lysates from J3.DR4.vec, J3.DR4.GILT, DM-331.vec and DM-331.GILT cells showing protein expression of GILT, HLA-DR, Ii, and HLA-DM. β-actin was utilized as a loading control. (B) Densitometric analysis was performed using β-actin as a reference protein band to quantitate relative protein expression. Data are representative of at least three separate experiments. Significant differences were calculated by student's *t test; *p<0.05, ns=not significant.*

Flow cytometric analysis confirmed that GILT expression did not influence cell surface expression of class II proteins (MFI: 245.06 vs. 254.16 in J3.DR4.vec and J3.DR4.GILT;

MFI: 181.62 vs. 183.60 in DM-331.vec and DM-331.GILT) in melanoma cells (Figure 2.3). Flow cytometric analysis also confirmed that J3.DR4.vec and J3.DR4.GILT cells expressed cell surface DR4 molecules, and the expression levels were not significantly altered by GILT, Figure 2.4. These data suggest that GILT expression does not alter HLA class II proteins, but may influence other components of the class II pathway in melanoma cells, contributing to enhanced immune recognition of melanoma.

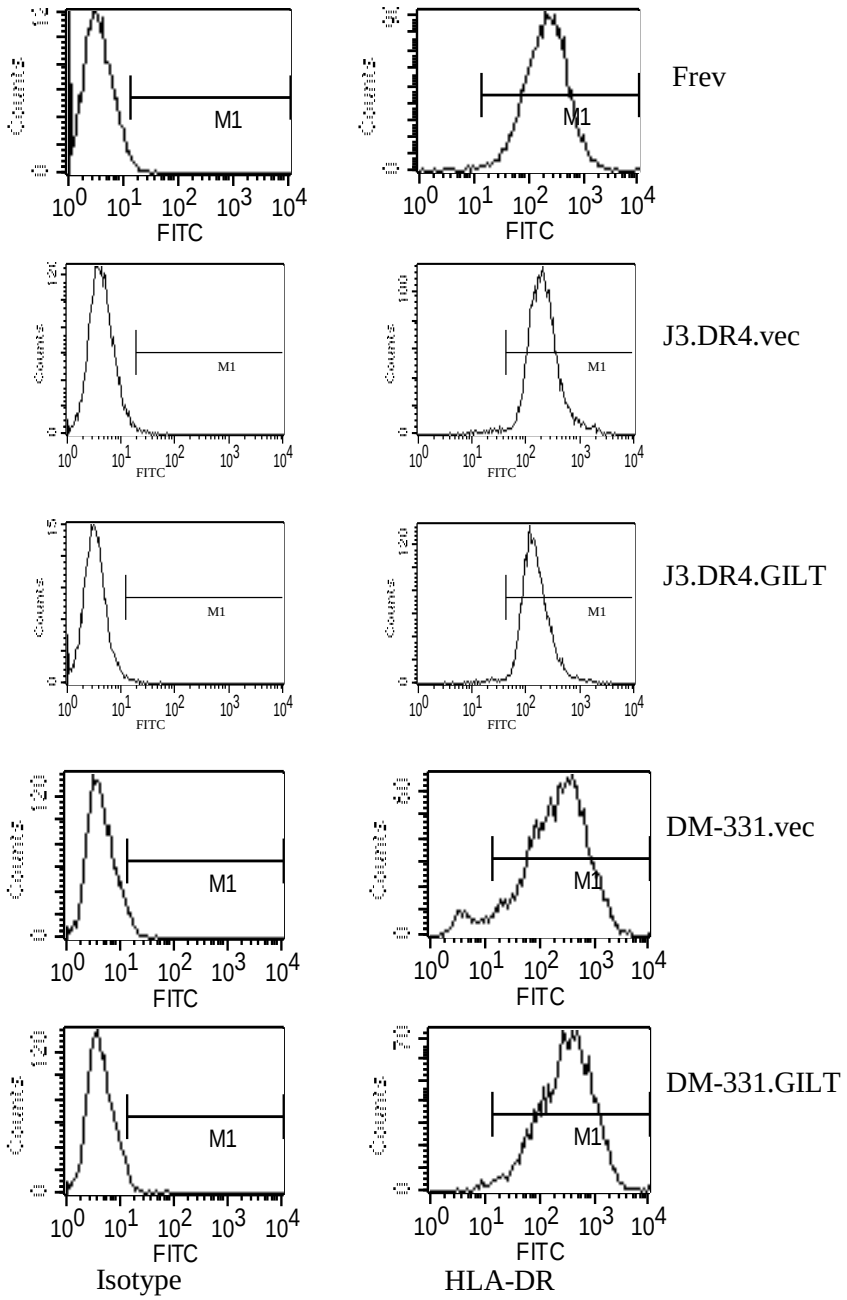

Figure 2.3 GILT expression did not alter cell surface HLA class II protein expression in melanoma cells. Flow cytometric analysis of HLA class II DR molecules. J3.DR4.vec, J3.DR4.GILT, DM-331.vec, and DM-331.GILT cells were stained with antibody against HLA-DR (mAb L243) for cell surface expression of HLA-DR molecules. NN4 was used as an isotype control. The B-cell line Frev which constitutively express HLA-DR molecules was used as a positive control. Data are representative of three separate experiments.

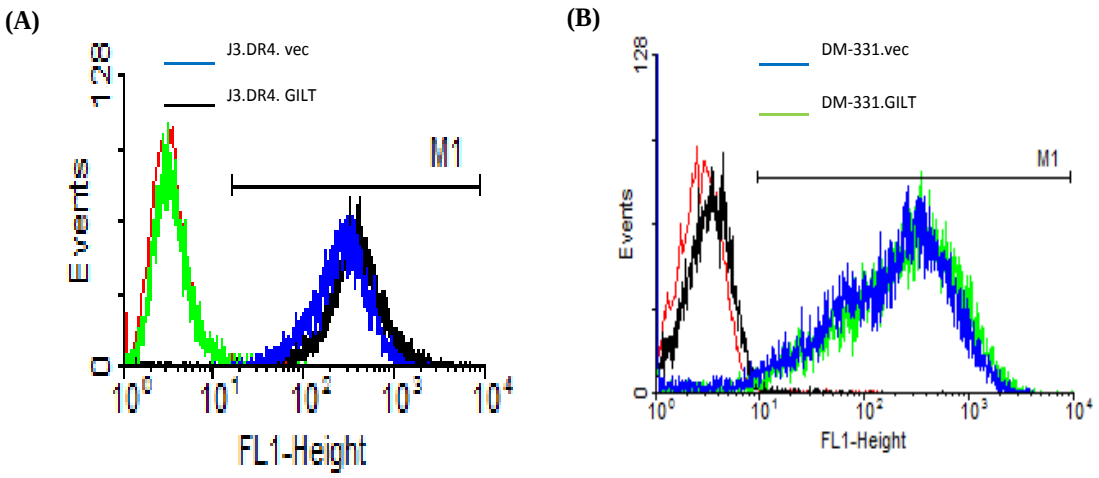

Figure 2.4 GILT expression did not alter cell surface HLA-DR4 expression in melanoma cells. Flow cytometric analysis of HLA class II DR4 molecules. J3.DR4.vec, J3.DR4.GILT, DM-331.vec, and DM-331.GILT cells were stained with antibody against HLA-DR4 (359-F10) for cell surface expression of HLA-DR4 molecules. IN-1 antibody was used as an isotype control. Data are representative of three separate experiments.

GILT expression upregulates intracellular CD80/CD86 molecules in melanoma cells.

A contributing component to the lack of optimal CD4+ T cell activation is the absence or low levels of CD80 and CD86 molecules on melanoma cells [141]. A central goal of improved melanoma immunotherapeutic design is an enhanced immune response that includes the activation of both the cytotoxic CD8+ T cells and the supportive CD4+ helper T cells. Along with Ag presentation by HLA class II molecules on the surface of melanoma cells, the secondary signal received by T cells plays a key role in enhancing and prolonging the activation of CD4+ T cells. The secondary signal may come from the interaction between CD86 and CD28 molecules as melanoma cells do not express detectable CD40 molecules [142, 143]. However, the majority of human melanoma cells do not express detectable cell surface CD80/CD86 molecules, and thus, they may not provide sufficient costimulatory signals for T cell recognition. The expression of CD86

may be turned on and/or enhanced through IFN-γ stimulation following signaling via the JAK/STAT pathway, particularly through STAT1. Given GILT's IFN-γ inducible nature, our laboratory has demonstrated that GILT is indeed regulated by STAT1 [109]. J3.DR4.vec and J3.DR4.GILT melanoma cells were stained with anti-CD80, anti-CD86, and fluorescence-labeled secondary antibody and analyzed by confocal microscopy. These data suggest that GILT expression slight elevates CD80 while it markedly upregulates CD86 in J3.DR4.GILT cells, seen in Figure 2.5.

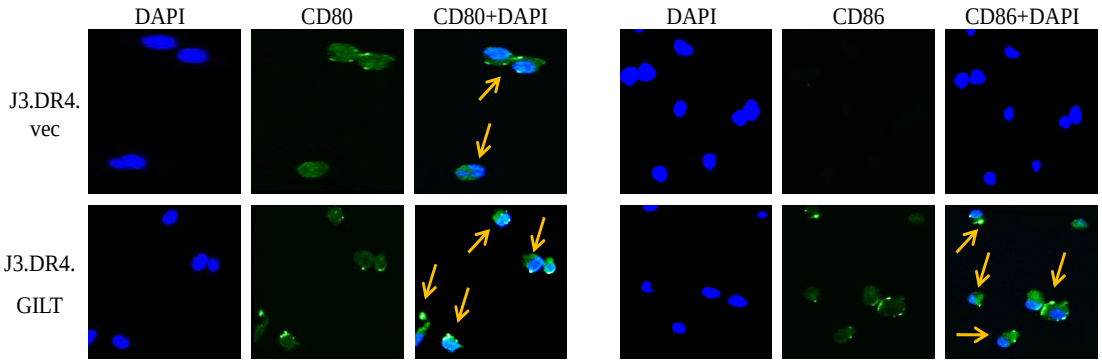

Figure 2.5 GILT-positive cells express higher levels of costimulatory molecules CD80 and CD86. J3.DR4 cells transfected with empty vector or GILT were simultaneously stained with primary antibodies against CD80 and CD86 proteins, followed by Alexa488-labeled secondary antibody as described in the methods. Slides were analyzed by Leica TCS SP5 confocal laser scanning microscope using Las-AF software. Representative confocal microscopy images of J3.DR4.vec and J3.DR4.GILT cells indicate increased levels of CD80 and CD86 expression (green) with nuclear staining DAPI (blue), overlapped (arrows) in the right hand corners.

This upregulation of costimulatory molecules could promote T cell activation in melanoma cells [144]. To examine further, J3.DR4.vec and J3.DR4.GILT cells were stained with fluorescence-labeled anti-CD80/CD86 antibodies and analyzed by flow cytometry. A slight increase in cell surface expression of CD80 and CD86 molecules was observed, Figure 2.6.

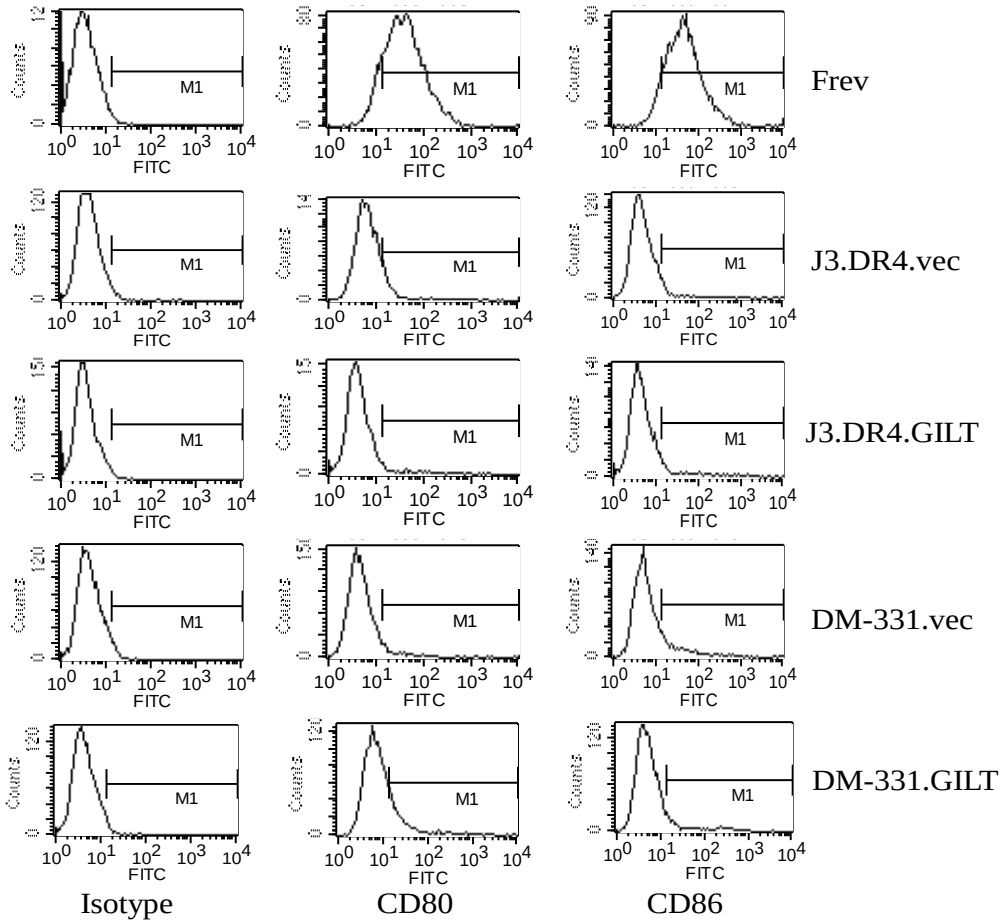

Figure 2.6 GILT expression minimally alters cell surface expression of costimulatory molecules CD80 and CD86, but significantly elevates intracellular CD80/CD86 in melanoma cells. Flow cytometyric analysis of cell surface CD80 and CD86 molecules. J3.DR4.vec, J3.DR4.GILT, DM-331.vec, and DM-331.GILT cells were stained with CD80-FITC and CD86-FITC, and a rabbit IgG isotype control. Cells were then analyzed by flow cytometry for cell surface expression of CD80 and CD86 molecules. The B-cell line, Frev which constitutively express CD80 and CD86 molecules was used as a positive control. Data are representative of at least three separate experiments.

However, further studies failed to detect a significant change in cell surface CD80/CD86 molecules in additional melanoma lines (data not shown). This change in CD80/CD86 expression could result from a variation of cell types. Interestingly, GILT

expression significantly elevated intracellular CD80 and CD86 protein expression as determined by western blot analysis (Figure 2.7), supporting my immunofluorescence data (Figure 2.5). This indicates that GILT may play a role in the alteration of CD80/CD86 molecules in melanoma cells.

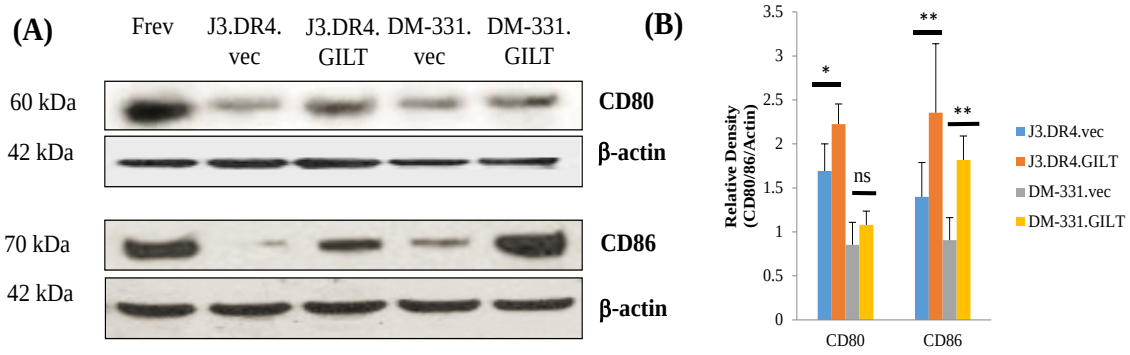

Figure 2.7 GILT-positive cells express higher levels of intracellular CD80 and CD86 protein expression. (A) Western blot analysis of CD80 and CD86 molecules. Frev, J3.DR4.vec and J3.DR4.GILT, DM-331.vec, and DM-331.GILT cells were subjected to western blotting for CD80 and CD86 molecules. β-actin was utilized as a loading control. (B) Densitometric analysis was performed using β-actin as a reference protein band to quantitate relative protein expression. Data are representative of at least three separate experiments. Significant differences were calculated by student's *t test; *p<0.05, **p<0.01, ns=not significant.*

GILT colocalizes with acidic cathepsins B and D in melanoma cells.

The importance of acidic cathepsins in class II Ag processing and presentation cannot be overstated. Cysteinyl and aspartyl cathepsins are responsible for the processing of self-Ags into smaller peptides for presentation to CD4+ T cells. Our laboratory has previously shown that GILT expression upregulates active forms of cathepsins [97, 139, 140], which may help processing of Ags/peptides for class II presentation. GILT expression in melanoma cells may thus enhance the reductive cleavage of self-Ags, allowing protein unfolding. These partially processed polypeptides are very susceptible to degradation by acidic cathepsins. Without reductase/cathepsin

activity, endogenous and exogenous Ags cannot be efficiently processed into functional epitopes for class II loading, an adaptation used by melanoma cells to avoid immune detection. Whether GILT is playing a direct role in governing this increase in cathepsin protein expression or activity remains unknown. Therefore, J3.DR4.GILT cells were cultured and analyzed through confocal microscopy to assess the localization of cathepsins and GILT when co-expressed in melanoma cells. Cells were stained with either rabbit anti-CatB or CatD, and co-stained with goat anti-GILT antibodies, followed by rhodamine-conjugated anti-rabbit IgG and FITC-conjugated anti-goat IgG antibodies. Live images were acquired using a Leica TCS SP2 AOBS confocal system and processed with Leica software. In Figure 2.8, overlayed images from J3.DR4.GILT cells indicate that GILT colocalizes with acidic cathepsins in endolysosomal compartments of melanoma cells. This may imply a possible protein-protein interaction which could govern the increase in cathepsin expression and activity.

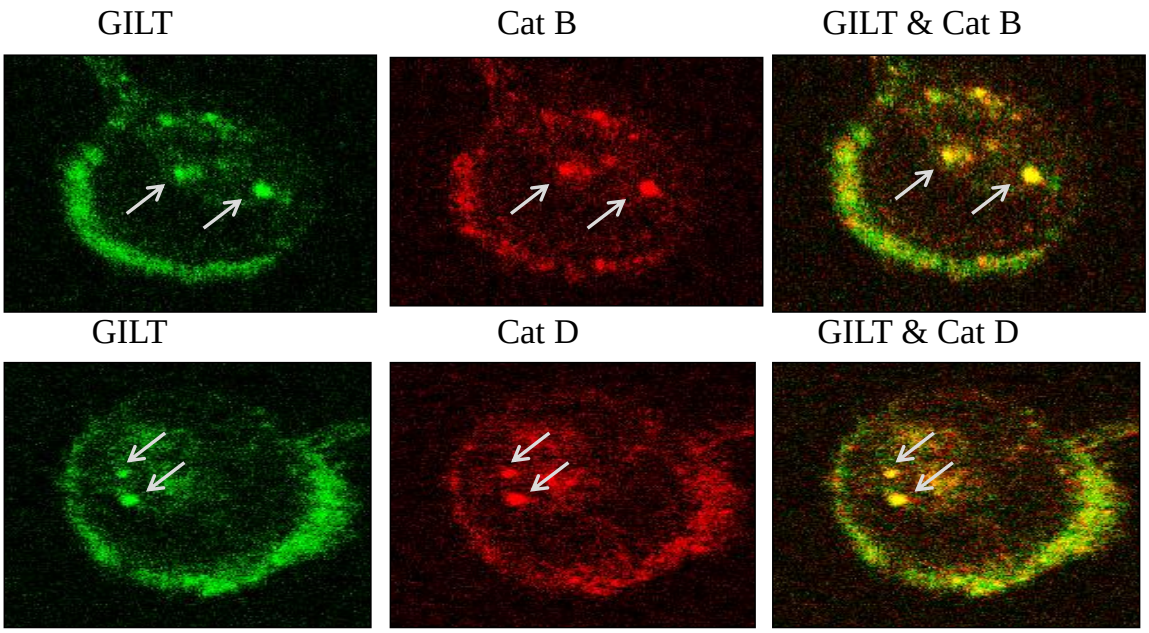

Figure 2.8 GILT colocalizes with cysteinyl and aspartyl cathepsins and enhances their expressions in human melanoma cells. J3.DR4.GILT cells were stained with either rabbit anti-CatB or CatD, and co-stained with goat anti-GILT, followed by rhodamine-conjugated anti-rabbit IgG and FITC-conjugated anti-goat IgG antibodies. Live images were acquired by using a Leica TCS SP2 AOBS confocal system and processed with Leica software. Colocalization of GILT (green) with CatB (upper panel) and CatD (lower panel) is indicated by yellow staining and arrows.

GILT expression enhances the activity of cysteinyl cathepsins B/S and aspartyl cathepsin D in melanoma cells.

Due to the colocalization of GILT with acidic cathepsins, I further investigated whether GILT influences cathepsin activity in human melanoma cells. While cysteinyl Cat B processes Ags, Cat S degrades Ii into smaller intermediate peptides with the end result being the class II-associated Ii peptide (CLIP) [92, 95, 145, 146]. Without this critical reaction, the removal and degradation of Ii would not occur, which effectively blocks peptide loading onto HLA class II molecules. Thus, I first examined the activity of cysteinyl cathepsin B in J3.DR4.vec, J3.DR4.GILT, DM-331.vec, and DM-331.GILT cells. Interestingly, Cat B activity was significantly increased (J3.DR4.vec=3,873 vs.

J3.DR4.GILT=4,499.3, $p \leq 0.05$; DM-331.vec=1520.67 vs. DM-331.GILT=4272, $p \leq 0.01$) in two different melanoma cell lines transfected with GILT (Figure 2.9). Similarly, Cat S activity was significantly increased in GILT-transfected J3.DR4.GILT (12,348 vs. 7730, $p \leq 0.01$) and DM-331.GILT (7,477 vs. 6521, $p \leq 0.05$) cells (Figure 2.9). However, there were no significant changes in Cat L activity in DM-331.vec, and DM-331.GILT cells, rather Cat L activity was relatively lower in J3.DR4.GILT cells when compared to J3.DR4.vec cells (data not shown). It remains unclear why GILT had an alternative effect on Cat L, although both Cat S and Cat L can process Ii, facilitating HLA class II maturation [97]. Altogether, these results suggest that GILT expression enhances the activity of cysteinyl cathepsins B and S in human melanoma cells. This increase in protease activity in J3.DR4.GILT and DM-331.GILT cells may help generate a greater pool of functional epitopes, contributing to enhanced Ag presentation.

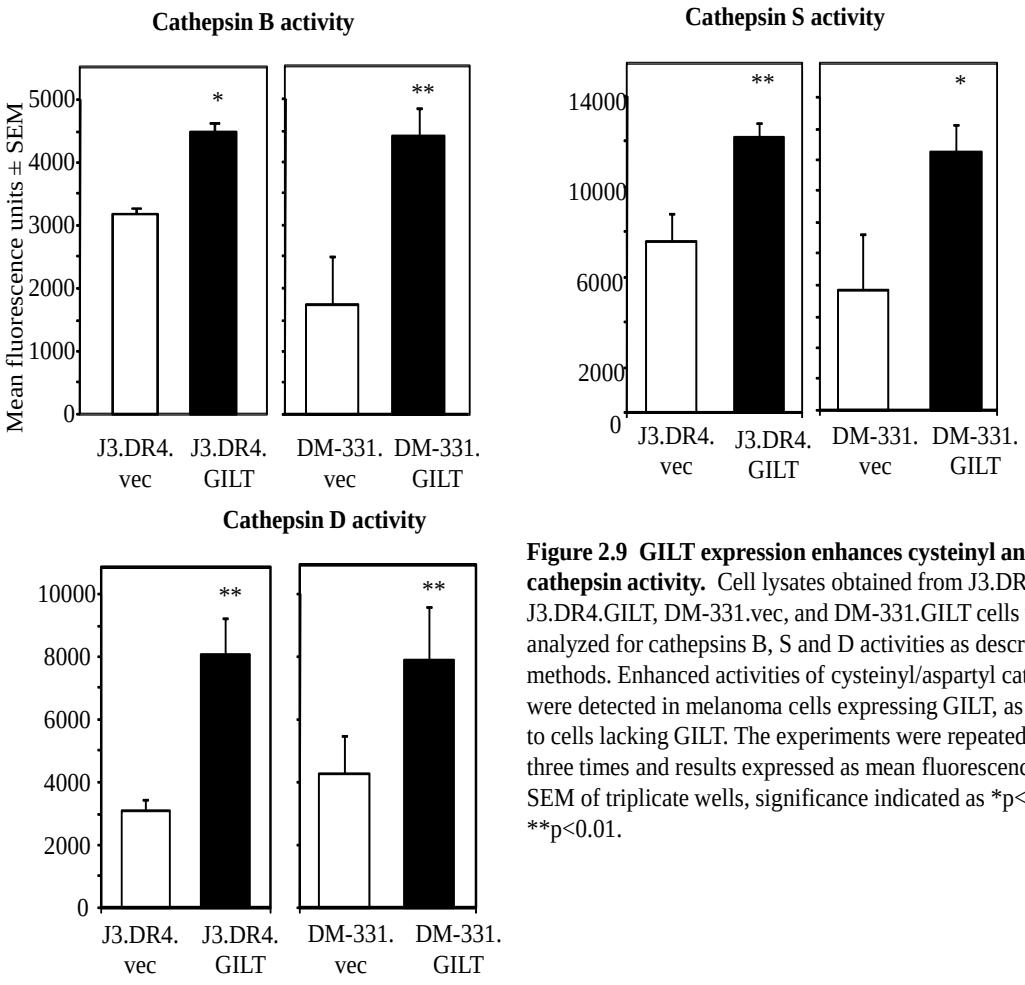

Figure 2.9 GILT expression enhances cysteinyl and aspartyl cathepsin activity. Cell lysates obtained from J3.DR4.vec, J3.DR4.GILT, DM-331.vec, and DM-331.GILT cells were analyzed for cathepsins B, S and D activities as described in the methods. Enhanced activities of cysteinyl/aspartyl cathepsins were detected in melanoma cells expressing GILT, as compared to cells lacking GILT. The experiments were repeated at least three times and results expressed as mean fluorescence unit ± SEM of triplicate wells, significance indicated as *$p<0.05$, **$p<0.01$.

Cathepsin D is an integral acidic protease involved in Ag processing and exhibits site-specific cleavage and splicing of Ags, which is important for short peptide loading onto HLA class II molecules [95, 96]. An increase in cathepsin D expression and activity would aid melanoma cells in enhanced Ag processing and presentation of class II-peptide complexes to CD4+ T cells. Thus, I performed cathepsin D activity assays, and I demonstrated that GILT expression upregulated cathepsin B enzymatic activity in two unique melanoma cell lines (Figure 2.9), suggesting that GILT expression may be able to generate more functional peptides for class II presentation and CD4+ T cell recognition.

These findings also suggest that GILT expression enhances select cysteinyl and aspartyl cathepsin enzymatic activity in melanoma cells, which would allow for an improved processing and generation of melanoma Ags for HLA class II presentation.

Mass spectroscopy and fragmentation of cysteinylated versus reduced Igκ$_{188\text{-}203}$ peptides.

Because GILT expression enhances cathepsins' activity, I next sought to examine whether GILT-positive melanoma cells generate a greater pool of functional peptides as compared to GILT-negative cells. Melanoma cells J3.DR4.vec and J3.DR4.GILT were incubated with whole Ag IgG for 6 hours in HBSS and supernatants were collected and subjected to LC-MS mass analysis to search for functional (reduced) κ188-203 peptide. A greater pool of reduced IgGκ188-203 peptide was present in J3.DR4.GILT cells as compared to J3.DR4.vec cells, confirming GILT's ability to functionally reduce antigenic peptides needed for T cell recognition, shown in Figure 2.10. Mass spectroscopic analysis also suggested that J3.DR4.GILT cells produced a greater pool of peptides as compared to J3.DR4.vec cells (Figure 2.10).

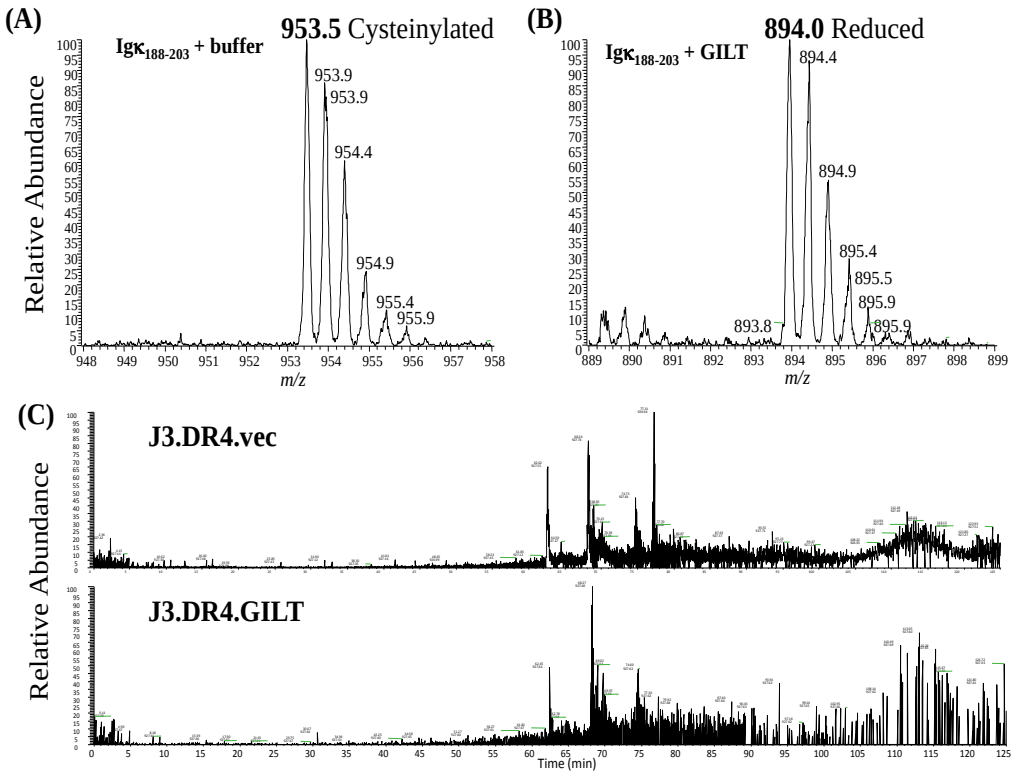

Figure 2.10 Mass spectroscopy and fragmentation of cysteinylated versus reduced Igκ$_{188-203}$ peptides. (A) Cysteinylation of the κ$_{188-203}$ peptide was determined by the detection of ionized species at 954 m/z. (B) GILT catalyzed the reduction of cysteinylated-κ$_{188-203}$ as ionized species at 894 detected. (C) Extracted ion chromatograph of peptides generated by J3.DR4 and J3.DR4.GILT cells. LC-MS mass spectrometry was performed on supernatant obtained from J3.DR4 and J3.DR4.GILT cells fed with IgG. Data suggest that J3.DR4.GILT cells generated a greater pool of reduced peptides.

Further analyses by LC-MS showed that a greater pool of oxidized peptides (77.9% vs. 40.7%) was generated by cells lacking GILT, when a cysteine-containing peptide was analyzed (Figure 2.11). Interestingly, no major alterations were observed when a non-cysteine-containing peptide was analyzed (Figure 2.12).

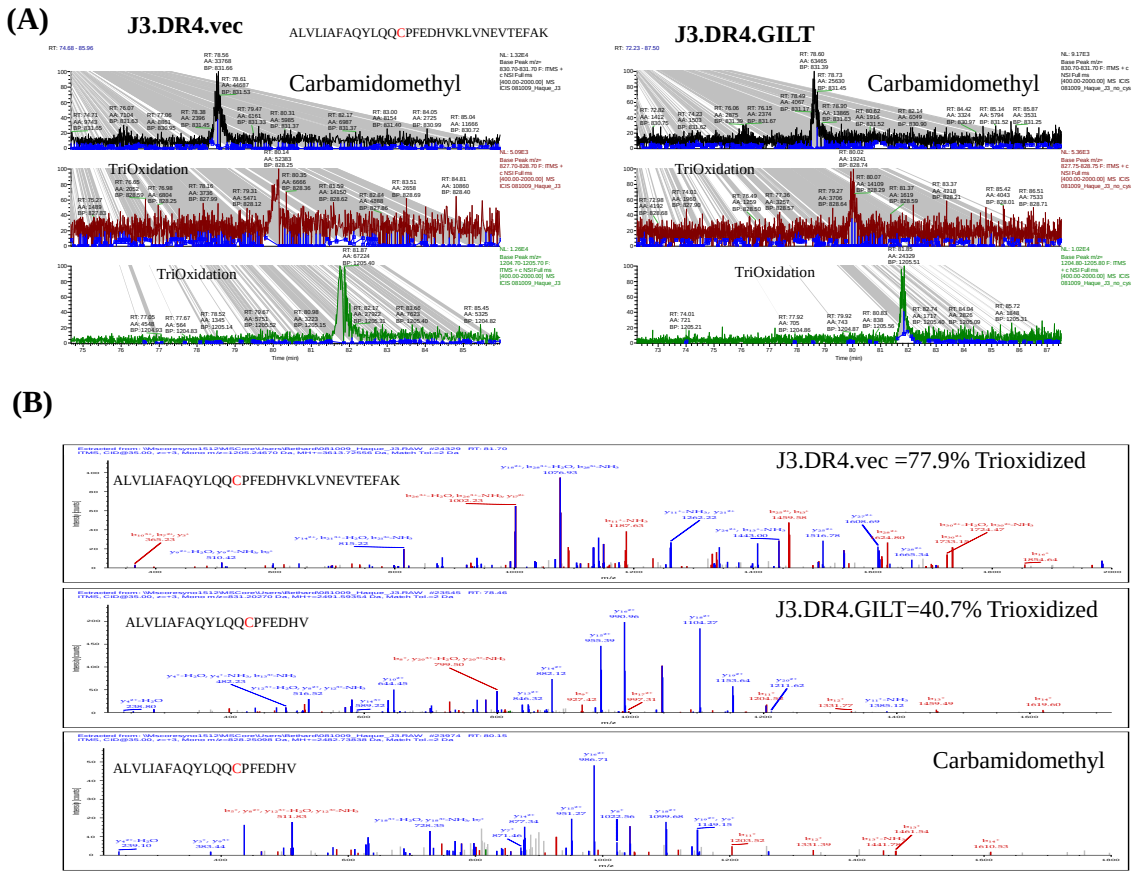

Figure 2.11 Percent occupation of cysteine oxidation in supernatants obtained from cells with or without GILT. (A) J3.DR4 and J3.DR4.GILT cells were fed with IgG in serum free HBSS for 4h. Supernatants were collected by centrifugation and analyzed by mass spectroscopy as described in the methods. Extracted Ion Chromatograph (XIC) of the peptide ALVLIAFAQYLQQCPFEDHVK identified in supernatants obtained from cells±GILT. 831.66 is the mass of the +3 charge state for the peptide ALVLIAFAQYLQQCPFEDHVK with the cysteine chemically modified by iodoacetamide (+57). 828.25 is the +3 charge state of ALVLIAFAQYLQQCPFEDHVK which contains a tri-oxidized cysteine. 1205.4 is +3 charge state of the peptide ALVLIAFAQYLQQCPFEDHVKLVNEVTEFAK which contains a tri-oxidized cysteine and 1 trypsin missed cleavage. The percent occupation of oxidation was calculated using the area under the curve from the XIC (the total area of the oxidized peptides divided by the total area of the peptide × 100). Cells expressing GILT had a 40.7% tri-oxidized cysteine while cells lacking GILT had a significantly higher level of oxidation with 77.9% of the peptide being tri-oxidized. (B) Tandem MS spectra (MS/MS) of the reduced and oxidized forms of the peptides ALVLIAFAQYLQQCPFEDHVK and ALVLIAFAQYLQQCPFEDHVKLVNEVTEFAK, with the cysteine detected as either carbamidomethylated or tri-oxidized. The top spectra identified ALVLIAFAQYLQQCPFEDHVKLVNEVTEFAK with the cysteine tri-oxidized with an Xcorr value of 5.39. The site of oxidiation was confirmed by the presence of the b14 ions 1610.8 (+1) and 805.9 (+2)) and the y18 ion 805.9(+2). The middle tandem MS spectrum was identified as ALVLIAFAQYLQQCPFEDHVK with a trioxidized cysteine and an Xcorr value of 3.36. The site of oxidation was confirmed by the presence of the b14 ions 1610.8(+1) and 805.9(+2) and the y8 ions 1022 (+1) and 511.7(+2). The bottom MS/MS spectra was identified with an Xcorr of 4.78 as the peptide ALVLIAFAQYLQQCPFEDHVK, with the cysteine carbamidomethylated. The modification was localized by the presence of the b14 ions 1619(+1) and 810(+2) and the y8 ion 516(+2).

GILT transfected melanoma cells produce more functional epitopes for HLA class II-mediated presentation to CD4+ T cells.

Since GILT expression enhanced both aspartyl and cysteinyl cathepsin activity in melanoma cells, it was pertinent to investigate whether GILT expression in melanoma cells could generate more functional peptides for HLA class II presentation and T cell recognition. J3.DR4.vec and J3.DR4.GILT cells were incubated overnight with the whole IgGκ in HBSS. Cell supernatants were collected, filtered by a 0.45μM filter, and analyzed by mass spectrometry. Data obtained showed an increase in the generation of the peptide pool in GILT expressing melanoma cells (~2x more peptide in J3.DR4.GILT cells, based on Peak area analyzed), and that more oxidized peptides were found in the supernatant of melanoma cells lacking GILT (Figure 2.12). These data suggest that GILT expression may help produce more functional peptides for presentation via the class II pathway.

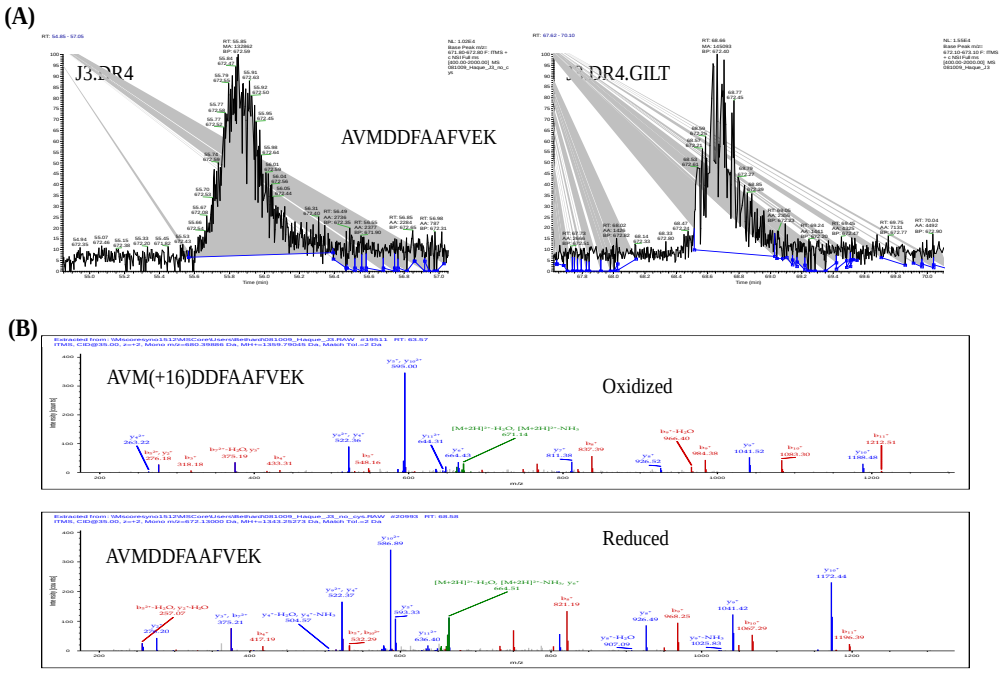

Figure 2.12 Percent occupation of methionine oxidation in supernatants obtained from cells with or without GILT. Cells (J3.DR4 and J3.DR4.GILT) were fed with IgG in serum free HBSS for 4h. Supernatants obtained were analyzed by mass spectroscopy. (A) Extracted ion Chromatograph (XIC) of the peptide AVMDDFAAFVEK identified in cell supernatants obtained from J3.DR4 and J3.DR4.GILT cell. 672.5 was identified as the reduced form of peptide AVMDDFAAFVEK, and determined to be the +2 charge state. The oxidized form of this peptide, 680.5 (+2 charge state) was below the quantitation limit as a peak was unable to be extracted to calculate the area. Based on the areas of the unoxidized form of this peptide, there is no significant change in oxidation of methionines in J3.DR4.GILT supernatant. (B) Tandem MS spectra (MS/MS) of the reduced (672.1) and oxidized (680.1) forms of the peptide AVMDDFAAFVEK. The top spectra represent the oxidized form of the peptide AVMDDFAAFVEK. This peptide was identified with an Xcorc value of 3.15. Localization of the oxidized amino acid was determined by the presence of the b3 ion at 318.3 and the y10 ions at 1188.5 (+1) and 594.7 (+2). The bottom spectrum was identified as the reduced peptide AVMDDFAAFVEK with an Xcorr of 3.53.

GILT expression enhances HLA class II-mediated Ag processing and presentation.

We have previously reported that GILT expression restores CD4+ T cell recognition of human melanoma cells [101]. In an effort to further understand the role of GILT in melanoma, melanoma cell lines J3.DR4.vec, J3.DR4.GILT, DM-331.vec, and DM-331.GILT were incubated with the whole Igκ Ag overnight under the same medium conditions. After incubation, cells were washed and co-cultured with the T cell hybridoma line 2.18a, which recognizes $Ig\kappa_{188\text{-}203}$ epitope, for 24 hours. Cell supernatants were stored, and the T cell production of IL-2 was quantitated by ELISA.

Analysis of functional Ag presentation showed that GILT expression enhanced CD4+ T cell recognition of melanoma cells, shown in Figure 2.13. This data supports the notion that increased cathepsins' enzymatic activity in GILT-expressing melanoma cells might have induced enhanced Ag processing and presentation capability as well as T cell responses in melanoma cells.

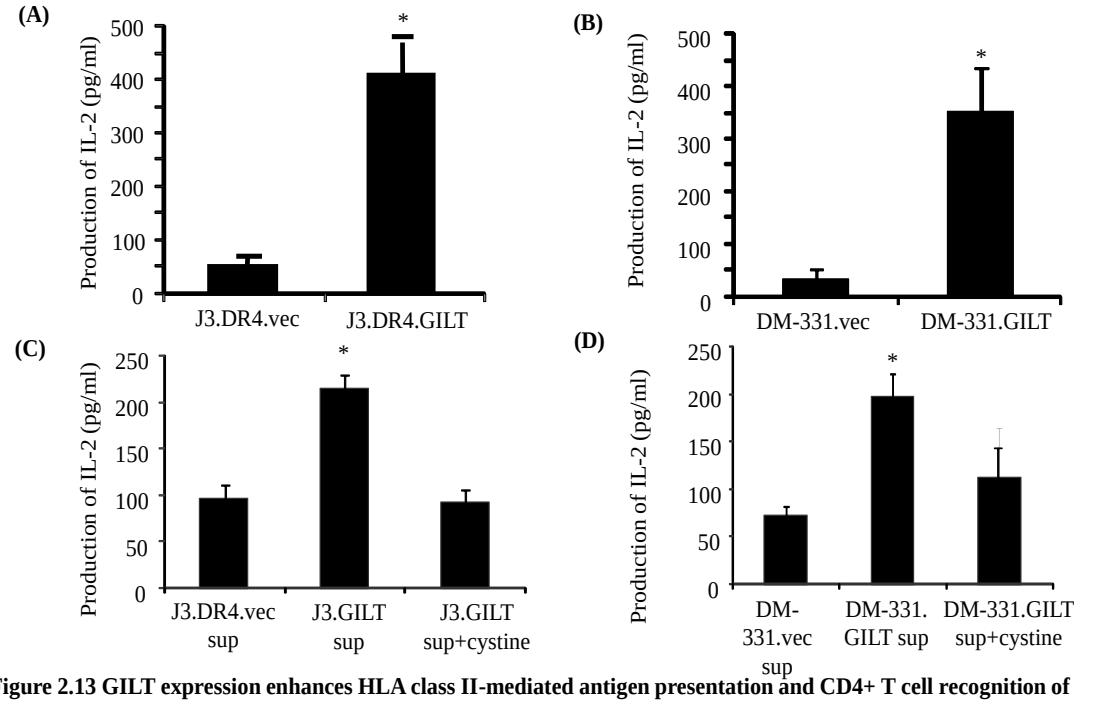

Figure 2.13 GILT expression enhances HLA class II-mediated antigen presentation and CD4+ T cell recognition of tumors by producing a greater pool of functional epitopes. (A-B) Human melanoma cell lines J3.DR4.vec, J3.DR4.GILT, DM-311.vec, and DM-311.GILT were incubated with whole Igκ Ag overnight at 37ºC. Cells were then washed, and co-cultured with the $\kappa_{188-203}$ peptide specific CD4+ T cell hybridoma line (2.18a) for 24 h. T cell production of IL-2 in the culture supernatant was measured by ELISA. The production of IL-2 is used as an indication of Ag presentation and T cell recognition. Data are expressed as mean pg/ml +/- SD of triplicate wells of at least three independent experiments. *$p<0.01$. (C-D) Melanoma cells J3.DR4.vec, J3.DR4.GILT, DM-331.vec, and DM-331.GILT were incubated overnight with whole Igκ Ag in HBSS at 37ºC. Cell supernatants were transferred to paraformaldehyde fixed J3.DR4.vec (C) and DM-331.vec (D) cells for overnight at 37ºC. Supernatants from GILT-expressing cells were also incubated with L-cystine (290 μM) as described. Cells were then washed and co-cultured with the $\kappa_{188-203}$ peptide specific CD4+ T cell hybridoma 2.18a for 24h. T cell production of IL-2 was quantitated by ELISA. Data are representative of at least three separate experiments.*$p<0.001$.

Tumor cells either lack GILT or express low levels of this protein, helping them evade immune recognition. In this chapter, I have found that cells incubated with cysteine-containing Ag were poor presenters of epitopes to T cells, and GILT expression

helped or enhanced T cell recognition. To investigate if GILT-expressing cells are better targets for T cells, cells +/- GILT were incubated with IgG in HBSS, and supernatants collected were tested on J3.DR4.vec and DM-331.vec for their ability to stimulate CD4+ T cells as previously described in the Materials and Methods. Cells were fixed with 1% paraformaldehyde to prevent internalization and processing of Ags, washed, and co-cultured with the peptide-specific T cell hybridoma 2.18a. J3.DR4.vec cells incubated with supernatant obtained from IgG-fed J3.DR4.vec cells did not optimally stimulate T cells. By contrast, J3.DR4.vec cells incubated with supernatant obtained from IgG-fed J3.DR4.GILT cells optimally stimulated T cells. Addition of oxidized cystine in the J3.DR4.GILT-supernatant significantly downregulated epitope presentation by J3.DR4.vec cells to T cells (Figure 2.13), indicating that GILT expression in tumors may drastically become better targets for CD4+ T cells, and cysteinylation blocks T cell recognition via the class II pathway. These data also suggest that epitopes generated by GILT-expressing cells are presented by GILT-negative cells in the context of HLA class II molecules.

Discussion & Conclusions

An important characteristic in the immune evasion of melanoma tumors is the alteration of tumor Ag presentation or interruption in the HLA class II Ag presentation pathway. Restoring the HLA Class II presentation pathway in melanoma cells has been shown to support tumor destruction [97, 101]. However, melanoma cells lack an important enzyme, GILT, perturbing epitope presentation via the HLA Class II

machinery. Therefore, investigation of the role of GILT in the epitope generation for the class II pathway and its involvement in stimulating CD4+ T cell recognition is essential in the development of improved immunotherapeutic strategies.

In this study, we have shown that GILT enhances multiple components of the HLA class II pathway, such as Ii and HLA-DM. Expression of Ii is important for stabilizing HLA class II molecules by effectively forming a trimer within the endoplasmic reticulum, thus regulating HLA class II presentation [147-149]. HLA-DM acts as a peptide editor upon the class II DR complex to determine if the correct epitope binds to the binding groove [150, 151]. Thus, DM can accelerate the reaction from unstable to stable class II: peptide complex for immune recognition [97]. GILT expression also enhanced intracellular expression of CD80/CD86, but this was not translated on the cell surface. An increase in intracellular CD80/CD86 does correlate with the expression on the cell surface [152]. However, this upregulation of costimulatory molecules by GILT could lead to a reduction in T cell tolerance [153] and immune avoidance by melanoma cells.

Professional APCs express high levels of GILT which is crucial for Ag processing and presentation to CD4+ T cells. However, melanoma and other tumors, express low to no detectable levels of GILT which could be correlated to the tumor cells' inability to display a broad repertoire of functional class II-peptide complexes on their cell surface to T cells [111].

Professional APCs possess all the machinery to optimally processes and present Ags to T cells while malignant tumor cells lack some of the processing machinery needed

to generate a large repertoire of functional HLA peptide complexes necessary for a robust CD4+ T cell response [97, 101, 102].By further understanding the steps and factors involved in Ag processing reactions, new potential targets for immunotherapy may emerge. This study suggests that GILT expression in melanoma cells enhances HLA class II Ag processing. GILT expression also enhances the enzymatic activity of cathepsins B, S, and D, which correlates with our previous finding that GILT causes an increased expression of active forms of cysteinyl and aspartyl cathepsins [97]. Intracellular proteases such as cysteinyl cathepsins B and S are essential for degradation of endogenous and exogenous Ags, and each serves an important role in the processing of peptides for presentation via HLA class II molecules. Aspartyl cathepsin D activity was significantly upregulated, which may contribute to the enhanced processing of self-Ags/peptides. This suggests that Ags, both endogenous and exogenous, may be readily processed by GILT-expressing tumor cells, which could allow for more functional epitopes available for presentation via the class II pathway [154]. The final event would then end with an increase in immune recognition and a stronger anti-tumor immune response. Since melanoma express their own tumor Ags such as NY-ES0-1, gp100, and tyrosinase [155-157], the increase in enzymatic activity by GILT-expressing melanoma cells could be exploited for the induction of tumor Ag-specific T cells. Further understanding GILT's role in Ag processing and presentation in melanoma may lead to the development of new and more effective immunotherapeutics against metastatic melanoma.

The presence of GILT influences several key components of the class II pathway in melanoma. It enhances the expression of the cathepsins and increases Ag processing and presentation, leading to increased stimulation of CD4+ T cells. Other studies have shown that GILT is important in the development of the overall T cell response to protein Ags that contain disulfide bonds [97, 101, 103]. With the combination of GILT-facilitated reduction as well as proteolysis in the endosomal/lysosomal compartments in melanoma cells, it is safe to assume that the generation of class II epitopes would be enhanced, but this had never been tested. We present evidence that the pool of Ag peptides/epitopes generated by the presence of GILT have increased functionality, illustrating GILT's ability to reduce oxidized or cysteinylated peptides to a more functional form. This is also supported by the observed increase in GILT/cathepsins. The presence of GILT produced more functional epitopes from whole Igκ, which then was able to increase CD4+ T cell recognition and IL-2 production. This action was inhibited when supernatant was incubated with the presence of cystine, which suggests that cysteinylation inhibits peptide presentation and GILT expression may overcome inefficient processing of self-Ags/peptides. Data presented here suggests that epitopes generated by GILT-expressing cells are better recognized by CD4+ T cells than those of GILT-negative cells. Enhancing the presentation of known melanoma Ags by GILT-expressing cells could be exploited through the whole cell vaccine immunotherapy strategy. Allowing the generation of *in vitro* T cells with specific Ags expressed by melanoma cells would also exploit immunological memory against reoccurring malignant cells.

Chapter 3: GILT expression negatively regulates PAX3 in human melanoma cells.

PAX3 and its Role in Melanoma Pathogenesis

Because of the aggressive nature and the immune avoidance by melanoma, current research has focused on factors that amplify advanced disease. Recent studies suggest that melanoma cells revert to an embryonic program of gene expression involved in neural crest cell migration to support developmental plasticity and metastasis [158]. This includes studying molecules involved in melanocyte generation and differentiation. One such factor that has been found in late stage melanomas is a transcription factor called paired box 3 (PAX3). PAX3 is a transcriptional regulator involved in melanocyte development as well as myogenesis and the development of the central nervous system [159, 160]. PAX3 contains four domains: the paired domain, the homeodomain, the octapeptide, and the transactivation domain. The paired domain facilitates protein-protein interactions and DNA binding [72]. The homeodomain functions in regulating the DNA binding ability of the paired domain [161, 162]. The octapeptide acts as a protein-interaction epitope while the transactivation domain mediates PAX3-DNA interactions [161]. During embryonic development, neural crest cells express PAX3 while they develop into melanoblasts and migrate to the epidermis. Here, melanoblasts differentiate into melanocytes, and PAX3 is a key component in the migration and proliferation of these cells [163]. PAX3 is also expressed in melanocyte stem cells, where it represses terminal differentiation, retains the ability to enter the cell cycle, and inhibits apoptosis [164-167]. Mutations in PAX3 result in Waardenburg syndrome which includes abnormalities of the nervous system, eyes, nose, and pigmentation defects affecting skin, hair, and otic pigment cells [168, 169]. Many mutations within PAX3 can result in

Waardenburg syndrome, but most mutations occur in the paired domain [170]. PAX3 expression has also been found in medulloblastoma, benign peripheral glial tumor neurofibroma, Erwin's sarcoma, supratentorial primitive neuroectodermal tumor, gastric cancer, and pediatric alveolar rhabdomyosarcoma [171].

When neural crest cells develop into melanoblasts and then melanocytes, PAX3 is translocated to the nucleus via Importin13, and forms a complex with Sry-like HMG box 10 (SOX10) to activate Microphthalmia transcription factor (MITF) [172-174]. MITF is crucial for melanoblast survival during and immediately following migration from the dorsal neural tube to the migration staging area [160]. PAX3, SOX10, and MITF determine the balance between melanocyte differentiation and maintenance of melanoblast and melanocyte stem cells, which is Wnt-dependent [164, 175]. However, once a threshold of PAX3 expression is achieved, PAX3 is downregulated, and later phases of terminal differentiation continue [165]. MITF then signals to melanin synthesis proteins Tyrosine related protein-1 (Trp-1), Tyrosinase (Tyr), and Dopachrome Tautomerase (Dct) for complete melanocyte differentiation [164].

Along with melanoblast maintenance and melanocyte differentiation, PAX3 is also involved in cell survival. Known anti-apoptotic factors like Bcl-Xl, p53, and PTEN are direct downstream targets of PAX3. During embryogenesis, PAX3 is involved in neural crest development through the inhibition of p53-mediated apoptosis [176]. PAX3 also inhibits PTEN expression, at least in myogenesis [177]. Increased expression of PAX3 leads to PTEN downregulation and a decrease in apoptosis through the PTEN/AKT pathway [178]. Transcription of Bcl-Xl is also directly regulated by PAX3 in

rhabdomyosarcoma [179], and MITF regulates Bcl-2 in melanocytes and melanoma [180]. The anti-apoptotic function of PAX3 aids in the migration of undifferentiated cells, which may enhance melanoma cell survival.

Regulation of PAX3 is essential for melanocyte development. PAX3 protein expression can be regulated by phosphorylation and ubiquitination. A Ser205 phosphorylation site within PAX3 has been found, but it has only been observed in proliferating mouse primary myoblasts [181]. Ubiquitination of PAX3 has been shown in adult muscle stem cells [182]. Also, PAX3 interacts directly with Death domain associated protein (Daxx), which was found through its interaction with Fas/CD95 in the cytoplasm [161]. Daxx acts as a repressor of transcription factors in the nucleus, where Daxx may be mediated by STAT1 activation [183]. It binds to PAX3 through epitopes in the homeodomain and the octapeptide regions [161]. The Daxx-mediated inhibition of PAX3 can be blocked by the recruitment of Daxx to the nuclear bodies by promyelocytic leukemia protein (PML). Daxx also inhibits a PAX3 direct downstream target receptor tyrosine kinase MET [184]. This recruitment of Daxx to PAX3 can ultimately restrict the development and differentiation of melanoblasts into melanocytes.

Multiple studies have looked into the relationship between STAT3 and PAX3. STAT3 is a direct transactivator of the PAX3 promoter [185]. Mutant V600E BRAF enhances STAT3 phosphorylation and increases PAX3 expression in melanocytes [186]. One study determined that silencing of STAT3 or PAX3 with siRNA was shown to inhibit the growth of melanoma cells, particularly in melanoma cells that have acquired resistance to vermurafenib [29].

Another regulator of PAX3 is transforming growth factor beta (TGF-β), a cytokine that controls numerous effects on multiple cells [187, 188]. These functions include cellular behavior, differentiation, survival, migration, proliferation, and/or adhesion [189]. TGF-β also protects homeostasis by acting as a tumor suppressor [190]. In melanoma cells, high levels of TGF-β are secreted within the tumor microenvironment, but tumor cells fail to respond and growth inhibition is prevented [191]. While there are other regulators of PAX3, TGF-β has an important role in the maintenance of PAX3 in adult melanocytes. With limited UVR, keratinocytes residing in the epidermal layer of the skin secrete moderate levels of TGF-β, which signals through serine/threonine kinase receptor complexes (RI-RII) on the surface of melanocyte [192]. This binding at the cell membrane activates the Smad proteins to accumulate in the nucleus, which then controls targets of the TGF-β/Smad complex [193, 194]. Once TGF-β is bound to the RI-RII receptor, R-Smad is phosphorylated and forms a complex with Smad4 and Ski [195]. Ski forms this complex in melanocytes and directly inhibits the transcription of PAX3 [196]. Another study also showed that treating melanocytes with varying concentrations of TGF-β led to the down-regulation of PAX3 mRNA and protein expression [196].

On the other hand, levels of TGF-β are reduced when keratinocytes are stimulated with UVR. Studies suggest that TGF-β expression is also suppressed at both the transcriptional and protein level following UVR of the skin [196-198]. The repression of TGF-β is caused by the UVR-induced expression of both Jun N-terminal kinase (JNK) and the tumor suppressor p53. Collectively, JNK and p53 activate the transcription of

activating protein 1 (AP-1) [199, 200]. This allows p53 to stimulate the production of pro-opiomelanocortin/melanocyte stimulating hormone (POMC/MSH) in keratinocytes [23, 201], which releases the αMSH ligand that binds to the melanocortin-1 receptor (MC1R) on the melanocyte cell surface [201]. Once the αMSH ligand binds to MC1R, a signal cascade that works with adenylate cyclase (AC) leads to the production of cyclic adenosine monophosphate (cAMP) [16]. As levels of cAMP reach a certain threshold, the phosphorylation of cAMP response element binding transcription factor (CREB) occurs via protein kinase A [201].

CREB stimulates both PAX3 and SOX10 which together form a complex to activate MITF. MITF, the master regulator of melanocyte differentiation, plays multiple roles in melanoma. Loss of MITF results in cell cycle arrest and apoptosis, moderate levels lead to proliferation and survival, and increased expression results in differentiation [180, 202]. MITF and PAX3 can also independently initiate the expression of MET, which plays a role in cell migration and growth as well as in cancer progression and metastasis [17, 203, 204]. However, when deregulation occurs, PAX3 may play a role in the pathogenesis of melanoma [160, 161, 164, 196, 205]. PAX3 expression is deregulated in a significant proportion of melanomas [206, 207] (Figure 3.1). PAX3 has been found in healthy melanocytes, benign nevi, and melanoma tumors [206, 208-210]. PAX3 has also been used as a staging marker for melanoma and in the detection of circulating melanoma cells [160, 211, 212]. PAX3 has been recognized as an immunogenic protein, where it has been found in primary tumors as well as advanced diseases such as stages 1 and 4 [213, 214]. This indicates that the regulation of PAX3

could be an important facet in melanoma initiation, progression, and metastasis. The direct role that PAX3 plays during intermediate stages of melanoma (i.e. II and III) must be identified to better understand the process of melanoma progression. Given PAX3's expression in late stage metastatic melanoma but absence in intermediate stages, targeting PAX3 could potentially shift the nature of melanoma tumors to a less aggressive, less metastatic form.

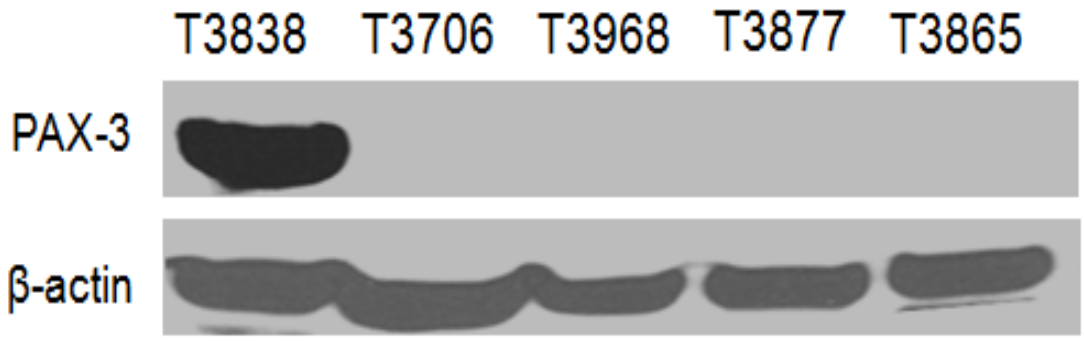

Figure 3.1 PAX3 is differentially expressed in human melanoma tumors. Five melanoma tumor samples of different stages were tested for PAX3 protein expression via western blot analysis. Sample T3838 showed a marked PAX3 protein expression, which correlates with the highly metastatic and late stage of the tumor. Four other melanoma patient samples did not express detectable levels of PAX3 proteins. Further information from Hollings Cancer Center indicated that T3838 was a stage 4 metastatic tumor with invasive bone metastasis. The other four samples either were not early stage tumors, or the metastasis information was not provided.

Previous studies have shown that GILT enhances HLA class II presentation and T cell recognition. If GILT has this secondary role in improving cancer cell aggressiveness, PAX3 would be a good candidate see if GILT has any effect on its gene/protein expression. PAX3 is known as a transcription factor in the differentiation of melanocytes, and is implicated in tumorigenesis and anti-apoptosis. If GILT can alter expression of PAX3, it may be able to reduce the cells to a less aggressive, less metastatic

form. Thus if GILT insertion can alter the expression of PAX3, it may be able to reduce the cells to a less aggressive, less metastatic form, while shedding light on the potential benefit of targeting PAX3 in the design future melanoma immunotherapy.

Hypothesis

I tested the hypothesis that GILT expression downregulates PAX3 molecules in human melanoma cells via protein-protein interaction, activation of autophagy and lysosomal degradation pathway.

Research Strategy

Experiment 1: Examined PAX3 and Daxx gene expression in melanoma cells +/- GILT.

Experiment 2: Determined GILT, PAX3, and Daxx protein expressions in melanoma cells +/- GILT.

Experiment 3: Studied the relationship between PAX3 and Daxx in human melanoma cells.

Experiment 4: Analyzed multiple GILT mutants to determine its effect on PAX3 expression.

Experiment 5: Investigated the pathway GILT utilizes to regulate PAX3 and downstream targets in GILT +/- melanoma cell lines.

Materials and Methods

Cell lines

Human melanoma cell lines DM-331, HT-144, and J3.DR4.vec were cultured as described in Chapter 2 and were used in these experiments. The human melanoma cell line J3 was cultured in the same media conditions, but was transfected with a mutated GILT protein where cysteine at position 46 was mutated to a serine (Dr. Suzanne Ostrand-Rosenberg, University of Maryland, Baltimore, MD).

Table 3.1 Cell lines utilized for chapter 3.

Melanoma Cell Line	Conditions/Treatments	Reason for use
J3.DR4	+/- GILT, +/- C46S GILT mutant, +/- 20nM bafilomycin	Retrovirally transduced to express DR4, to determine role of GILT in PAX3 regulation, displayed high levels of PAX3
HT-144	+/- GILT	Constitutive expression of DR4, to determine the role of GILT in PAX3 regulation, displayed high levels of PAX3

DNA transfection assays

Human melanoma cell lines DM-331, HT-144, and J3.DR4 were transfected with a plasmid encoded with GILT cDNA and a puromycin drug resistance gene or a vector-encoded plasmid with the same puromycin drug resistance gene using a lipofectamine transfection reagent (Sigma-Aldrich, St. Louis, MO) as described in Chapter 2 of this study.

Preparation of cell lysates & Protein determination

Transfected cells were grown to 80% confluence and subjected to complete lysis

buffer, and cell lysates were assessed for protein concentration as previously described in this study.

Western blotting

Once protein levels were quantified following cell lysate and protein determination, equal concentrations of vector and GILT matched cell lines were run onto a NuPAGE 4-12% gel and transferred as previously described in this study.

Antibodies and reagents

Nitrocellulose membranes were subjected to probing with various antibodies. The antibodies used were PAX3 (Santa Cruz), Daxx (Santa Cruz), Beclin-1(Santa Cruz), LC3 (Bioscience), GILT (Santa Cruz), and Actin (Santa Cruz). Nitrocellulose membranes were incubated for 2-3 hours, rolling, at room temperature with a given antibody at a predetermined concentration (as per manufacturer standard) in a solution of 2.5% milk in TBS-T. Following incubation time, blots were washed for 30 minutes in TBS-T before being probed with antibody species specific secondary antibodies (anti-goat, anti-rabbit, and anti-mouse IgG, Invitrogen and Santa Cruz) for one hour. Finally, blots were washed again in TBS-T for 30 minutes then subjected to Luminata Crescendo Western HRP Substrate (Millipore Corporation, Billerica, MA) and assessed as described in western blot methods. Images were taken using BioRad GelDoc XRS photocenter while subjected to ultraviolet light. Bafilomycin A1 (InvivoGen) was diluted to 20nM in culture medium and used to block autophagy in melanoma cells overnight.

Confocal microscopy

HT-144.vec and HT-144.GILT cells were grown to 80% confluence to then be subjected to staining via confocal microscopy as described in Chapter 2 of this study.

Immunoprecipitation

Transfected cells were grown to 80% confluence and collected as a pellet in a 15ml conical tube and stored at -80^{o}C until use. Cell lysis was performed as previously described with about 200 µg-500 µg of protein needed. 60 µl of protein/bead mix per sample tube was aliquotted and spun down for 10 seconds at 10,000 rpm. Supernatant was removed and beads were placed on ice. Protein determination provided the appropriate amount of cell lysate needed along with adding complete lysis buffer to tubes containing the beads to reach a total volume of 300 µl. Tubes were then placed on the rotator at 4^{o}C for 2 hours. Samples were spun down for 2.5 minutes at 10,000 rpm and supernatant was transferred to a new tube while pellet was discarded. GILT antibody (Santa Cruz) was used to pull down proteins in these cells and it was added at a 1:100 dilution to the supernatant. Tubes were then placed on the rotator at 4^{o}C for 1 hour. Bead mix previously described was performed and added to the cell lysate/antibody mixture in each tube containing protein beads. Tubes were placed on the rotator at 4^{o}C overnight. Next, samples were spun down for 5 minutes at 10,000 rpm and supernatant was aspirated. 800 µl of wash buffer (cell lysis buffer without protease inhibitors) was added to each tube and spun for 5 minutes at maximum speed. Supernatant was aspirated and

the wash step was repeated for a total of 4 washes. During the last wash, a master mix of lysis buffer (8 µl/sample), 4x sample buffer (8 µl/sample), and DTT (4 µl/sample) was prepared for all samples. After aspirating the final wash step, 20 µl of the master mix was added to each sample. Samples were then heated on at heat block at 100^{o}C for 10 minutes. Samples were quickly spun down for about 10 seconds and 15 µl of each samples was loaded onto NuPAGE 4-12% Bis-Tris gels (Invitrogen) and run at 200 volts for 50 minutes. Bis-Tris gels containing protein were then transferred to nitrocellulose membranes (Osmonics) employing a transfer chamber subjected to 30 volts for one hour. Nitrocellulose membranes were then removed and blocked in a solution of 5% milk in TBS-T overnight at 4^{o}C. After incubation, the nitrocellulose membranes were probed with protein specific mAbs. Probed nitrocellulose membranes were next assessed using autoradiography film, following incubation with 3ml of Luminata Crescendo Western HRP Substrate (Millipore Corporation, Billerica, MA) for 3 minutes. Autoradiography films were scanned using a Canon MP250 scanner/printer and analyzed using a BioRad Geldoc XRS photocenter, where densitometric software enabled for the quantification of protein densities.

Statistical Analysis

Data from each experimental group were subjected to statistical analysis. ANOVA with post-hoc tests, Repeated Measures ANOVA with post-hoc tests, or Student's *t*-tests were used, as appropriate. Student's TTEST was performed on a minimum of three independent values to determine significance. Significance was then

determined as having a p value less than or equal to 0.05 as represented by an asterisk, or less than or equal to 0.01 as represented by a double asterisk. The standard deviation of all recorded values for a given experiment were also determined and are represented by error bars on all figures, this data is representative of all obtained values for each given figure with an N of at least 3. Finally, densitometry was performed on all electrophoresis gels, using a BioRad GelDoc XRS photocenter. Using contoured image selection software a relative density for each primer band was determined, along with a density value for its corresponding actin band. Density readings were taken in triplicate using three contoured readings: one tight, one medium, and one wide contour image for each band was used. Each primer band density was then divided by the recorded density of its corresponding actin yielding a relative density for each band. These data were then used to generate both significance and standard deviations as determined above. Two-sided tests were used in all cases and P values <0.05 were considered statistically significant.

Results

GILT downregulates PAX3 and upregulates Daxx proteins in human melanoma cells.

PAX3 has been indicated in melanoma tumorigenesis and metastasis [17, 203]. Therefore, targeting PAX3 may lead to a less aggressive state of melanoma. First, PAX3 expression had to be established in melanoma cell lines. In Figure 3.2, HT-144 cells were stained with PAX as well as SOX10 and MITF, and confocal microscopy confirmed PAX3 expression in the cytosol of these cells.

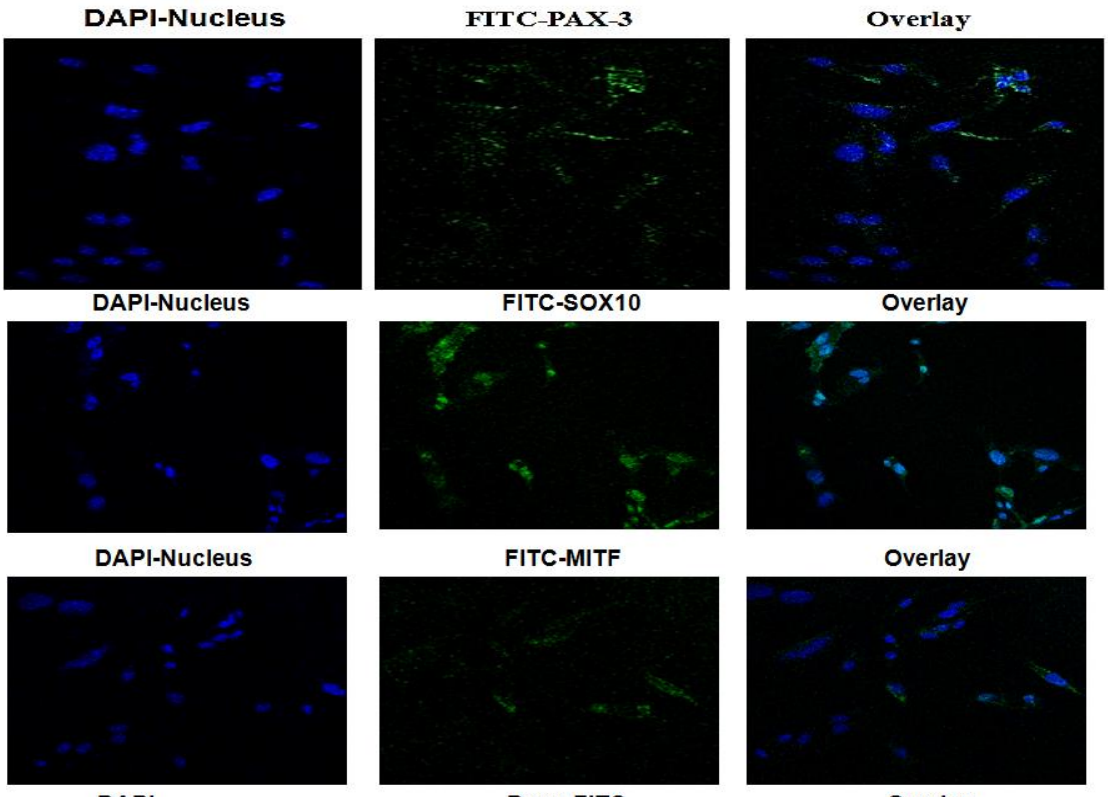

Figure 3.2 PAX3, SOX10, and MITF expression in human melanoma cells. HT-144 cells expressed the highest levels of PAX-3 and were tested for nuclear staining using confocal microscopy. However, PAX-3 is mainly expressed in the cytosol. Cells were also tested for the downstream molecules SOX10 and MITF using confocal microscopy. Staining confirms that both molecules are expressed in these cells.

To determine if GILT would have an effect on such tumorigenic molecules, I tested GILT transfected melanoma cell lines for PAX3 expression. Whole cell lysates were prepared and tested through western blot analysis for PAX3 showed expression in cell lines J3.DR4.vec, HT-144.vec, and DM-331.vec (Figure 3.3). Whole cell lysates were determined due to the main location of PAX3 is in the cytosol. As shown in Figure 3.6, the insertion of GILT effectively and significantly downregulated PAX3 protein expression in all three cell lines.

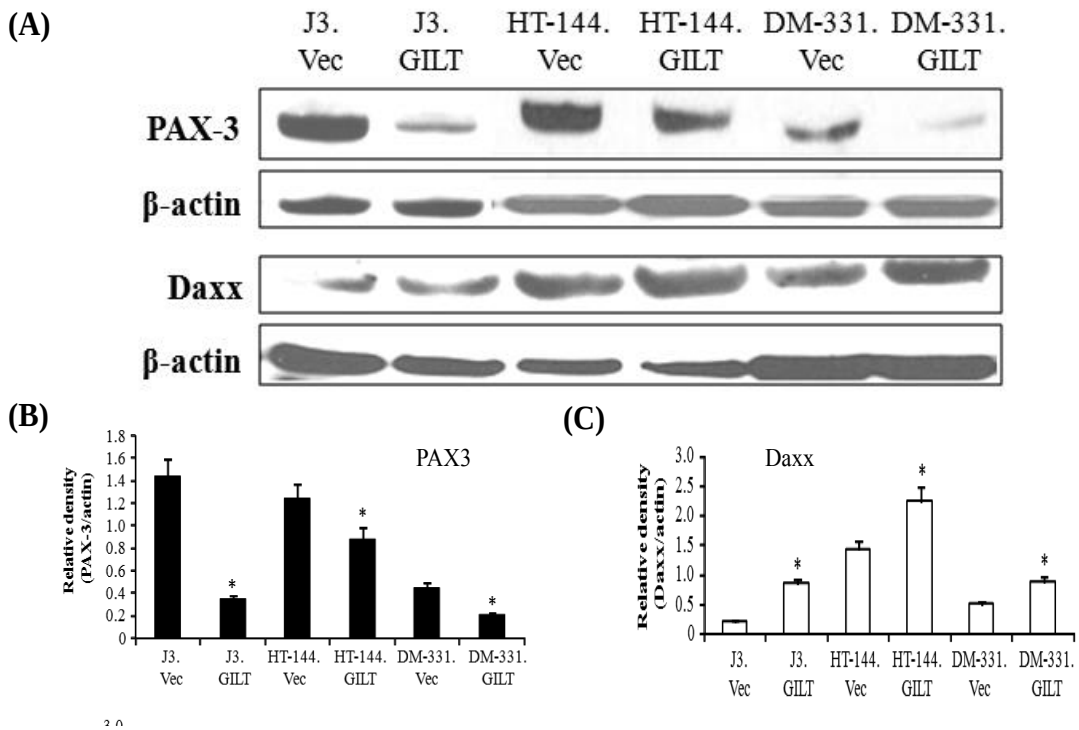

Figure 3.3 GILT expression alters PAX3 and Daxx proteins in human melanoma cells. Melanoma cell lines J3, HT-144, and DM-331 were stably transfected with vector or GILT cDNA as described in the methods. (A) Western blot analysis for PAX3 and Daxx protein expression in melanoma cell lines +/- GILT. β-actin was used as a loading control. Densitometric analysis of the protein bands detected in Figure 1b. β-actin was used as a reference to quantitate the relative expression of PAX3 **(B)** and Daxx **(C)** proteins in both vector- and GILT-transfected J3, HT-144 and DM-331 melanoma cells. Data suggest that GILT expression significantly reduces PAX3 proteins while upregulating Daxx proteins in human melanoma cells. * = p <0.05

Daxx may be regulated through a STAT1-dependent pathway [183]. Our lab has already shown that GILT is regulated by STAT1, not CIITA [109]. Because of the downregulation of PAX3 observed in GILT-positive cells compared to GILT-negative cells, GILT may be utilizing Daxx as an intermediate in the negative regulation of PAX3 via STAT1. Therefore, I tested the same melanoma cell lines +/-GILT, and western blot analysis determined a significant increase of Daxx protein expression in all GILT transfected cell lines (Figure 3.3).

GILT colocalizes with PAX3, not Daxx, in human melanoma cells.

Due to GILT's effect on PAX3 expression, I next examined the mechanism GILT utilized to downregulate PAX3 expression. As previously stated, GILT is localized within endosomal/lysosomal compartments while PAX3 is found both in the cytosol and within the nucleus. Confocal microscopy was used to determine if GILT and PAX3 had any direct interactions within the cell. Using the melanoma cell line HT-144.GILT, confocal microscopy revealed that GILT and PAX3 do in fact colocalize together within the cell, as seen in Figure 3.4. Based on the protein expression results, I tested whether Daxx and GILT also colocalize within the cell. Both Daxx and GILT are regulated through STAT1 signaling. Due to this similarity, Daxx may be acting as the intermediate protein resulting in PAX3 reduction. I used confocal microscopy on HT-144.GILT cells to determine if a protein-protein interaction between GILT and Daxx existed in these cells. However, there was no observable colocalization between GILT and Daxx (Figure 3.4). This finding is incredibly interesting, as PAX3 has never been found localized within endosomal/lysosomal compartment, as the finding with GILT suggests. These data supports the notion that GILT is interacting with PAX3 through a possible protein-protein interaction, resulting in its downregulation.

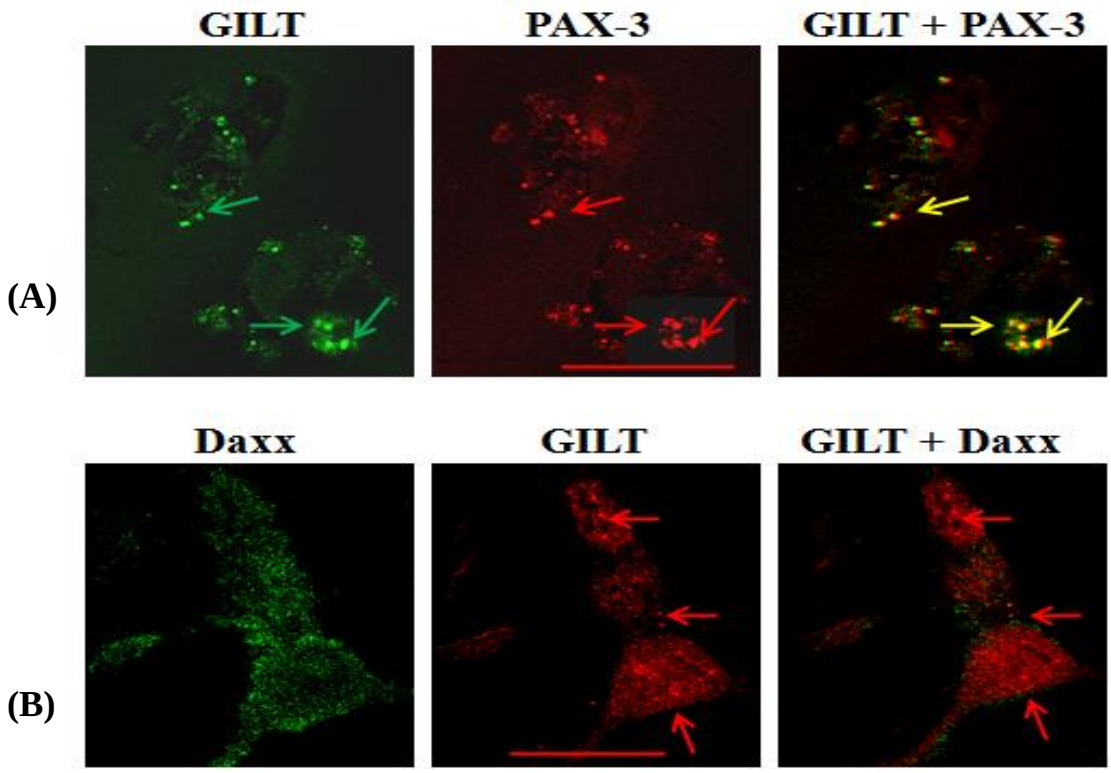

Figure 3.4 GILT colocalizes with PAX3 molecules in HT-144.GILT melanoma cells. **(A)** HT-144.GILT melanoma cells were subjected to confocal microscopy using antibodies against GILT (left panel, green arrows) and PAX3 (middle panel, red arrows) proteins. Overlay shows colocalization of PAX3 and GILT proteins (right panel, yellow arrows) in HT-144.GILT cells. Bar, 26.1 µM. **(B)** Confocal microscopy of HT-144.GILT cells for Daxx (left panel, green) and GILT (middle panel, red) molecules. Overlay shows no colocalization of Daxx and GILT proteins (right panel, red arrows) in HT-144.GILT cells. Bar, 17.6 µM. Data are representative of three separate experiments.

GILT interacts with PAX3 proteins in human melanoma cells.

Immunoprecipitation was used to definitively prove the direct interaction between these two proteins (Figure 3.5). Following the immunoprecipitation protocol outlined in the methods section of this chapter, IP GILT was used to pull down all of the proteins, which directly bind and interact with GILT within the cell. IB probing of this extracted lysate for PAX3 confirmed a direct protein-protein interaction between GILT and PAX3 in both J3.DR4.vec and HT-144 melanoma cell lines. These results are confirmed as GILT specific

through the control lysate which used a nonspecific NN4 antibody IP, followed by PAX3 probing IB.

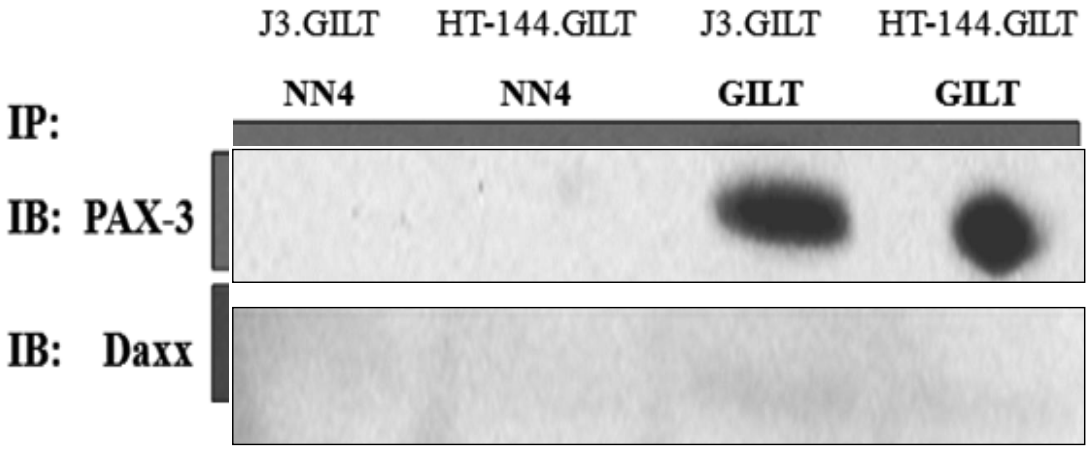

Figure 3.5 GILT interacts with PAX3 proteins through a direct protein-protein interaction in human melanoma cells. Co-immunoprecipitation studies in J3.GILT and HT-144.GILT cells for GILT/PAX3 proteins using antibodies against GILT proteins. The NN4 antibody was used as an isotype control. Immunoblotting was performed by using antibodies against PAX3 and Daxx molecules. Data are representative of at least three separate experiments.

Functional GILT is required for PAX3 downregulation in human melanoma cells.

To further investigate the role of GILT in the negative regulation of PAX3, I tested whether functional GILT was necessary for the decrease in PAX3 protein. A previous study was done to test multiple GILT mutants [215]. It was observed that when the cysteine at position 46 was mutated to a serine within the GILT protein, cells expressed the mature GILT form at 30kDa, but did have reductase activity. Therefore, this mutant GILT was transfected into the J3 cell line by the Ostrand-Rosenberg lab, and this cell line was tested for PAX3 protein expression. Western blot analysis in Figure 3.6 determined that J3.DR4.vec cells expressed high levels of PAX3. With the insertion of

GILT, there is a markedly decrease in PAX3 expression. However, in J3 cells transfected with mutated GILT, PAX3 proteins recover to levels similar to J3.DR4.vec cells. These data suggests that functional GILT is required for the downregulation of PAX3 protein in human melanoma cells.

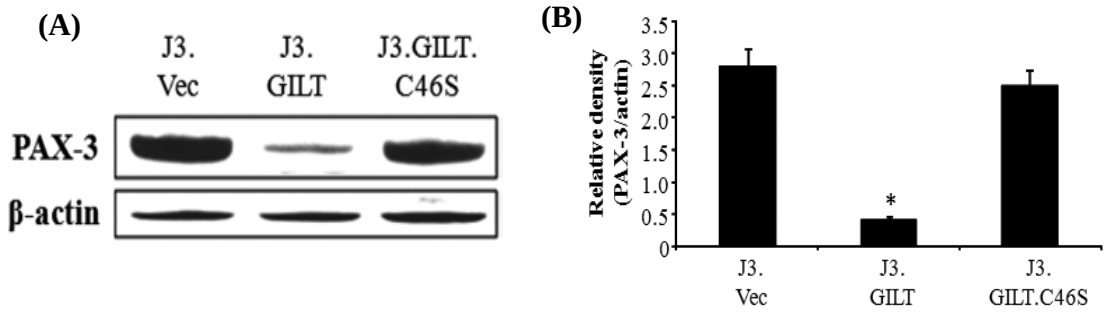

Figure 3.6 GILT induction regulates PAX3 protein expression in melanoma cells. (A) J3.Vec, J3.GILT and the cysteine mutant J3.GILT.C46S were analyzed by western blotting for steady state PAX3 protein expression. β-actin was used as a loading control. (B) Densitometric analysis of the protein bands detected in Figure 1b. β-actin was used as a reference to quantitate the relative expression of PAX3 proteins in J3.vec, J3.GILT, and the mutant J3.GILT.C46S melanoma cells. Data suggest that functional GILT expression is required in the downregulation of PAX3 in human melanoma cells. * = $p < 0.05$

<u>GILT expression regulates PAX3 through the autophagy and lysosomal degradation pathway in human melanoma cells.</u>

GILT resides with the endosomal/lysosomal compartments of cells, while PAX3 mainly is expressed in the cytoplasm [161]. It was previously shown that GILT expression downregulates PAX3 through a protein-protein interaction, and functional GILT is necessary for this decrease. However, the mechanism underlying the interaction between GILT and PAX3 remains to be elucidated.

Autophagy is a lysosome-dependent degradation process designed to maintain cellular homeostasis by clearing damaged cytosolic organelles and long-lived proteins [216]. It can be activated under cellular stress such as nutrient starvation, pathogen

infection, and under pathological conditions, including vascular diseases, neurodegenerative diseases, and cancer [217]. Once autophagy is activated, this process helps reduce oxidative damage and maintains redox homeostasis [218].

Therefore, autophagic proteins were tested in melanoma cell lines +/- GILT insertion through western blot analysis (Figure 3.7). The cell lines J3.DR4 and HT-144 were chosen for this experiment, due to the high levels of PAX3 in the vector cell lines, and the significant downregulation when transfected with GILT. Results indicate that GILT expression increased Beclin-1 proteins while decreasing LC3 protein. The presence of GILT affects multiple proteins involved in autophagy. Because GILT is able to downregulate PAX3, it is possible that GILT is leading PAX3 through the lysosomal degradation pathway.

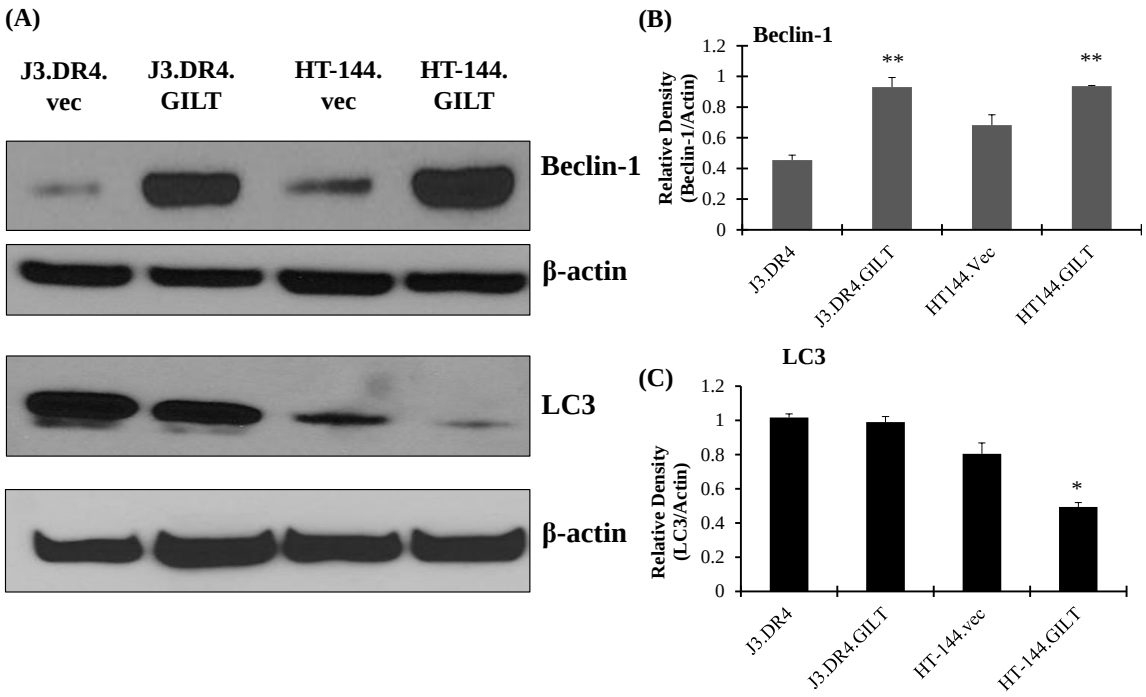

Figure 3.7 GILT expression affects multiple proteins involved in autophagic processes. (A) Western blot analysis of whole cell lysates from J3.DR4.vec, J3.DR4.GILT, HT-144.vec, and HT-144.GILT cells showing protein expression of Beclin-1 and LC3. β-actin was utilized as a loading control. (B-C) Densitometric analysis for each protein tested, which was significant in Beclin-1 and LC3 for HT-144.GILT cells, as indicated by *. Data are representative of at least three separate experiments.*$p<0.05$, **$p<0.01$.

To test whether GILT regulates PAX3 through this pathway, cells were treated with 20nM bafilomycin overnight. Bafilomycin has been shown to inhibit the late phase of autophagy. This treatment prevents maturation of autophagic vacuoles by inhibiting fusion between autophagosomes and lysosomes. Therefore, J3.DR4 +/- GILT expression were treated with bafilomycin overnight, whole cell lysates were obtained, and subjected to western blot analysis. Shown in Figure 3.8, J3.DR4 cells were probed for PAX3 as well as Beclin-1 and GILT. When cells are treated with bafilomycin, there is a significant increase in PAX3 expression, specifically in GILT positive cells. Beclin-1 and GILT were used as controls to determine the effectiveness of bafilomycin treatment. This data suggests that when autophagy/lysosome is blocked, PAX3 expression is able to

endure. When GILT is present in melanoma cells. GILT is able to regulate PAX3 through the autophagy and lysosomal degradation pathway.

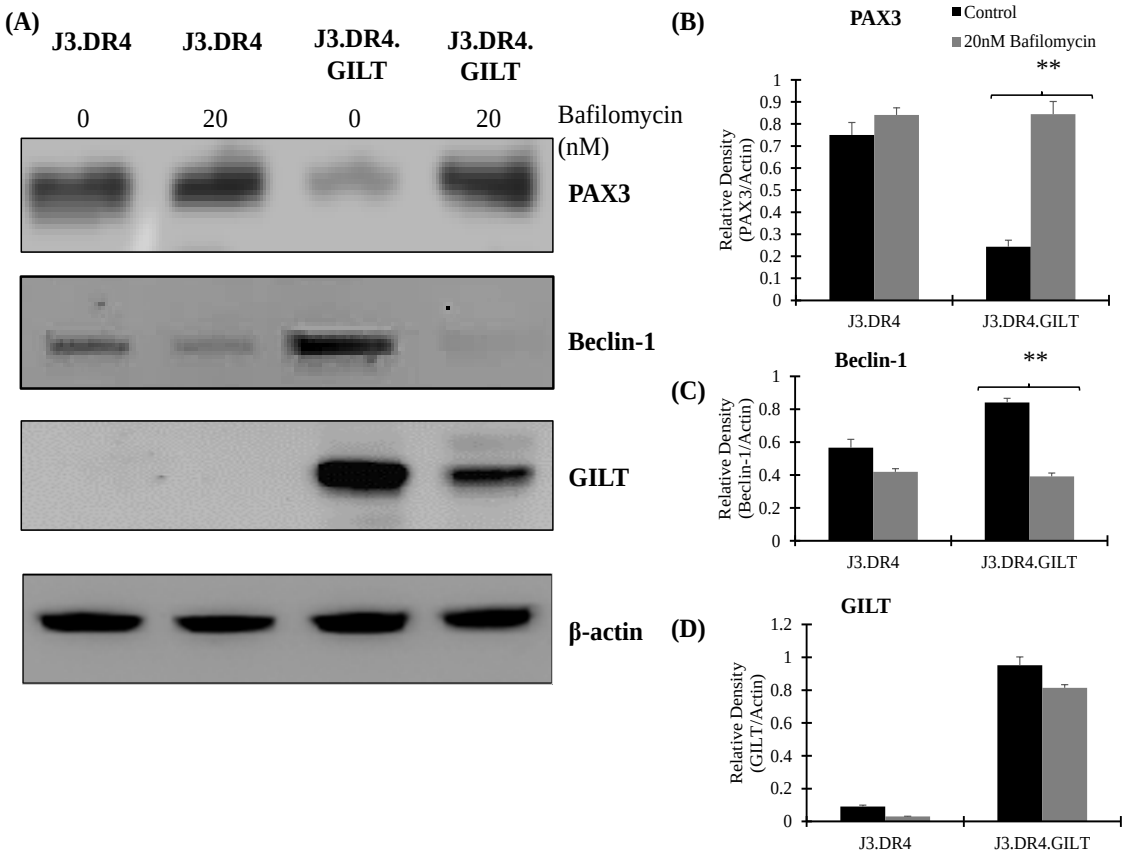

Figure 3.8 GILT regulates PAX3 through the autophagy and lysosomal degradation pathway. (A) Melanoma cell lines J3.DR4 and J3.DR4.GILT were treated with or without 20nM bafilomycin overnight, which blocks proteins from processing via the lysosomal degradation pathway. Western blot analysis from whole cell lysates of these cell lines were probed for PAX3, Beclin-1, and GILT expressions. β-actin was utilized as a loading control. (B-C) Densitometric analysis for each protein tested, which was significant in J3.DR4.GILT cells with or without bafilomycin, as indicated by *. Data are representative of at least three separate experiments.*$p<0.05$, **$p<0.01$.

Discussion & Conclusions

The major focus of this chapter was related to PAX3 and its signaling and their influence in late stage melanoma. PAX3 is a tumorigenic and immunogenic molecule that is susceptible to targeted therapies [87]. Only in this study, results presented earlier in this chapter showed that the insertion of GILT in melanoma cells led to a downregulation in both

PAX3 mRNA and protein expression. PAX3 has also been indicated in late stage metastatic melanoma. This has been confirmed in melanoma patient tumors and finding PAX3 expression in a stage IV melanoma tumor, where metastasis was present in the brain as well as bone. These results indicate that PAX3 may be an important factor in facilitating late stage metastasis.

To examine PAX3 regulation, I investigated the protein Daxx, because it has been shown that it binds to PAX3 and inhibits its expression [68]. Studies have shown that both GILT and Daxx are regulated through STAT1 signaling [60, 101]. Data in this study showed that GILT insertion enhanced Daxx expression at the proteins levels. However, confocal microscopy showed that GILT does not colocalize with Daxx in melanoma cells. This result indicates that although GILT and Daxx may not have a direct relationship with one another, Daxx may still have an effect on the decrease of PAX3 protein expression.

Once ruling out the indication that GILT was using Daxx in the regulation of GILT, GILT's direct role on PAX3 expression was examined. For the first time, results show that GILT and PAX3 colocalize together in melanoma cells through the use of confocal microscopy. Immunoprecipitation confirmed this result, determining that GILT directly interacts with PAX3 in a protein-protein interaction leading to its reduction. This finding was further enhanced when a GILT mutant was transfected into the J3.DR4.vec cell line and tested for PAX3. With the mutant GILT having the protein expression but no reductase activity, it was found that PAX3 expression was recovered to almost control levels. Data suggests that functional GILT is required for PAX3 downregulation.

Never before has it been documented that GILT would have any effect on PAX3, because GILT is localized in the endosomal/lysosomal compartments while PAX3 is mainly

in the cytosol and partially in the nucleus [52, 67]. Within the endosomal/lysosomal compartments, proteins may trafficked through and tagged for autophagy through the lysosomal degradation pathway. Knockdown of PAX3 expression in melanoma cells can lead to reduced or arrested cell growth, and induction of apoptosis and/or senescence [158, 206, 219] These results support the notion that PAX3 is susceptible to targeting, which could lead to a less metastatic phenotype of this disease.

Chapter 4: Modulation of GILT and PAX3 by Ganoderic acid DM enhances radiation and chemoimmunotherapy of melanoma.

Introduction

In metastatic melanoma, standard treatments alone such as radiation, chemotherapy, and immunotherapies have been ineffective when treating this disease. Despite toxicities, high-dose radiation and chemotherapeutic drugs have become a general mainstay for cancer treatment, destroying cancer cells by inducing apoptosis [220]. However, it has become increasingly important to search for natural products that are less toxic and can produce favorable immune responses. One such candidate for antitumor responses is the *Ganoderma lucidum* mushroom. For thousands of years, the *G. lucidum* mushroom has been used in herbal medicine where it was initially thought to maintain vitality and increase life expectancy [221]. It was reported that *G. lucidum* presented a wide array of biological effects including prevention of chronic diseases, such as hepatitis, hepatopathy, hypertension, and cancer [222, 223]. Recent research suggests that the Ganoderic acid extracts from this mushroom may have wide-ranging medicinal benefits, most notably its toxicity to tumor cells with limited toxicity to healthy bystander cells [223]. Various Ganoderic acid subtypes have been tested for efficacy in multiple inflammatory and malignant diseases such as inflammation, bronchitis, and cancer [224-226]. Crude extracts of the *G.lucidum* mushroom have shown cytotoxicity in various tumor cell lines [227-231]. Among the active compounds in *G. lucidum*, triterpenoids have been demonstrated as one of the main components responsible for pharmacological activities including immunomodulation, anti-oxidative, anti-metastasis, and anti-tumor effects [232-234]. Of all the extracts, Ganoderic acid DM (GA-DM) has the most

hydrophobic structure and is devoid of interfering hydroxyl or acetyl side chain groups. GA-DM has been found to inhibit osteoclastogenesis by regulation of c-Fos and nuclear factor of activated T cells c1 and exerts anti-prostate cancer effects partially via inhibiting 5α-reductase activity [226, 235]. While the effects of Ganoderic acids on breast, lung, and prostate cancer cell lines have been well-established [223, 226, 229, 231, 236-238], much less was known about its potential role as a therapeutic agent in metastatic melanoma.

Our lab is the only group to test GA-DM on melanoma cell lines. We have shown that GA-DM could influence intracellular machinery of melanoma cells for HLA Class II processing and presentation to T cells for immune recognition [239]. We also showed that GA-DM treatment induces autophagic and apoptotic events as well as immune activation in human melanoma cells. GA-DM treatment showed an increase in caspase 9, caspase 3, bcl-2-like protein 4 (Bax), cytochrome c, and apoptotic protease activating factor 1 (Apaf-1), a possibly activated extrinsic pathway of programmed cell death (Figure 4.1). Anti-tumor efficacy of GA-DM in B16 melanoma model in vivo was investigated and demonstrated a slowed tumor progression with a significant reduction in tumor volume [239]. These findings suggest a huge potential of GA-DM as an immunotherapeutic agent for treating malignant melanoma.

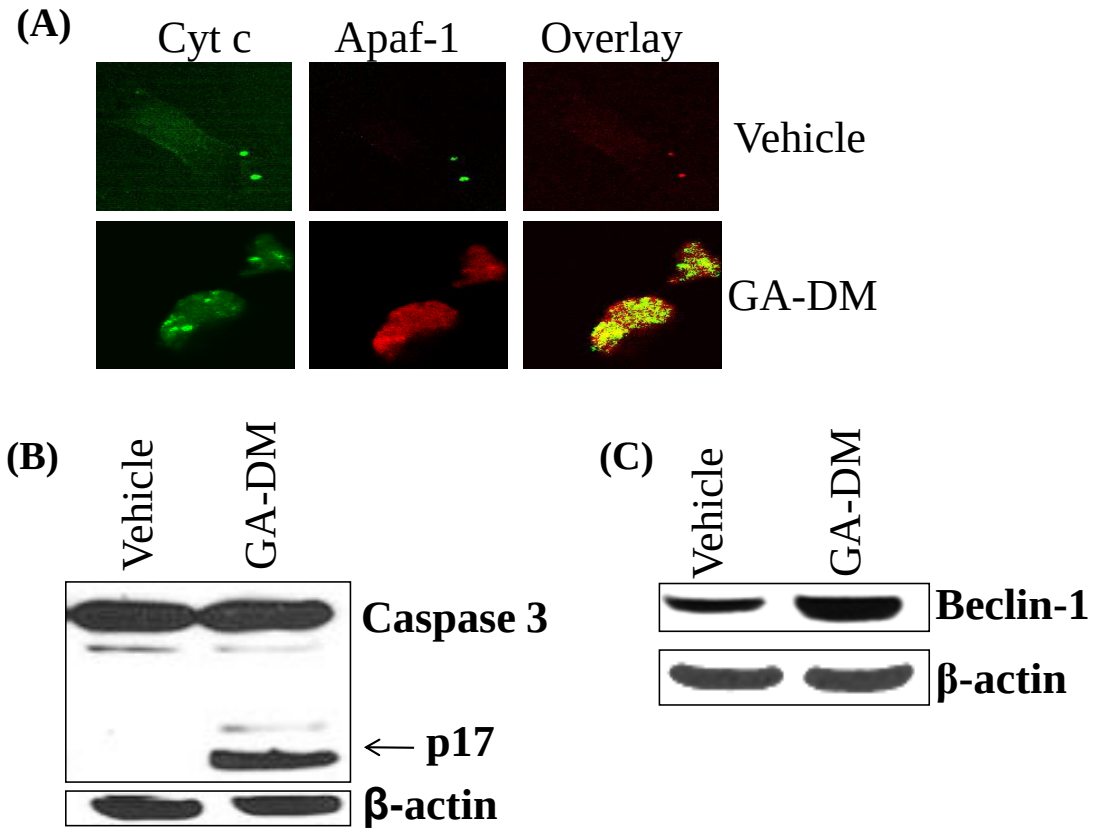

Figure 4.1 GA-DM affects apoptotic and autophagic proteins in human melanoma cells. (A) J3.DR4.vec cells were treated with GA-DM overnight and stained for cytochrome c and Apaf-1 proteins through confocal microscopy. In overlayed images of cells treated with GA-DM, an increase in cytochrome c release and Apaf-1 proteins is observed compared to vehicle. (B) Western blot analysis of J3.DR4.vec cells treated with GA-DM indicates activation of caspase 3 with cleaved caspase 3p17 expressed. (C) Autophagic protein Beclin-1 shows higher protein expression in J3.DR4.vec cells treated with GA-DM compared to vehicle, suggesting that melanoma cells are undergoing autophagic processes. β-actin was used as a loading control in (B) and (C). Data is representative of 3 independent experiments.

As previously stated, our lab has tested the efficacy of GA-DM on multiple human melanoma cell lines. Figure 4.2 is a proposed model of what is happening when melanoma cells are treated with GA-DM. As shown, it is postulated that DNA damage is occurring, leading to an increase in p53 while reducing Mouse double minute 2 homolog

(MDM2). The activation of p53 leads to p21 increased expression, and p21 is able to block the binding of CDK4 with Cyclin D. CDK4 and Cyclin D are cell cycle regulators, and when this is disrupted, G1 cell cycle arrest occurs. This will ultimately lead to tumor suppression. There are many other targets that may be involved in GA-DM-mediated melanoma cell death. Such molecules like the BH3-only proteins as well as apoptotic proteins may play a role leading to cellular death. It is currently unknown whether this treatment has any effect on these molecules.

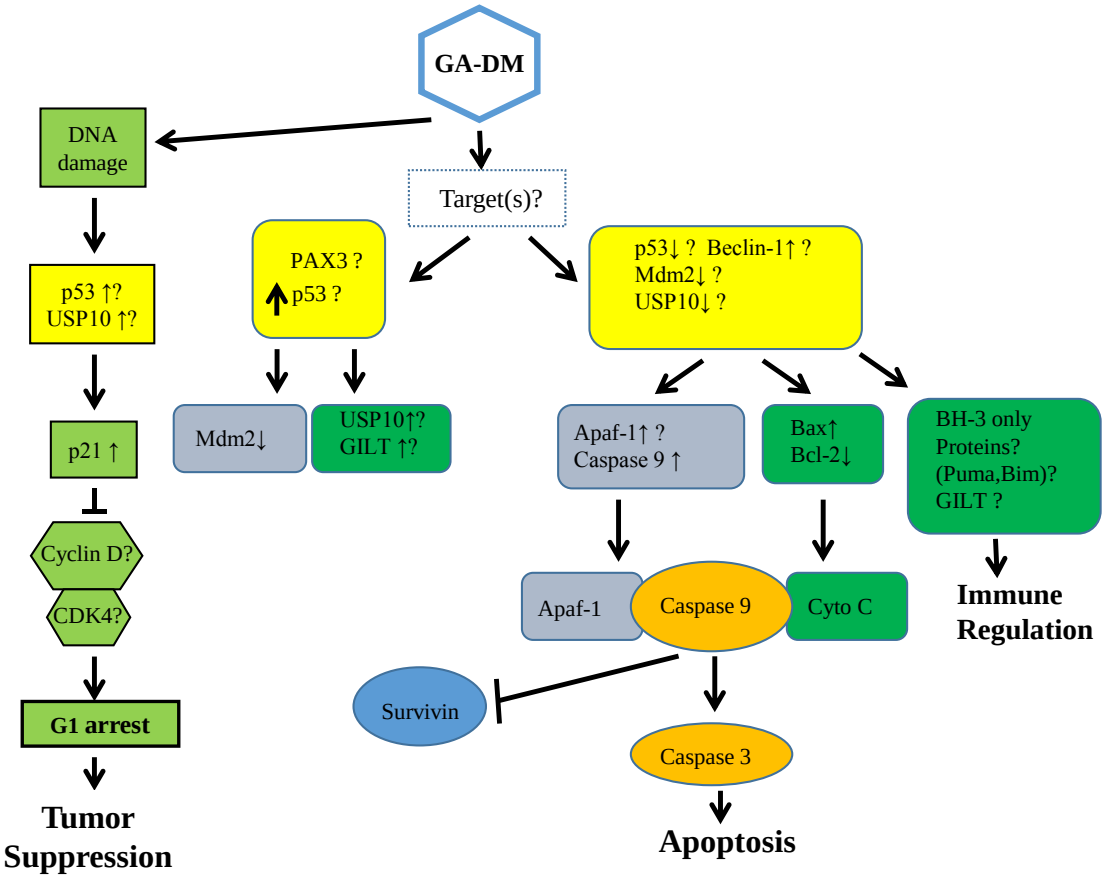

Figure 4.2 A hypothetical model for testing the effects of GA-DM on melanoma growth *in vitro* and *in vivo*. This diagram is a hypothetical signaling pathway when melanoma cells are treated with GA-DM. When cells are treated, it is postulated that DNA damage is occurring, leading to an increase in p53 while downregulating Mdm2. This will lead to an increase in p21, thus blocking the binding of Cyclin D with CDK4, leading to G1 arrest of melanoma cells and ultimately tumor suppression.

Understanding the role of GILT on PAX3 reduction may allow melanoma cells to be sensitized to radiation treatment, a commonplace treatment of melanoma patients. In addition, GA-DM has been shown to induce apoptotic protein expression. Utilizing a combination treatment of radiation and GA-DM may induce cellular death while enhancing immune responses. My preliminary data suggests GILT insertion sensitizes melanoma cells to radiation therapy. Other studies have also found that knockdown of PAX3 expression in melanoma cells can lead to reduced or arrested cell growth, and induction of apoptosis and/or senescence [158, 206, 219]. Because of the preliminary data of GILT decreases PAX3 protein expression as well as the role of PAX3 in cell survival, blocking PAX3 expression could allow melanoma cells to be susceptible to cellular death. This indicates that GILT may be a possible target in immunotherapy. Because GILT may downregulate PAX3 to sensitize cells to radiation therapy, this simultaneous targeting of GILT and PAX3 by GA-DM may enhance radiation and chemoimmunotherapy of melanoma *in vivo*.

On the other hand, ionizing radiation has been used for treatment for cancer for more than 100 years [240]. Recent studies have shown that endogenous type I interferons (IFNs) play a role in radiation-mediated anti-tumor immunity by enhancing the ability of dendritic cells to cross-prime CD8+ T cells [241]. It was previously stated that radiation therapy has had some success when combined with multiple immunotherapies [53, 56, 57]. To further investigate the role of radiation therapy, in vivo studies have been done to test the efficacy of this treatment. One study revealed that antitumor immune responses were present in a B16 mouse model receiving either 15Gy single dosage or fractionated (5 x 3Gy) of localized ionizing radiation [242]. It was

found that local tumor irradiation increases the Ag-presenting capability within tumor-draining lymph nodes and increases the numbers of T cells within tumor-draining lymph nodes that secrete IFN-γ upon tumor peptide stimulation [242]. Radiation also increased the numbers of immune cells infiltrating the tumors, including TILs that both secrete IFN-γ upon tumor peptide stimulation and exhibit lytic activity [242]. Another *in vivo* study displayed similar results that radiation-induced type I IFNs play a role in increasing CXCR3 chemokine levels within the tumor, which affects the initial recruitment of immune cells into the tumor microenvironment, when using the B16 mouse model and local single high-dose radiation (15Gy) treatment [240]. This study also showed the increasing intratumoral IFN-α levels exogenously after radiation, to further improve the ability of the therapy to bring about tumor control. These studies, as well as others, indicate a positive immune, anti-tumor response when malignant cells are treated with radiation therapy *in vivo*.

Radiotherapy combined with multiple immunotherapies have shown promise, as previously described in Chapter 1 of this study. With the low success rates of current treatments for melanoma, the treatment strategy of combining GA-DM as an immunotherapy and radiation as the standard treatment would be ideal in destroying cancer cells while simultaneously increasing antitumor immunity.

Hypothesis

I tested the hypothesis that Ganoderic acid DM modulates GILT and PAX3 to enhance radiation and chemoimmunotherapy of melanoma.

Research strategy

Experiment 1: Examined cell viability of GILT +/- melanoma cells after varying radiation, GA-DM, and the combined GA-DM/radiation treatments.

Experiment 2: Investigated apoptotic molecules (p53, caspase 3, caspase 9, etc.) and cell cycle checkpoints (Cyclin D, CDK4, p21, etc.) in GILT +/- melanoma cells subjected to radiation, GA-DM, and the combined GA-DM/radiation treatments.

Experiment 3: Analyzed tumor volume and survival in no treatment, radiation, GA-DM, and the combined GA-DM/radiation treatment utilizing the murine B16 melanoma model.

Experiment 4: Analyzed cytokine production, T cell infiltration, and other immune components (MDSCs, M2, etc) in no treatment, radiation, GA-DM, and the combined GA-DM/radiation treatment *in vivo*.

Materials & Methods

Cell lines

Human melanoma cell lines HT-144.vec and J3.DR4.vec were cultured as described in Chapter 2. The B16 mouse melanoma cell line was a gift from Dr. Mark Rubinstein (Medical University of South Carolina, Charleston), and was cultured in complete RPMI supplemented with HEPES and non- essential amino acids Invitrogen) as described previously. B16/Ab mouse melanoma cell line, which was transfected to express MHC class II, was a gift from Dr. Suzanne Ostrand-Rosenberg (University of

Maryland, Baltimore, MD). It was cultured in complete RPMI supplemented with FBS. The mouse T cell hybridoma BO4, which is specific for HEL_{74-88}/I-A^b was maintained in complete RPMI supplemented with 10% FBS + β-ME.

Table 4.1 Cell lines utilized for chapter 4.

Melanoma Cell Line	Conditions/Treatments	Reason for use
J3.DR4	+/- GILT, +/- 20uM GA-DM, +/- 5-20Gy	Retrovirally transduced to express DR4, to determine role of GILT in PAX3 regulation *in vitro*, displayed high levels of PAX3
HT-144	+/- GILT, +/- 20uM GA-DM, +/- 5-20Gy	Constitutive expression of DR4, to determine the role of GILT in PAX3 regulation *in vitro*, displayed high levels of PAX3
B16	+/- 20uM GA-DM, +/- 5-20Gy, +/- Ab (MHC class II)	Constitutive expression of PAX3 and GILT, mouse melanoma to determine treatment efficacy *in vivo*

DNA transfection assay

Human melanoma cell lines HT-144.vec and J3.DR4.vec were transfected with a plasmid encoded with GILT cDNA and a puromycin drug resistance gene or a vector-encoded plasmid with the same puromycin drug resistance gene using a lipofectamine transfection reagent (Sigma-Aldrich, St. Louis, MO) as described in Chapter 2 of this study.

Antigens, peptides, and antibodies

Hen egg lysozyme (HEL) was purchased from Sigma-Aldrich (St. Louis, MO). The mouse HEL_{74-88} peptide (NLCNIPCSALLSSDI) was produced using Fmoc

technology and an Applied Biosystems Synthesizer as described [139, 140]. Peptide purity (>99 %) and sequence were analyzed by reverse phase HPLC purification and mass spectroscopy. Peptides were dissolved in DMSO and stored at -20℃ until used [103]. The primary antibodies used were human Bax (B-9), p53, MDM2, CDK4, Cyclin D, p21, PAX3, c-MET, and GILT, (Santa Cruz Biotechnology Inc., Santa Cruz, CA); and b-actin (clone AC-15) (Sigma, St. Louis, MO). The secondary antibodies used were horseradish peroxidase conjugated anti-mouse (Pierce, Rockford, IL, USA), anti-rabbit or anti-goat IgG (Santa Cruz).

Ganoderic acid DM preparation

Ganoderic acid DM (GA-DM), originally isolated from the *Ganoderma lucidum* mushroom, was purchased from Planta Analytica, LLC (Danbury, CT) (Cat# G-032). The purity of GA-DM was determined by the vendor as 99.9 % using LC/MS analysis. GA-DM was dissolved in DMSO (Sigma) to make a 10 mM stock solution for use in the cytotoxicity assay. For all GA-DM treatments, DMSO final concentration was ≤1 %.

Preparation of cell lysates and western blotting

J3.DR4, HT-144.vec, and B16 cells were cultured for 24 hours in the presence of vehicle alone, 20, or 40 μM of GA-DM. Following treatment, cells were washed and cell lysate was obtained using a standard lysis buffer (10 mM Trizma base, 150 mm NaCl, 1 % Triton X-100). Equal protein concentrations from designated cell lysates were separated on a 4–12 % Bis/Tris NuPage gel (Invitrogen, Grand Island, NY). Proteins

were transferred onto a nitrocellulose membrane (Pierce, Rockford IL), and probed with antibodies for the expression of Bax, p53, MDM2, CDK4, Cyclin D, p21, PAX3, c-MET, and GILT. The secondary antibodies used were horseradish peroxidase conjugated anti-mouse (Pierce), anti-rabbit or anti-goat IgG (Santa Cruz Biotechnology). Monoclonal antibody for b-actin was used as a protein loading control.

Radiation, GA-DM, and Combination in vitro assays

J3.DR4, HT-144.vec, and B16 cells +/- GILT were grown to 80-90% confluence. Cells were washed two times with DPBS, trypsinized, and collected in 5ml media. Cells were spun down at 7000rpm for 5 minutes, media aspirated, the pellet was broken up, and reconstituted in 2ml of media. Cells were counted and reconstituted as $5x10^5$ cells per 500µl of media in 15ml conical tubes. No treatment cells (Vector-0, GILT-0) were placed on ice. Multiple radiation treatments were as follows: 5, 10, and 20Gy for appropriate tubes. After radiation, cells were mixed well, and 100µl of each cell type with each treatment were plated in triplicate on a flat bottom 96-well plate (cat# 3595, Corning Incorporated). For GA-DM or combination treatments, GA-DM was then added to appropriate wells for the final concentrations of 0 and 20µM. An additional 100µl of media was added to each well, bringing the total volume to 200µl per well. Plates were incubated for 48 hours or 5 days at 37 °C. After incubation, 50µl of 2.5% trypsin was added to each well. Plates were incubated 20-30 minutes at 37 °C, and checked under the microscope to determine if cells had lifted. Using a multichannel pipette, 100µl was removed from each well and placed in a protein estimation plate. Each well was

collected and counted using the trypan exclusion method for the number of live cells. Experiments were repeated at least three times and the data were expressed as percent cytotoxicity ± SD of triplicate wells.

Annexin V staining and flow cytometry

B16 cells were cultured for 5 days in the presence of vehicle alone, 20μM of GA-DM, 10Gy radiation, or combination of GA-DM and radiation. Following treatment, cells were collected and washed with staining buffer (PBS + 1 % heat-inactivated BGS) (HyClone) 2 times, and resuspended in 1x annexin binding buffer (cat. no. 556454, BD Bioscience: 0.1 M HEPES (pH 7.4), 1.4 M NaCl, and 25 mM CaCl2) at $1x10^6$cells/ml. 100ul were transferred to individuals tubes were cells were stained with 5ul of Annexin V-FITC (cat. no. 556420, 556419, BD Bioscience) alone, 5ul of 7-AAD (cat# 51-68981E, BD Bioscience)alone, and double staining of annexin V and 7-AAD. Cells were incubated for 15 minutes at room temperature. 400ul of 1x annexin binding buffer was added, and samples were transferred to FACS tubes. Samples were then analyzed on a FACScan using CellQuest software (BD Bioscience, Mountain View, CA) for apoptotic cells. Experiments were repeated at least three times.

MHC class II antigen presentation assay

B16/Ab cells ($5x10^5$cells/ml) were treated with either vehicle alone or 40 μM of GA-DM for 24 h at 37℃ in culture media in 96-well plate (cat#3595, Corning Incorporated). The $HEL_{74–88}$ peptide (10 μM) was added to the appropriate wells for the

last 4–6 h of incubation as described [139, 140] Cells were then washed and co-cultured with the $HEL_{74–88}$ peptide specific mouse T cell hybridoma (BO4) for 24 h. Following incubation, the plates were stored at -80℃ until tested for mouse IL-2 production. T cell production of mouse IL-2 was measured by enzyme-linked immunosorbent assay (ELISA) according to the manufacturer's instructions (R&D Systems, Minneapolis, MN, USA). Anti-IL-2 was purchased from Sigma-Aldrich. All assays were repeated at least three times.

In vivo tumor induction and evaluation

Tumors were induced by the subcutaneous injection of B16 cells (1x105 cells, >90% viability by Trypan blue exclusion) into the right flanks of 6-8 week old C57BL/6 mice from the Jackson Laboratory. Treatment was initiated by i.p. injection of GA-DM (25 mg/kg) at day 7 and day 11 for GA-DM only and Combination groups[239]. Localized radiation therapy was initiated at 1.5Gy fractions on days 8, 10, 14, and 16 after tumor injection for 6Gy overall per mouse, using 6 MeV and/or 9 MeV electron beams from a Varian 2100C linear accelerator located in Radiation Oncology and administered by personnel in radiation oncology [40]. Following treatment, tumor volumes were determined at periodic intervals using a digital caliper by measuring the longest diameter (a) and the next longest diameter (b) perpendicular to (a). Using these measurements, the tumor volume was calculated by the formula: $V = ab^2 \times \frac{\pi}{6}$ [243]. The mice were kept under observation until tumor volume was determined to be 1,400 mm^3 or when mice showed signs of severe stress. At this point, the mice were requisitely

euthanized. Tumor samples were collected to be fixed in 10% formalin, and kept in 70% ethanol. Serum was collected to be tested for cytokine production, and spleens were process to be tested for multiple cell populations via flow cytometry. Treatment or control groups consisted of six mice in experiment #1 and three mice in experiment #2. All work with mice was approved by the MUSC Animal Protocols Review Board and was performed in accordance with the National Institutes of Health Guide for Care and Use of Laboratory Animals.

Statistical Analysis

Data from each experimental group were subjected to statistical analysis. ANOVA with post hoc tests, Repeated measures ANOVA with post hoc tests or Student's t tests were used, as appropriate. Densitometry was measured as described in Chapters 2 and 3 of this study. Two-sided tests were used in all cases and p values <0.05 were considered statistically significant. Analysis of survival curves was done by the log-rank test. Parametrical analysis was done using a one-way ANOVA with the Bonferroni multiple comparison test. The estimates are based on a random effects model which uses linear regression and random intercepts to account for repeated measures over time. Comparisons between two groups over time were performed by two-way ANOVA. Comparisons between two groups were performed by the Student's t test (parametric) or Mann-Whitney U test (nonparametric). A p value < 0.05 was considered significant.

Results

GA-DM treatment upregulates pro-apoptotic Bax proteins in human melanoma cells.

Previous studies have shown that GA-DM treatment may lead to G1 cell cycle arrest [232, 233]. Although those studies used higher concentrations, the goal for this study was to determine if a lower concentration of GA-DM may induce apoptotic proteins in melanoma cells. Therefore, J3.DR4 and HT-144.vec cells were treated with or without 20μM of GA-DM for 24 hours and then subjected to cell lysate preparation for western blot analysis. The apoptotic protein Bax was tested, which is an apoptosis regulator that complements and antagonizes Bcl-2 [239]. In Figure 4.3, cells incubated with GA-DM displayed a significant increase in Bax protein expression (J3.DR4, $p=0.008$; HT-144.vec, $p=0.04$). This data suggests that GA-DM treatment may induce apoptotic events in melanoma cells, especially in a lower concentration. However, further analysis of multiple apoptosis proteins must be examined.

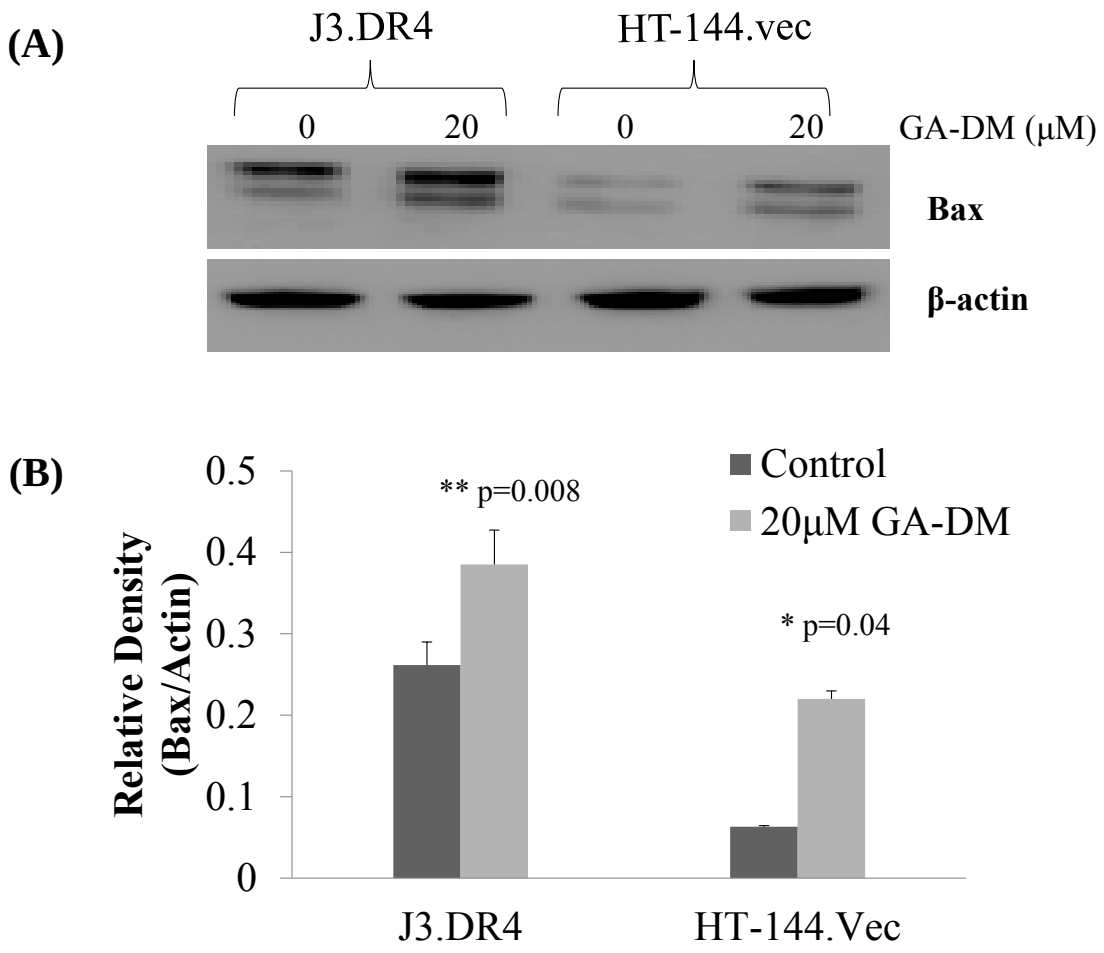

Figure 4.3 GA-DM treatment upregulates pro-apoptotic Bax proteins in human melanoma cells. (A) J3.DR4 and HT-144.vec melanoma cells were treated with 20μM GA-DM for 24 hours, and whole cell lysates were collected and analyzed through western blot analysis for Bax protein expression. GA-DM-treated cells expressed significantly higher levels of Bax proteins compared to untreated cells, as indicated by (B) densitometric analysis. Data are representative of at least three separate experiments.*$p<0.05$, **$p<0.01$.

GA-DM treatment upregulates p53 expression while suppressing MDM2.

Following this hypothetical model, I examined the tumor suppressor protein p53 and its counterpart MDM2. Normally, in unstressed cells, Mdm2 either binds itself to p53 to inactivate its transport or attaches ubiquitin to p53 to mark it for degradation by

the proteasome. Oftentimes, melanoma cells do not express p53 through loss-of-function, or p53 is mutated. In Figure 4.4, I tested melanoma cells J3.DR4 and HT-144.Vec with or without 24 hour GA-DM treatment (20μM). Cells were lysed, and protein expression was tested by western blot analysis. As shown, untreated cells expressed low levels of p53 protein while MDM2 expression was detected. However, cells treated with GA-DM displayed increased p53 expression while Mdm2 was greatly reduced. This data suggests that GA-DM treatment may lead to p53-dependent melanoma cellular death.

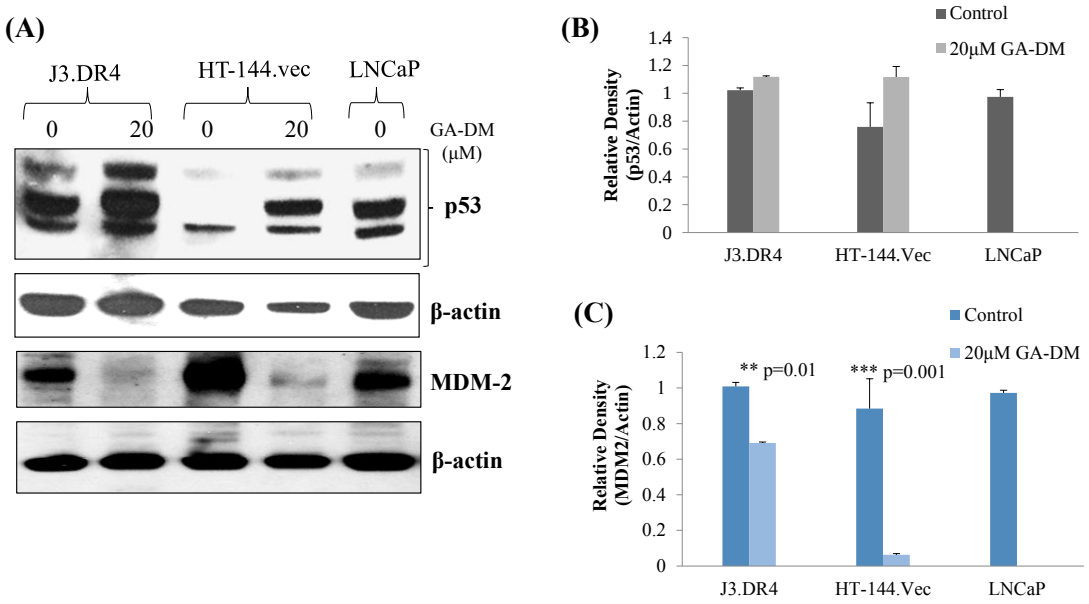

Figure 4.4 GA-DM treatment leads to apoptotic protein activation in human melanoma cells. Cells treated with 20μM GA-DM showed enhanced p53 expression while Mdm2 was decreased. LNCap, a human prostate cancer cell line, was used as a p53 positive control. This data suggests that GADM treatment may lead to p53-dependent melanoma cellular death. Data are representative of at least three separate experiments.*p<0.05, **p<0.01

GA-DM treatment influences cell cycle checkpoints in human melanoma cells.

Because of the increased p53 protein expression, I then tested the same cell lines

with the same treatment for expression of Cyclin D, CDK4, and p21. Typically, when p21 is activated, it blocks the binding interaction between CDK4 and Cyclin D, leading to cell cycle interruption. Using western blot analysis, it is shown in Figure 4.5 that GA-DM-treated melanoma cells expressed decreased CDK4 and increased Cyclin D compared to non-treated cells. In untreated cells, there is a dimer expression, but this is not seen in GA-DM treated cells. This may be due to the decreased expression of CDK4 observed. Also, there is an increase in p21 protein expression, further proving that this may disrupt Cyclin D/CDK4 interactions. This data suggests that GA-DM treatment affects cell cycle checkpoints in melanoma cells.

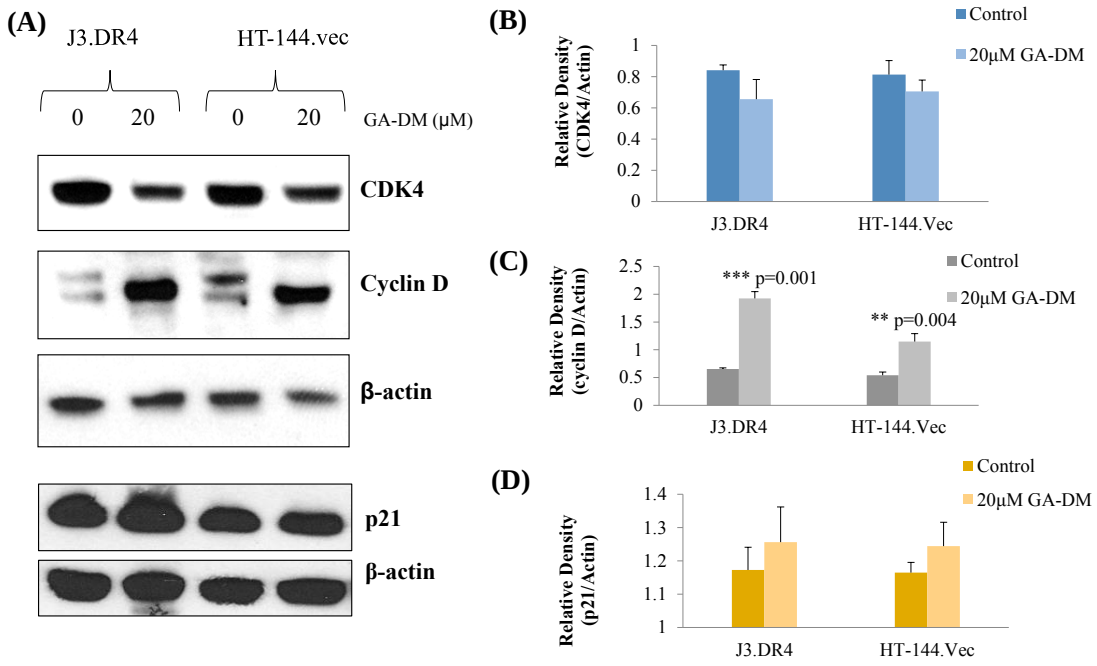

Figure 4.5 GA-DM treatment influences cell cycle checkpoints in human melanoma cells. (A) J3.DR4 and HT-144 melanoma cells were treated +/- GA-DM (20μM) for 24 hours and tested for protein expression by western blot analysis. GA-DM treatment downregulated CDK4 while affecting Cyclin D dimerization in both cell lines. GA-DM also upregulated p21 protein expression compared to untreated cells. This data suggests that GA-DM affects cell cycle checkpoints in melanoma cells. (B-D) Densitometric analysis for each protein tested, which was significant in Cyclin D, as indicated by *. β-actin was used as a loading control.

GA-DM treatment decreases PAX3 and c-MET proteins in human melanoma cells.

Data presented in the previous chapter suggested that GILT expression downregulated PAX3 in human melanoma cells. Our lab has previously shown that GA-DM could influence intracellular machinery of melanoma cells for HLA Class II processing and presentation to T cells for immune recognition [239]. Therefore, I wanted to investigate whether GA-DM treatment may also influence tumorigenic molecule PAX3 and its downstream target c-MET, due to their implications in cell survival and possible metastatic capabilities. Again, human melanoma cell lines J3.DR4 and HT-144.vec were treated with 20μM GA-DM and tested for PAX3 and c-MET proteins through western blotting. Figure 4.6 displays GA-DM-treated cells expressed significantly downregulated PAX3 and c-MET proteins compared to untreated cells (PAX3, $p=0.008$ & $p=0.005$; c-MET, $p=0.001$ & $p=0.008$). This data suggests that GA-DM may influence proteins with metastatic potential, which further adds to the anti-tumor properties that GA-DM possesses. Because both GILT insertion and GA-DM treatment may downregulate PAX3 in human melanoma cells, the next step would be to determine whether GA-DM may influence GILT expression to aid in PAX3 diminution.

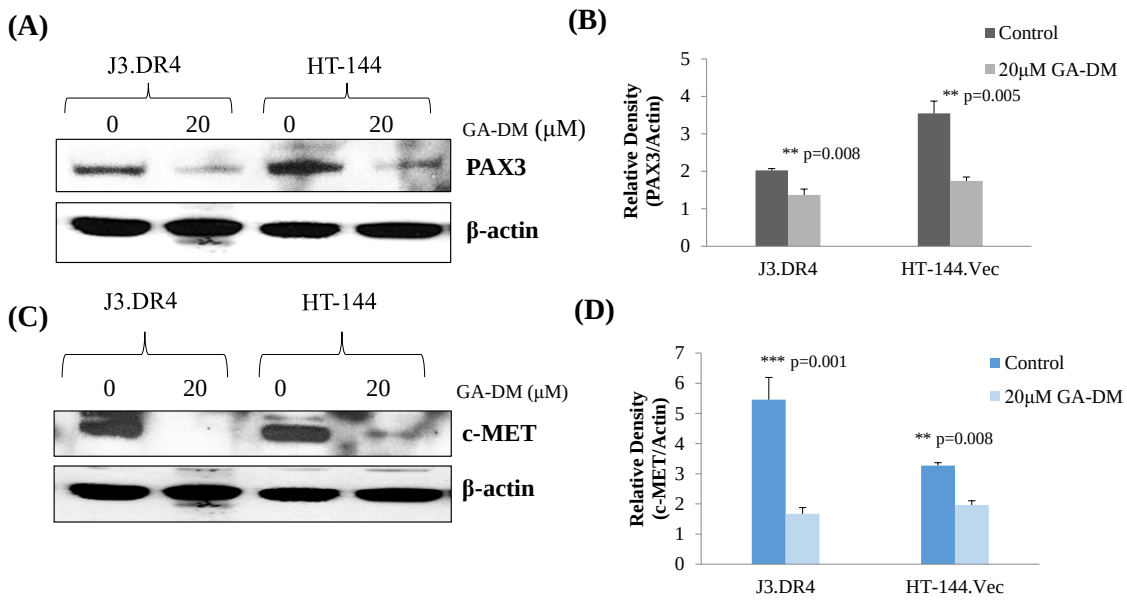

Figure 4.6 GA-DM treatment downregulates PAX3 and c-MET in human melanoma cells. J3.DR4 and HT-144.vec melanoma cells were treated with 20μM GA-DM for 24 hours, and whole cell lysates were collected and analyzed through western blot analysis for PAX3 and c-MET protein expressions. GA-DM-treated cells expressed significantly lower levels of (A) PAX3 and (C) c-MET proteins compared to untreated cells, as indicated by (B) and (D) densitometric analysis. β-actin was used as a loading control. Data are representative of at least three separate experiments.*p<0.05, **p<0.01

GA-DM treatment influences GILT and PAX3 proteins in mouse melanoma cells.

In order to test GA-DM treatment with radiation in vivo, the B16 mouse melanoma cell line was tested for PAX3 and GILT expression with or without GA-DM treatment. Unlike human melanoma cells, B16 mouse melanoma cells as well as normal melanocytes constitutively express PAX3 and GILT If treatment may increase the expression of GILT in these cells, the implications could be that Ag processing and presentation is potentially increased, cathepsins activity is enhanced, and that PAX3 inhibition may be occurring. Previous data suggests that human melanoma cells transfected with GILT displayed an increase in GILT expression when treated with GA-DM (data not shown). However, this had not been tested in a mouse melanoma cell line

with constitutive GILT expression. Therefore, after 24 hours of 20μM and 40μM GA-DM treatment, western blot analysis showed that GILT expression is increased in GA-DM treated cells compared untreated cells (Figure 4.7). Also, PAX3 expression was decreased when cells were treated with GA-DM in increasing doses. This indicates that GA-DM may enhance GILT expression as well as other components of the HLA Class II pathway while downregulating tumorigenic molecules involved in melanoma like PAX3.

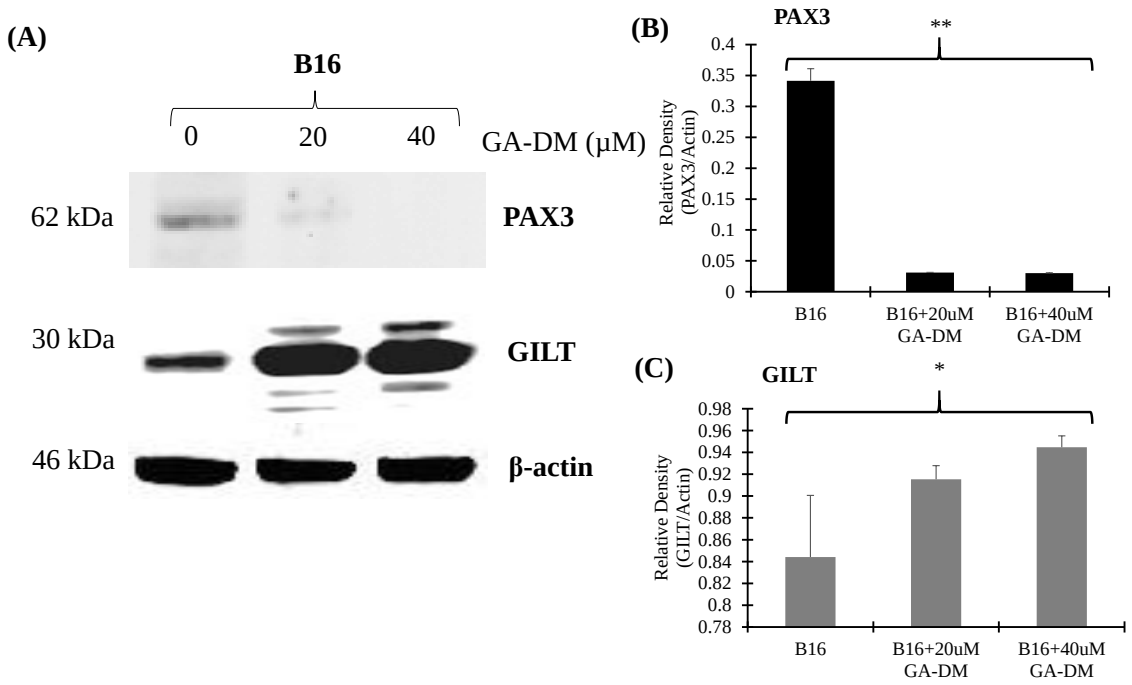

Figure 4.7 GA-DM treatment influences GILT and PAX3 proteins in B16 mouse melanoma cells. (A) B16 mouse melanoma cells were treated with 0, 20, or 40μM of GA-DM for 24 hours and tested for PAX3 and GILT protein expression via western blot analysis. Data suggests a significant decrease in PAX3 expression with GA-DM, while displaying a marked increase in GILT protein expression. Densitometric analysis for PAX3 (B) and GILT (C) determine significance as $p \leq 0.05$ (*) and $p \leq 0.01$ (**).

<u>GILT expression sensitizes melanoma cells to radiation therapy.</u>

PAX3 plays a role in cell survival during melanocytogenesis. However, it is unknown whether this is true in the development of melanoma. Interestingly, with GILT decreasing PAX3 expression in melanoma cells, the next step was to determine whether

this reduction would allow melanoma cells to be susceptible to cellular death. High-dose radiation is a common treatment for melanoma patients. Therefore, using lower doses of radiation through PAX3 targeting would be less toxic to patients. So, in Figure 4.8, I tested the melanoma cell lines HT-144.vec and HT-144.GILT in a radiation assay using different doses and incubated for 5 days. Cell viability was examined by the trypan blue exclusion method. Results show that the presence of functional GILT allowed more cells to die when compared to vector alone. This data suggests that PAX3 regulation by GILT sensitizes melanoma cells to radiation.

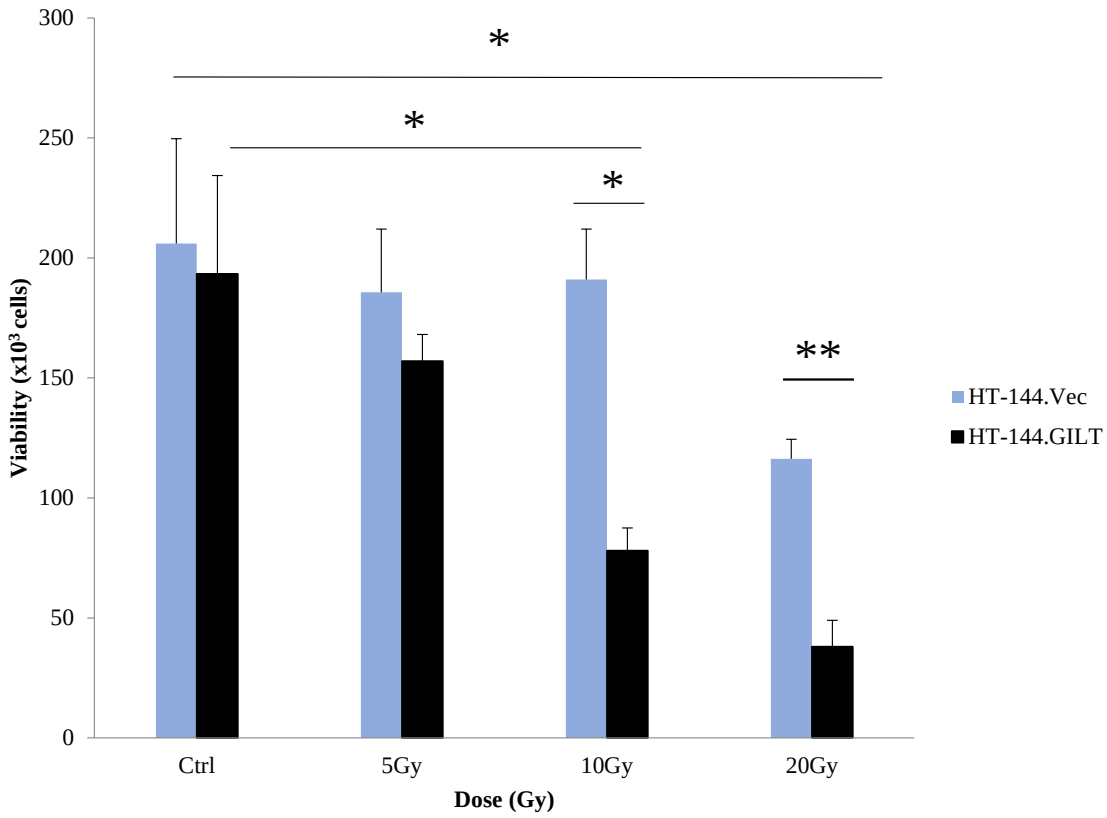

Figure 4.8 PAX3 targeting by GILT allows melanoma cell sensitization by radiation. Melanoma cell lines HT-144.vec and HT-144.GILT were subjected to different doses of radiation and incubated for 5 days. Cell viability was examined by the trypan blue exclusion method. Results show that cells with GILT were prone to cell death compared to vector alone, indicating that GILT expression sensitizes melanoma cells to radiation. Data are representative of at least three separate experiments.*p<0.05, **p<0.01

Mouse B16 melanoma cells were less viable 7 days after radiation treatment.

In order to test *in vivo*, the mouse melanoma cell line B16 was tested in a radiation assay as well. After growing B16 to 80-90% confluence, cells were subjected to varying doses of radiation (5, 10, or 20Gy) and incubated for 7 days. Cells were then

counted using the trypan blue exclusion method. As seen in Figure 4.9A, cell viability decreased with increasing doses of radiation. Due to these results, I used the radiation dose of 10Gy to further test the duration of cell viability. Therefore, B16 cells were cultured and subjected the cells to 10Gy radiation and incubated for a period of 3, 5, or 7 days and counted cells using the trypan blue exclusion method. In Figure 4.9B, cells were less viable as incubation increased after radiation exposure.

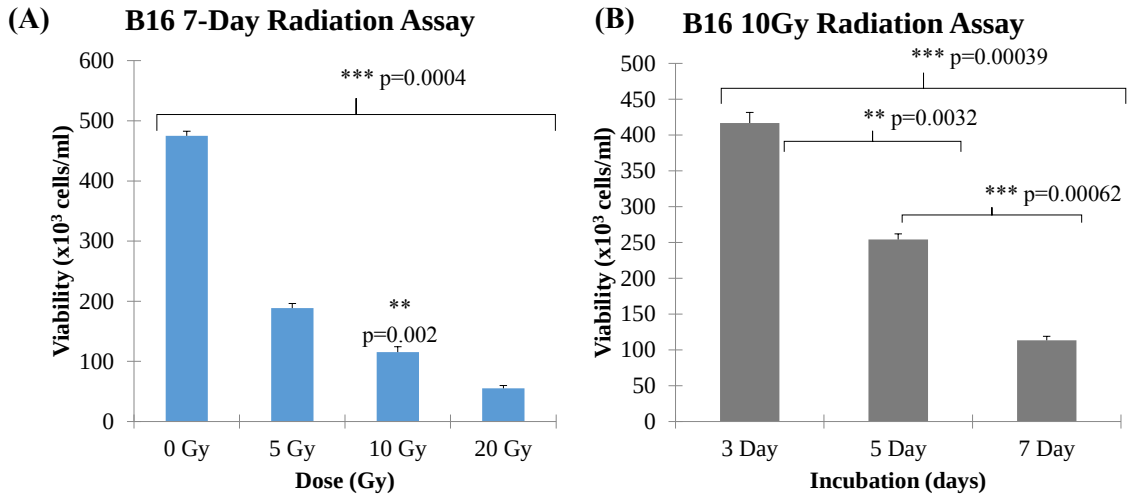

Figure 4.9 Radiation influences B16 growth. Mouse melanoma B16 cells were subjected to varying concentrations of radiation (0-20Gy) and incubated at multiple time points (3-7 days). Cells were collected, counted, and excluded using trypan blue. (A) B16 cells were exposed to varying doses of radiation and incubated for 7 days. There is a dose-dependent decrease in cellular viability with increased exposure to radiation. (B) B16 cells were exposed to 10Gy radiation and incubated from 3 to 7 days where a decrease in cell number was observed with longer incubation. Data are representative of at least three separate experiments.*p<0.05, **p<0.01

GA-DM treatment enhances radiation therapy of human and mouse melanoma cells.

Previous data showed that GILT expression downregulates PAX3, to aid in sensitizing melanoma cells to radiation therapy in both human and mouse melanoma cells. It was also found that GA-DM treatment enhanced GILT expression while decreasing PAX3 expression in both human and mouse melanoma cells. Therefore, I

wanted to test whether combining these treatments would further enhance cellular death. First, I tested HT-144 cells with or without GILT expression, and then subjected these cells to 10Gy radiation, 20uM GA-DM, or the combination of 10Gy with 20uM GA-DM treatments. Cells were incubated for 5 days, and cell viability was examined by the trypan blue exclusion method. Results indicate that cells with GILT expression were prone to cell death compared to vector alone, which was significantly enhanced in the combination treatment group (Figure 4.10).

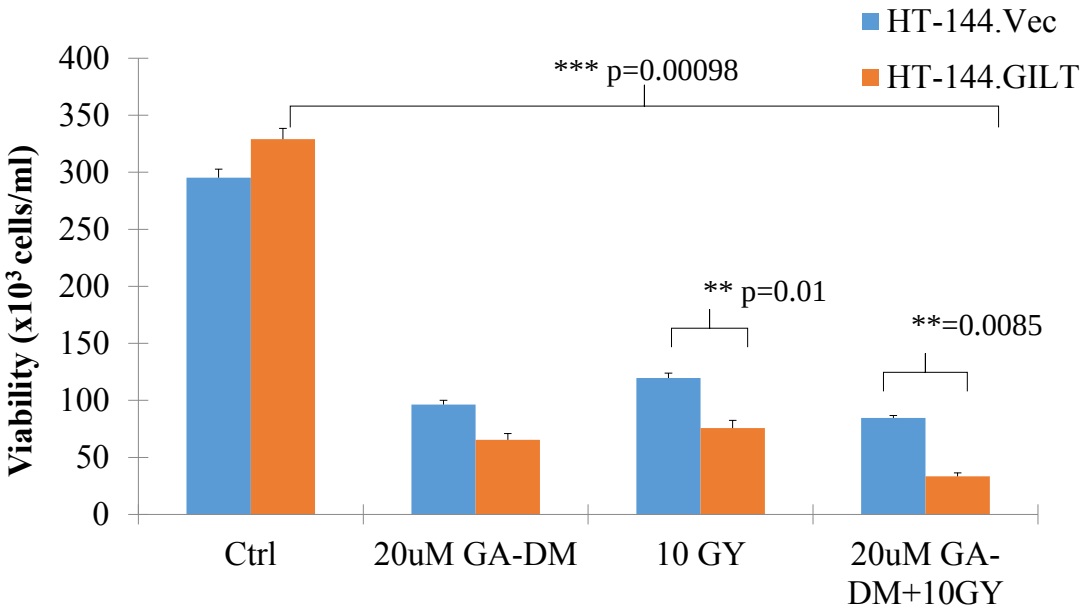

Figure 4.10 Combination treatment increases cellular death in human melanoma cells. Melanoma cell lines HT-144.vec and HT-144.GILT were subjected to 10Gy radiation, 20uM GA-DM, or the combination 10Gy and 20uM GA-DM treatments and incubated for 5 days. Cell viability was examined by the trypan blue exclusion method. Results indicate that cells with GILT were prone to cell death compared to vector alone, which was increased in the combination treatment group. Data are representative of at least three separate experiments.*p<0.05, **p<0.01

I also tested the B16 cell line using the same treatments, but grown for 7 days (Figure 4.11). Results show that, again, the combination treatment significantly enhanced cellular killing in B16 cells compared to radiation and GA-DM alone. This data suggests

that combination treatment may be a better strategy in killing melanoma cells than single treatments alone.

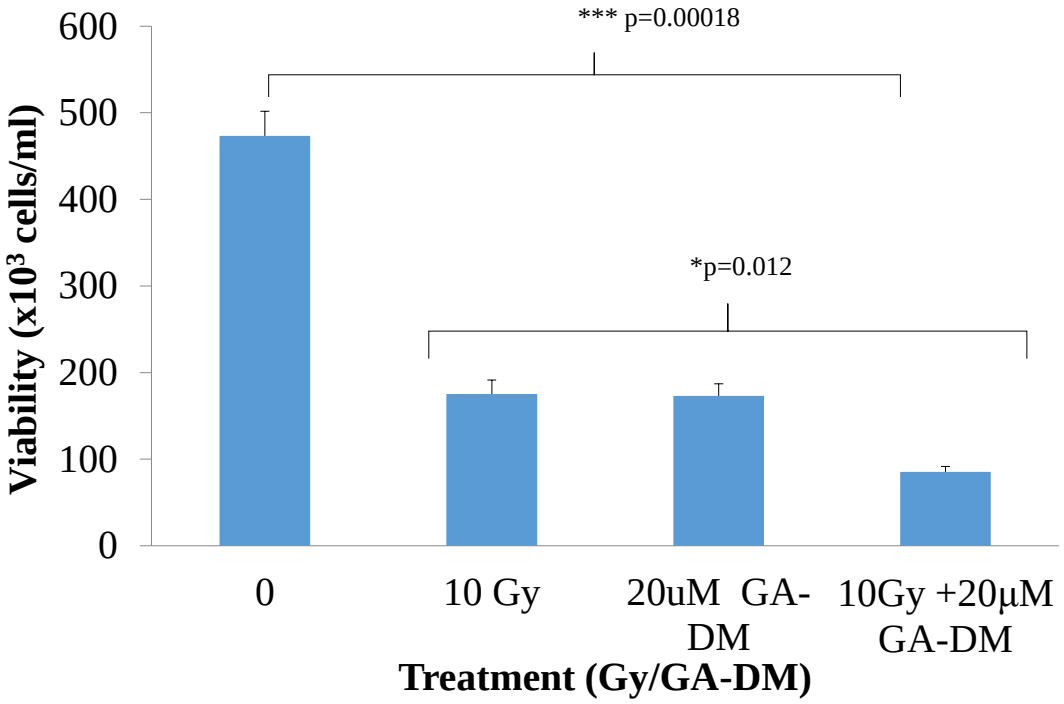

Figure 4.11 Combination treatment enhances cellular death in mouse melanoma cells. Mouse melanoma B16 cells were subjected to 10Gy radiation, 20uM GA-DM, or the combination 10Gy and 20uM GA-DM treatments and incubated for 7 days. Cell viability was examined by the trypan blue exclusion method. Results indicate that cells with GILT were prone to cell death compared to vector alone, which was significantly enhanced in the combination treatment group. Data are representative of at least three separate experiments.*p<0.05, **p<0.01

Combination treatments induce more apoptotic events compared to treatments alone.

In vitro data showed less cell viability in combination treatments among treatment groups in human and mouse melanoma cells. To investigate the mechanism of this cellular killing, B16 cells treated with radiation, GA-DM, or combination treatments were subjected to annexin V staining to determine of cells were undergoing apoptosis. Cells

were treated with 10Gy radiation, 20uM GA-DM, or the combination of 10Gy with 20uM GA-DM treatments, and cells were then collected on day 5. Cells were stained with annexin V which binds to the externalized phosphatidylserine during early stages of apoptosis. Flow cytometric analysis of treated B16 cells (Figure 4.12) show distinct subpopulations of low forward scatter (FSC) and high side scatter (SSC) profiles characteristic of apoptotic cells. Further analysis of cells showed higher proportion of the cells stained with annexin V combining both early and late stage of apoptosis. Apoptotic cells that double-stained with annexin V and 7-AAD, suggested further entry of 7-AAD into the apoptotic cells at an early stage where damage to the cell membrane occurred. Taken all together, data suggests that the combination treated cells led to increased apoptotic cell death compared to radiation and GA-DM alone.

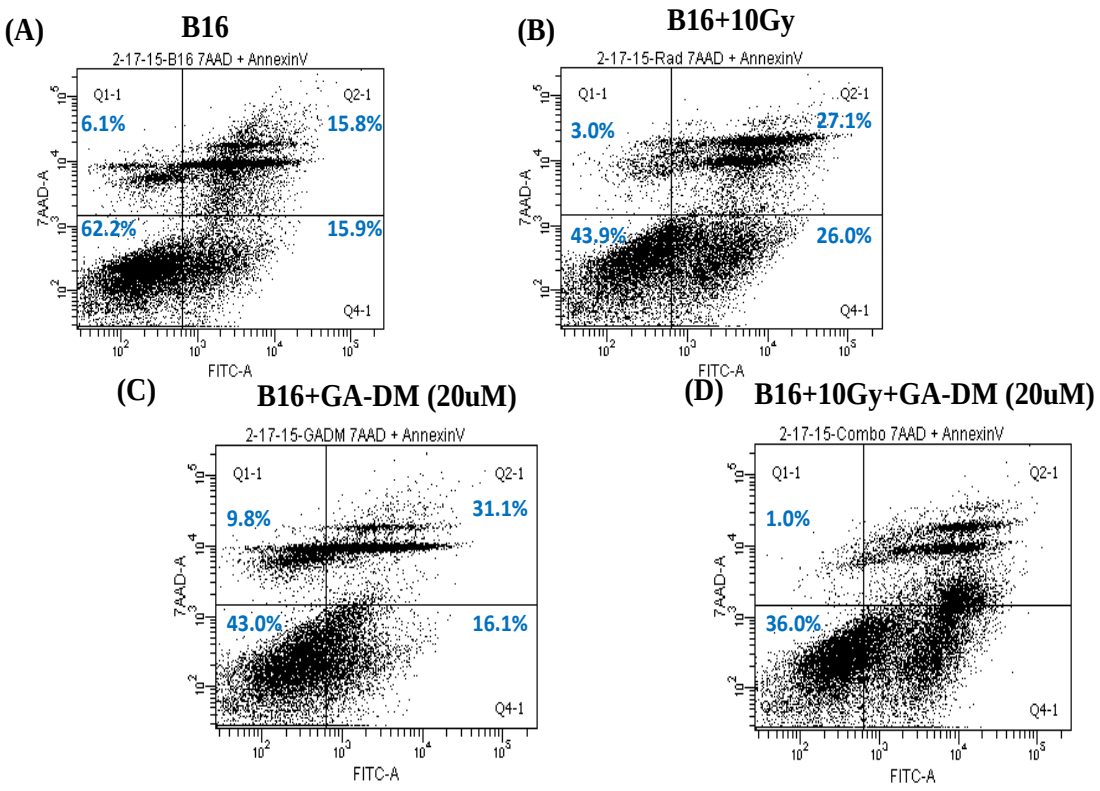

Figure 4.12 Combination treatment of GA-DM and radiation induces apoptosis in B16 cells. Contour diagrams of annexin V-FITC/7-AAD flow cytometry of B16 cells 5 days after (A) no treatment, (B) 10Gy irradiation, (C) 20uM GA-DM, or (D) combination of both treatments. Dot plot of forward and side scatter (20,000 events/samples, left panels), and annexin V/7-AAD double staining (right panels) were shown. The quadrant 4 (Q4-1) and quadrant 2 (Q2-1) represent the annexin V-positive early and late apoptotic cells, respectively.

<u>GA-DM enhances MHC class II-mediated antigen presentation by mouse melanoma cells.</u>

Our lab has previously shown that GA-DM can enhance HLA class II Ag presentation to T cells in human melanoma cells. Therefore, I wanted to test this in the mouse melanoma B16 to further investigate this treatment *in vivo*. B16/Ab cells were transfected by the lab of Dr. Ostrand-Rosenberg to express murine MHC class II. This cell line was given as a gift to our lab, where I tested for Ag processing and presentation to T cells. Cells were treated with or without 40uM GA-DM overnight and fed with $HEL_{74\text{-}88}$ peptide. The mouse T cell hybridoma BO4, which recognizes the I^a allele of

class II with peptide bond on B16/Ab cells, was co-cultured with B16/Ab cells, and supernatants were collected to test for IL-2 production via ELISA. The production of IL-2 is used as an indication of Ag presentation and T cell recognition. Figure 4.13 shows data shoes that GA-DM treatment enhances MHC class II-mediated Ag presentation and CD4+ T cell recognition of mouse melanoma cells. This data suggests GA-DM treatment further increases the CD4+ T cell response of melanoma cells while inducing cellular death affects.

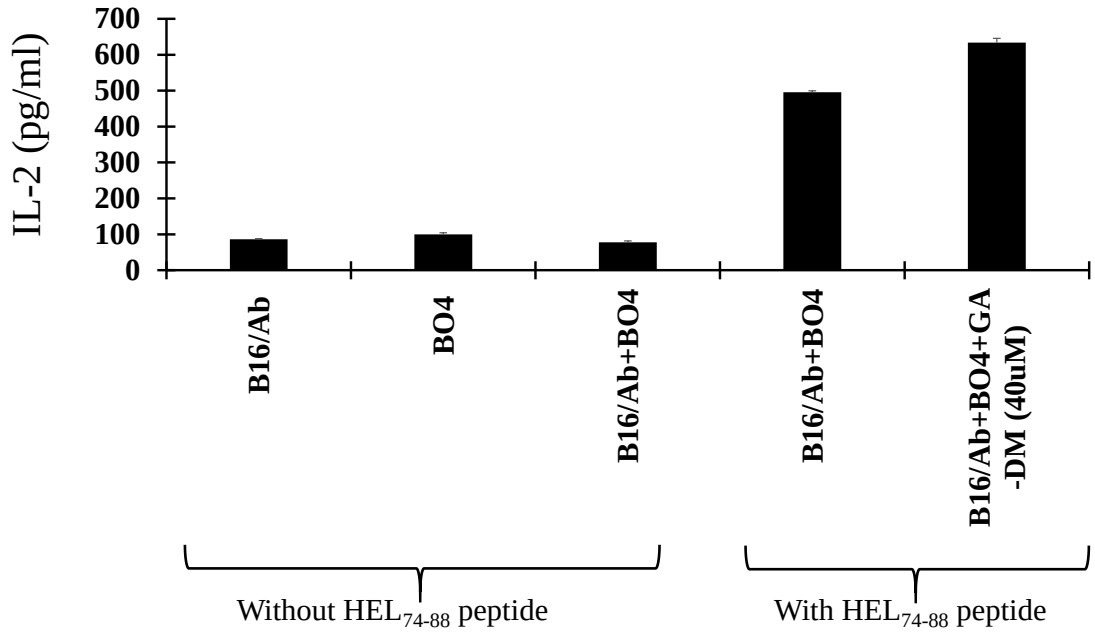

Figure 4.13 GA-DM treatment increases MHC class II-mediated Ag presentation and CD4+ T cell recognition of mouse melanoma cells. The mouse melanoma cell line B16/Ab was treated with or without 40uM GA-DM for 24 hours and then incubated with HEL_{74-88} overnight at 37°C. Cells were then washed, and co-cultured with the HEL_{74-88} peptide specific CD4+ T cell hybridoma line (BO4) for 24 h. T cell production of IL-2 in the culture supernatant was measured by ELISA. The production of IL-2 is used as an indication of Ag presentation and T cell recognition. Data are expressed as mean pg/ml +/- SD of triplicate wells of at least three independent experiments. *$p<0.01$.

Combination treatments significantly increased survival and decreased tumor volume, in treatment groups in vivo.

In order to investigate the potential therapeutic relevance of my in vitro data, the effects of the combination treatment, radiation only, and GA-DM only treatments were

examined in vivo using a B16 mouse melanoma model. Figure 4.14 is a schematic timeline of the treatments given. C57BL/6 mice were injected with $1x10^5$ cells subcutaneously in the right flanks.

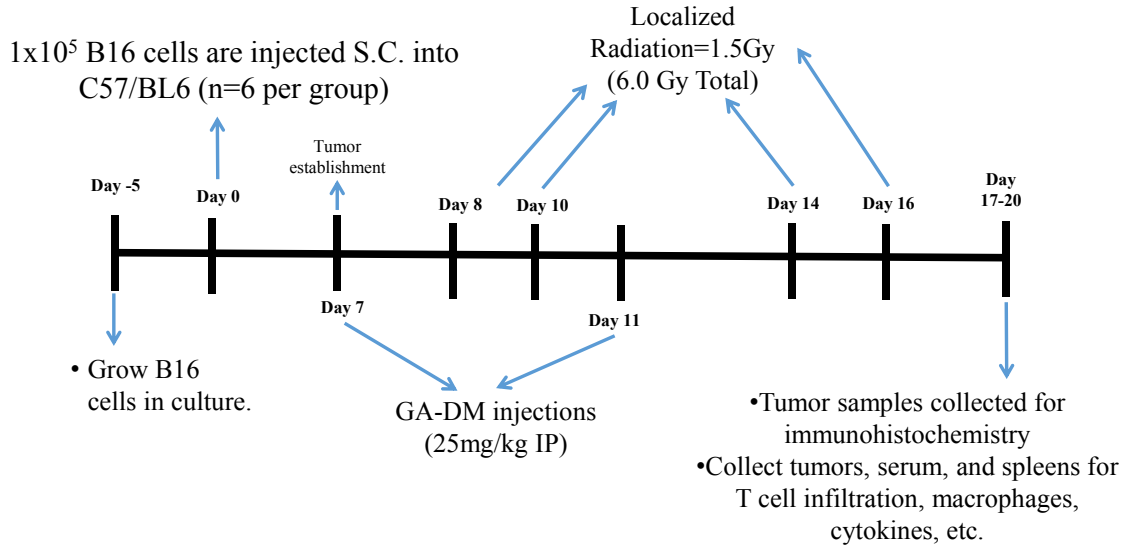

Figure 4.14 Schematic timeline of *in vivo* project for GA-DM and radiation treatments.

Tumors establish 7 days after injection, and GA-DM injections were given on days 7 and 11 at 25 mg/kg through i.p injection. Radiation treatments were given on days 8, 10, 14, and 16 for 6Gy overall. Tumors were measured as well as well-being of the mice until tumor volume reached over $1400mm^3$ or 15% weight loss.

Survival was also calculated in each experiment in vivo, as shown in Figure 4.15. The Kaplan-Meier curve displays a significant difference in survival overall, based on the log-rank test ($p=0.003$). The Combination treatment led to significantly enhanced survival compared to Control/Untreated and Radiation, $p=0.0031$ and $p=0.049$ respectively. There was no significant difference in survival between GA-DM alone versus Combination treatments. However, there were significant differences in survival

when comparing Control/Untreated with Radiation and GA-DM (p=0.02 and p=0.011, respectively). Table 4.2 summarizes the survival differences among treatment groups.

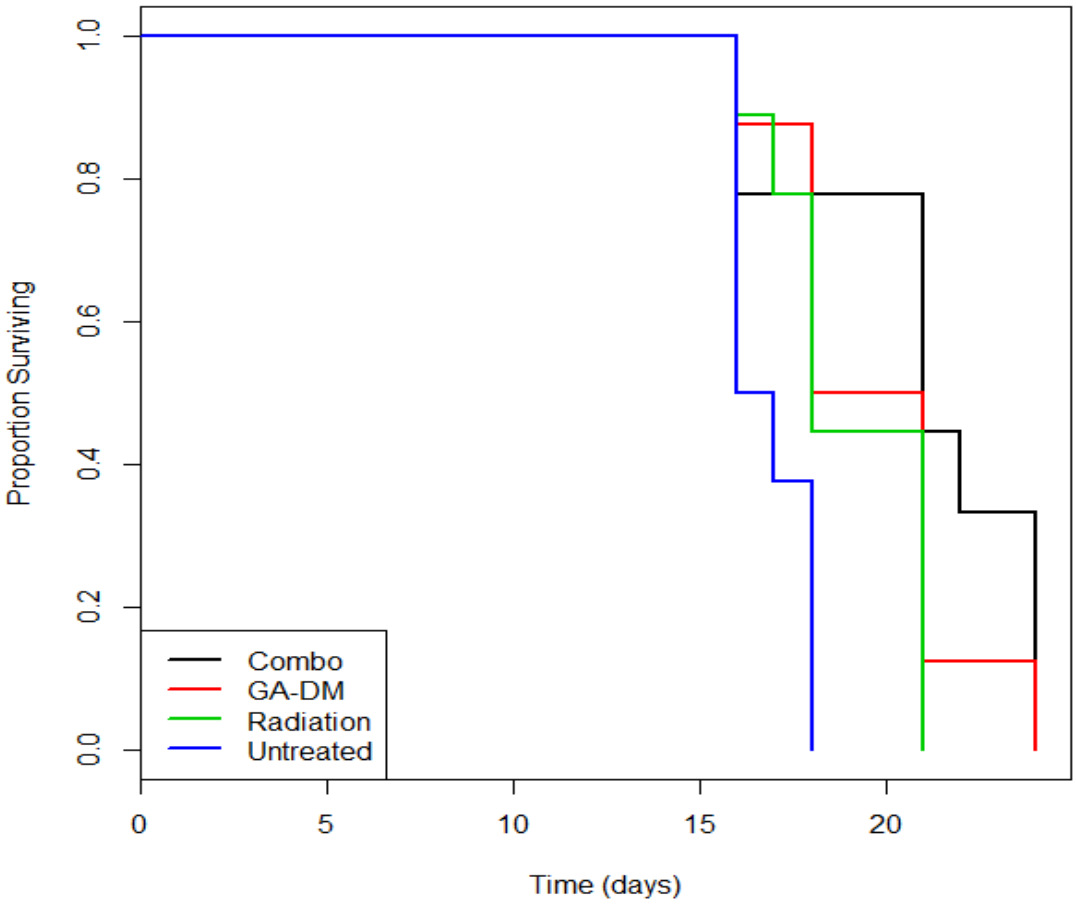

Figure 4.15 Combination and GA-DM groups displayed significantly prolonged survival among treatment groups. Kaplan-meier curves chart the survival for treatment groups. Overall survival was significant compared to the untreated group (p=0.003, log-rank test). The Combination treatment group displayed significantly enhanced survival compared to Untreated and Radiation groups (Untreated vs. Combo, p=0.0031, Radiation vs. Combo, p=0.049), although survival between GA-DM and Combo was not.

Table 4.2 Statistical Analysis of Survival among Treatment Groups.

Group 1	Group 2	p-value
Combination (black)	Control/Untreated (blue)	0.0031
Combination (black)	Radiation (green)	0.049
Combination (black)	GA-DM (red)	0.24
GA-DM (red)	Control/Untreated (blue)	0.011
Radiation (green)	Control/Untreated (blue)	0.02
GA-DM (red)	Radiation (green)	0.51
Values were calculated on the log-rank test, $p<0.05$ were considered statistically significant.		

In Figure 4.16, it was found that tumor volume was significantly reduced in the combinations treatment group at days 12 and 16, when compared to untreated, radiation only, and GA-DM alone (Tables 4.3, 4.4).

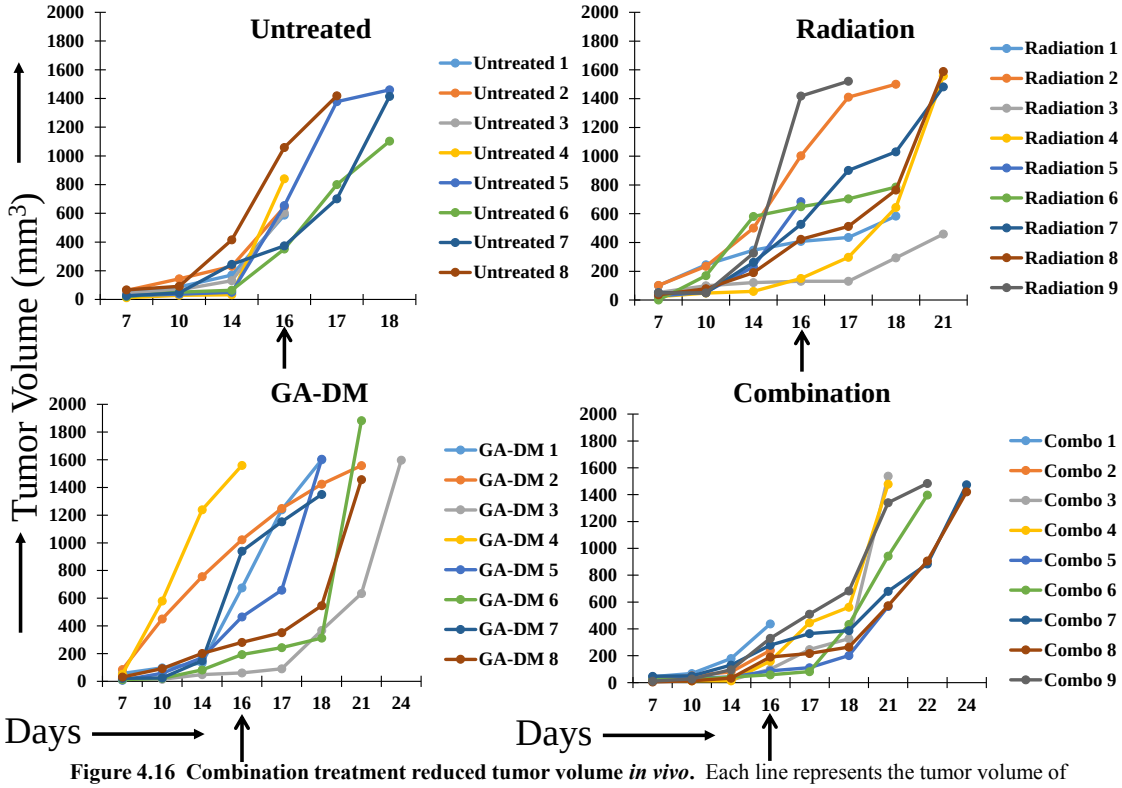

Figure 4.16 Combination treatment reduced tumor volume *in vivo*. Each line represents the tumor volume of one mouse for each treatment group. Tumor volume was delayed in the combination group compared to GA-DM and radiation alone. N=8, Control & GA-DM; N=9, Radiation & Combination

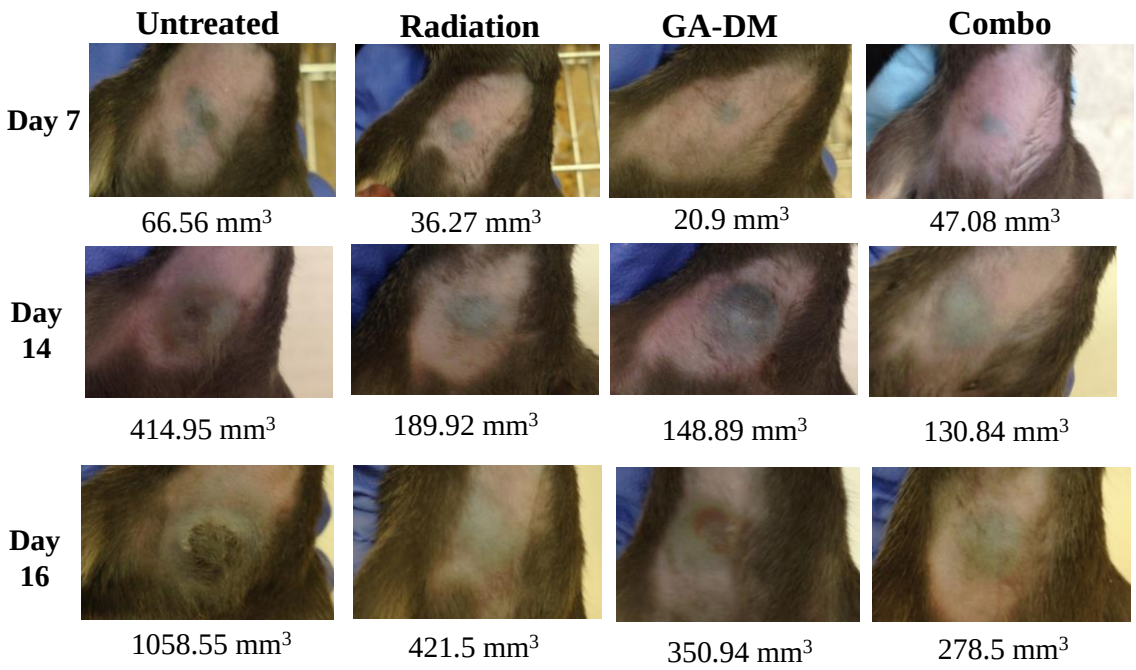

Figure 4.17 Combination treatment reduced tumor volume *in vivo*. A representative picture of one mouse per treatment group with appropriate tumor volume is displayed at days 7, 14, and 16.

Representative pictures were taken of one mouse per group to display increased tumor growth (Figure 4.17). The estimated tumor growth curves over time was graphed using a random effects model, which utilizes linear regression and random intercepts to account for repeated measures over time (Figure 4.18). Fold change in the tumor volume was also calculated among treatment groups. Inferences were based on days 12 and 16, where the fold change of the combination tumor volume was significantly lower compared to radiation and GA-DM groups at days 12 and 16, while combo and control was significant at day 16, shown in Figure 4.19.

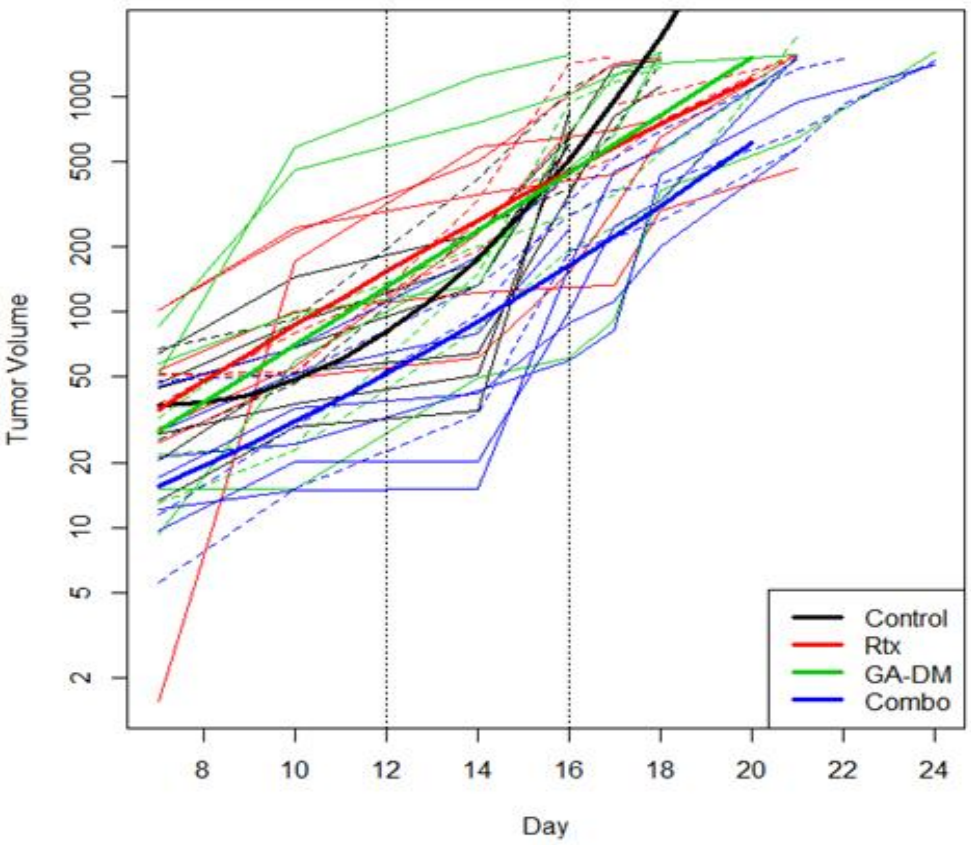

Figure 4.18 Estimated tumor growth curves per group over time. The estimates are based on a random effects model which uses linear regression and random intercepts to account for repeated measures over time. Due to the non-linear patterns, quadratic terms were included to account for curvature. Due to non-linearity, slopes cannot be compared. Two experiments were included: there is an experiment effect included in the regression model, the lines indicate experiment 1 (solid) vs. experiment 2(dashed).

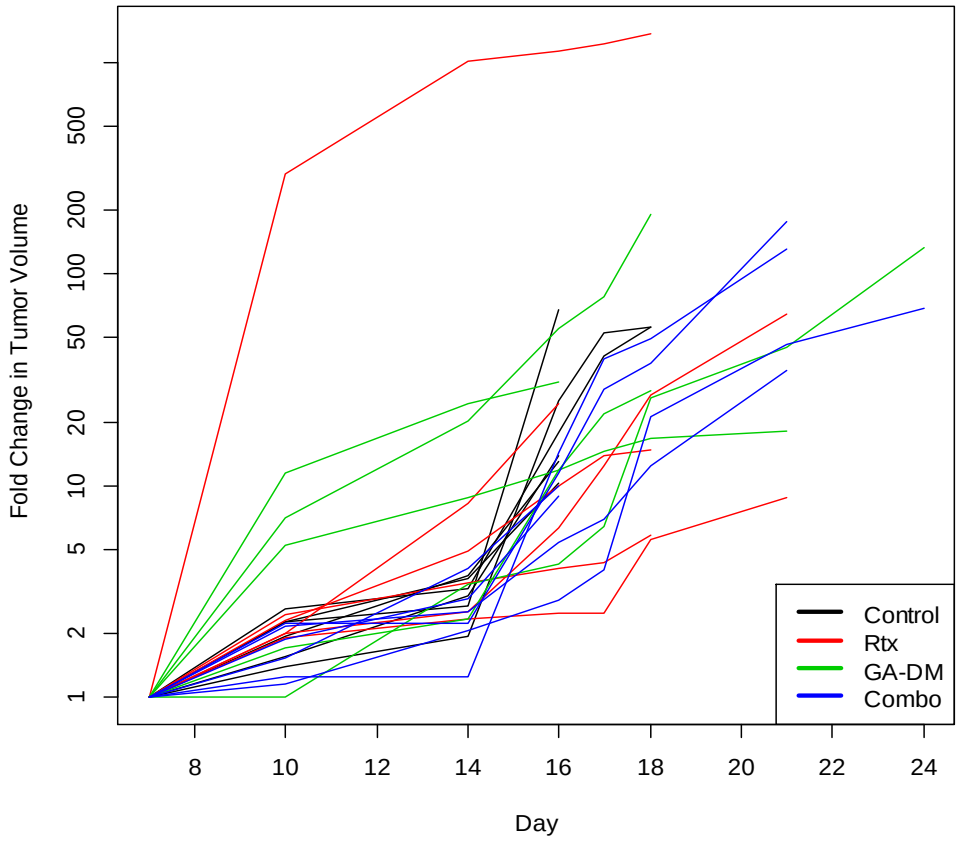

Figure 4.19 Fold change in tumor volume among treatment groups. Inferences were based on days 12 and 16. Statistical analysis suggests that the fold difference between Combo and Radiation and GA-DM treatment groups were significant at days 12 and 16, while Combo and Control was significant at day 16 (Tables 4.1 & 4.2).

Table 4.3 Tumor volume fold difference at Day 12.

Group 1	Group 2	**Day 12:** Fold difference in tumor size (group 2/group 1)	p-value
Control/Untreated (black)	Radiation (red)	1.90	0.064
Control/Untreated (black)	GA-DM (green)	1.60	0.17
Control/Untreated (black)	Combo (blue)	0.64	0.18
Radiation (red)	GA-DM (green)	0.84	0.59
Radiation (red)	Combo (blue)	0.34	0.0011
GA-DM (green)	Combo (blue)	0.40	0.0055
Inferences are based on comparing fitted tumor size at 12 days. Due to non-linearity, slopes cannot be compared.			

Table 4.4 Tumor volume fold difference at Day 16.

Group 1	Group 2	**Day 16:** Fold difference in tumor size (group 2/group 1)	p-value
Control/Untreated (black)	Radiation (red)	0.89	0.71
Control/Untreated (black)	GA-DM (green)	0.88	0.68
Control/Untreated (black)	Combo (blue)	0.32	0.0011
Radiation (red)	GA-DM (green)	0.98	0.96
Radiation (red)	Combo (blue)	0.36	0.0019
GA-DM (green)	Combo (blue)	0.37	0.0027
Inferences are based on comparing fitted tumor size at 16 days. Due to non-linearity, slopes cannot be compared.			

This data supports the previous data shown that combination treatments significantly reduce tumor burden. Altogether, this data suggests that the radiation/GA-

DM combination therapy possesses several antitumor properties that make it an attractive candidate for the development of novel therapeutic strategies.

Discussion & Conclusions

A defining feature of conventional anticancer therapies is their capacity to evoke cellular death by inducing cell apoptosis [239]. However, inherent or acquired resistances of cancer cells to mainstay treatments have been a major obstacle to complete treatment and sufficiently prevent tumor reoccurrence. Therefore, the search for new natural drugs that sensitize cancer cells to chemotherapy-mediated apoptosis, while also restoring antitumor immunity has increasingly become a focus of investigation [232, 239, 244]. This chapter shows that *G. lucidum*-derived triterpenoid GA-DM displays profound antitumor properties through alterations of cellular signaling and induction of apoptosis. GA-DM treatment leads to a p53-dependent apoptotic pathway, through multiple cell cycle checkpoints. It was also found GA-DM treatment enhanced GILT expression while downregulating PAX3 expression in B16 mouse melanoma cells, a similar trend found in human melanoma cell lines. This is further enhanced when combining with the mainstay treatment of radiation.

On the other hand, in the previous chapter, it was shown that functional GILT downregulates PAX3. Many studies have shown that targeting PAX3 leads to cell becoming susceptible to cellular death [206, 219]. Therefore, radiation treatment was used on both human and melanoma cells to determine cellular death. Results indicated that GILT expression led to enhanced killing of human melanoma cells compared to non-

GILT cells. B16, which naturally expresses GILT, also displayed increased cellular death with increasing doses of radiation. This suggests that the insertion of GILT in melanoma cells may lead to increased susceptibility for treatments. Combining radiation with GA-DM further enhanced cellular death in both human and mouse melanoma cells *in vitro*, compared to radiation and GA-DM alone. Annexin V staining supported this finding that combination treatments enhanced apoptosis in B16 cells compared to treatments alone. This promotes the efficacy of combining GA-DM treatment on melanoma cells with radiation therapy, utilizing the bioradiotherapy strategy.

Also, high-dose radiation and immunotherapies have proven to be highly toxic to patients with low response rates [194]. Thus, treatment strategies have been adopted to combine chemotherapy with immunotherapy to destroy cancer cells as well as elevate antitumor immunity to prevent further re-occurrence [245]. An agent that could enhance tumor immunogenicity while reducing tumor burden would be an ideal chemoimmunotherapeutic to overcome major obstacles in melanoma treatment [239]. Evidently, low concentrations of GA-DM have shown a much stronger effect in inducing an immune response, where surviving cells were capable of processing whole Ags for presentation to T cells. This chapter also highlighted that GA-DM enhanced MHC class II-mediated Ag presentation to CD4+ T cells in mouse melanoma cells. In order to investigate the potential therapeutic relevance of my in vitro data, the anti-tumor properties of GA-DM combined with radiation were examined in vivo using a B16 melanoma mouse model. I found that the administration of GA-DM combined with

radiation treatment significantly reduced tumor volume among treatment groups, which also significantly increased survival.

This study suggests that the radiation/GA-DM combination treatment makes for an attractive candidate for the development of novel therapeutics. GA-DM induced an upregulation of MHC class II that may prove to enhanced Ag presentation and T cell recognition of target cancer cells, confirming our previous findings in human melanoma cells. The beneficial effects of GA-DM with radiation were shown *in vivo* as evidenced by the significant decrease in tumor volume with significant increased survival.

Current treatments for metastatic melanoma include surgery, chemotherapy, high-dose radiation, and some immunotherapies. However, these treatments appear futile once the tumor has metastasized beyond localized lymph nodes. This stresses the need for improved disease targeting as well as new possibilities for combining treatments. Importantly, PAX3 plays a vital role in anti-apoptotic events during melanocyte development, and thus, targeting this tumorigenic protein may lead to a less aggressive, less metastatic form of melanoma. By targeting PAX3, melanoma cells may be susceptible to different types of treatments. [239]. Therefore, testing these treatments *in vivo* may reveal potential in using radiation-GA-DM combination treatment as a chemoimmunotherapy for treating metastatic melanoma.

Chapter 5: Summary and Conclusions

Metastatic melanoma is an aggressive disease that has been plaguing Western populations for many year. Finding a tolerable and effective treatment for melanoma has proven to be difficult. Current studies examining immunotherapies with common treatments have shown to provide the necessary boost to further improve tumor killing. The main goals of this dissertation were to examine the role of GILT in melanoma cells, determining the effect of GILT upon a known tumorigenic protein in metastatic melanoma, and investigating combination therapies to help combat this disease.

Data from the first aim of this study suggests multiple roles of GILT when present in melanoma cells. Although GILT's major role is in the catalysis of disulfide bonds formed between cysteine residues, it has been shown that GILT may also enhance cathepsin expression and activity. Localized in the endosomal/lysosomal compartments, it was found that GILT colocalizes with cathepsin B and D, which can lead to enhanced Ag processing and presentation. Bioassays testing for cathepsin activity confirmed this finding. With enhanced cathepsin activity, Ags undergo further splicing and processing to result in reduced, more functional peptides. These functional peptides can then be readily loaded onto HLA class II complexes to be presented and recognized by CD4+ T cells.

Because of enhanced cathepsin expression and activity with the presence of GILT, data acquired from mass spectroscopy suggests that GILT may aid in generating a greater pool of reduced, functional peptides and epitope generation. A greater pool of reduced IgG$\kappa_{188\text{-}203}$ peptide was present in J3.DR4.GILT cells as compared to J3.DR4.vec

cells, confirming GILT's ability to functionally reduce antigenic peptides needed for T cell recognition. In comparing GILT-positive to GILT-negative cells, cells with GILT expression were producing 44.7% tri-oxidized cysteine-containing peptides, which was significantly lower than 77.9% tri-oxidized cysteine-containing peptides generated from GILT-negative cells. With more functional peptides available, these peptides can be loaded onto class II molecules in presentation to CD4+ T cells, where we see enhanced IL-2 production from T cells. Enhancing presentation to the adaptive immune system can be exploited in a new immunotherapy approach, such as a whole cell vaccine strategy, as well as establishing memory in recurring malignant melanoma cells.

Results presented in the second aim of this dissertation also propose a new target and mechanism for late stage metastatic melanoma. The tumorigenic molecule PAX3 has been implicated in melanoma progression and metastasis. Data obtained showed that GILT decreases PAX3 protein expression. Confocal microscopy determined that this downregulation occurred through the colocalization of GILT and PAX3; this was confirmed that GILT and PAX3 have a protein-protein interaction through immunoprecipitation. Importantly, when using a GILT mutant transfected into the J3 melanoma cell line, functional GILT was required for PAX3 downregulation. GILT also was shown to enhance Daxx protein expression, a key regulator of PAX3. The elevated Daxx expression and the direct interaction with GILT may cause PAX3 downregulation. Also, GILT and Daxx may utilize the STAT1 pathway to regulate PAX3. Further studies will be conducted to determine how Daxx plays a role in the regulation of PAX3 when GILT is present.

This thesis also investigated the mechanism by which GILT is able to affect PAX3 expression. PAX3 has expression in both the nucleus and the cytosol, dominantly in the cytosol [87]. However, GILT's location is in the endosomal/lysosomal compartments. Data suggests that GILT is leading PAX3 to a lysosomal degradation fate. Because of GILT insertion, autophagic proteins like Beclin-1 and LC3 are influenced, and blocking lysosome function via bafilomycin allowed PAX3 proteins to endure in human melanoma cells with or without the presence of GILT. This suggests that GILT regulates PAX3 expression through the autophagy and lysosomal degradation pathway. Future studies of this aim may examine adapter proteins like heat shock proteins. These molecules are known for chaperoning other molecules and may be studied to determine how PAX3 relocates throughout the cell. Also, the PKC protein family may be studied as they have the ability to bind other signaling proteins, and they also have a role in modulating cellular processes such as vesicle trafficking and cell-cell communication [133]. Exploration of the autophagy and lysosomal degradation pathway may be examined to determine another role of GILT when present in melanoma cells. This aim showed that PAX3 is linked with late stage metastatic melanoma and is susceptible to targeted therapy. Such possibilities include using siRNA to block PAX3 transcription or using a cytotoxic drug targeting PAX3 to block its expression.

Aim three of this study investigated different therapeutic options to test upon both human and mouse melanoma cell lines and *in vivo*. GA-DM is a triterpenoid extract from *G. lucidum* that has many anti-proliferative properties, engaging intracellular signaling pathways, and induction of apoptosis. Apoptosis, a mechanism of programmed cell death,

is thought to be an important mechanism in tissue homeostasis [244]. This study outlined a model/signaling pathway that GA-DM treatment may lead melanoma cells through to induce apoptosis. Results from this thesis indicated that cells treated with GA-DM were lead to cellular death in a p53-dependent pathway. Cells with GA-DM treatment also saw a significant decrease in PAX3 expression in human and mouse melanoma cells. Importantly, GA-DM treatment significantly enhanced GILT expression in mouse melanoma cells. This increased expression of GILT by GA-DM may lead to an enhanced downregulation of PAX3. Allowing a downregulation of PAX3 may lead to susceptibility for melanoma cells to cellular death as well. On the other hand, melanoma cells that expressed GILT were also susceptible to radiation therapy compared to GILT-negative cells. This novel finding suggests that by treating melanoma cells with the combination of radiation with GA-DM, enhanced killing of melanoma cells may prove positive results *in vivo*.

B16 cells displayed susceptibility to both radiation and GA-DM treatment. These treatments also displayed a decrease in PAX3 expression while upregulating GILT. B16 cells transfected with MHC class II expression were also treated with GA-DM, and IL-2 was increased with GA-DM treatment compared to untreated cells. These findings led me to investigate whether the combination treatment may be beneficial in a mouse model. Therefore, using B16 in C57BL/6 mice, various treatments were tested to determine efficacy. Results indicated that the combination treatment increased survival and significantly reduced tumor volume among treatment groups. This study shows that

utilizing a combination treatment strategy may further enhance killing while inducing an immune response for potential memory for recurring cancer cells.

Future studies for this aim will investigate the immune components of the combination therapy *in vivo*. T cell infiltration will be examined within the tumor tissue among treatment groups at different time points. Previous studies in our lab have shown that T cells invade the tumor tissue by day 17 when mice were treated with 50 mg/kg GA-DM. It would be interesting to determine whether combination therapy may help in this aspect to help combat tumor growth. Other experiments will also look into the macrophage population within tumor tissue. Tumors may be examined via immunohistochemistry to determine the M1 versus M2 population of macrophages. Currently, the paradigm is that M1 macrophages express markers on the cell surface to suppress cancer progression while M2 macrophages promote it. Determining this facet within the tumor microenvironment, supported by serum cytokine expressions, may aid in the effectiveness that the combination therapy may have *in vivo*. Future studies for this project will also include optimizing multiple doses of both GA-DM and radiation therapy. This will help define the best overall dosage for both treatments by promoting tumor killing without cytotoxicity for the patient.

This study determined that combination treatments make for interesting candidates for the development of novel immunotherapeutics. If these strategies were used, we would hope to see a reduction in the aggressiveness and metastatic nature of melanoma cells. This study provides further insight into the complex nature of melanoma, and how novel targeting strategies are needed to combat this deadly disease.

List of References

1. Reed, K.B., et al., *Increasing incidence of melanoma among young adults: an epidemiological study in Olmsted County, Minnesota.* Mayo Clin Proc, 2012. **87**(4): p. 328-34.
2. Siegel, R., D. Naishadham, and A. Jemal, *Cancer statistics, 2013.* CA Cancer J Clin, 2013. **63**(1): p. 11-30.
3. Damsky, W.E., L.E. Rosenbaum, and M. Bosenberg, *Decoding melanoma metastasis.* Cancers (Basel), 2010. **3**(1): p. 126-63.
4. Ernfors, P., *Cellular origin and developmental mechanisms during the formation of skin melanocytes.* Exp Cell Res, 2010. **316**(8): p. 1397-407.
5. Wehrle-Haller, B. and J.A. Weston, *Soluble and cell-bound forms of steel factor activity play distinct roles in melanocyte precursor dispersal and survival on the lateral neural crest migration pathway.* Development, 1995. **121**(3): p. 731-42.
6. Ikeya, M., et al., *Wnt signalling required for expansion of neural crest and CNS progenitors.* Nature, 1997. **389**(6654): p. 966-70.
7. Hari, L., et al., *Lineage-specific requirements of beta-catenin in neural crest development.* J Cell Biol, 2002. **159**(5): p. 867-80.
8. Rimm, D.L., et al., *Frequent nuclear/cytoplasmic localization of beta-catenin without exon 3 mutations in malignant melanoma.* Am J Pathol, 1999. **154**(2): p. 325-9.
9. Garraway, L.A., et al., *Integrative genomic analyses identify MITF as a lineage survival oncogene amplified in malignant melanoma.* Nature, 2005. **436**(7047): p. 117-22.
10. Larue, L. and V. Delmas, *The WNT/Beta-catenin pathway in melanoma.* Front Biosci, 2006. **11**: p. 733-42.
11. Tang, A., et al., *E-cadherin is the major mediator of human melanocyte adhesion to keratinocytes in vitro.* J Cell Sci, 1994. **107 (Pt 4)**: p. 983-92.
12. Khoja, L., et al., *Circulating tumour cells as tumour biomarkers in melanoma: detection methods and clinical relevance.* Ann Oncol, 2015. **26**(1): p. 33-9.
13. Uzarska, M., et al., *Chemoprevention of skin melanoma: facts and myths.* Melanoma Res, 2013. **23**(6): p. 426-33.
14. de Maleissye, M.F., et al., *Parents' attitudes related to melanocytic nevus count in children.* Eur J Cancer Prev, 2010. **19**(6): p. 472-7.
15. Bennett, D.C., *Ultraviolet wavebands and melanoma initiation.* Pigment Cell Melanoma Res, 2008. **21**(5): p. 520-4.
16. Meyle, K.D. and P. Guldberg, *Genetic risk factors for melanoma.* Hum Genet, 2009. **126**(4): p. 499-510.
17. Tsao, H., et al., *Melanoma: from mutations to medicine.* Genes Dev, 2012. **26**(11): p. 1131-55.
18. Kamijo, T., et al., *Functional and physical interactions of the ARF tumor suppressor with p53 and Mdm2.* Proc Natl Acad Sci U S A, 1998. **95**(14): p. 8292-7.
19. Zhang, Y., Y. Xiong, and W.G. Yarbrough, *ARF promotes MDM2 degradation and*

stabilizes p53: ARF-INK4a locus deletion impairs both the Rb and p53 tumor suppression pathways. Cell, 1998. **92**(6): p. 725-34.
20. Lin, K., et al., *High frequency of p53 dysfunction and low level of VH mutation in chronic lymphocytic leukemia patients using the VH3-21 gene segment.* Blood, 2003. **102**(3): p. 1145-6.
21. Muthusamy, V., et al., *Amplification of CDK4 and MDM2 in malignant melanoma.* Genes Chromosomes Cancer, 2006. **45**(5): p. 447-54.
22. Fargnoli, M.C., et al., *MC1R variants increase melanoma risk in families with CDKN2A mutations: a meta-analysis.* Eur J Cancer, 2010. **46**(8): p. 1413-20.
23. Moustakas, A., *TGF-beta targets PAX3 to control melanocyte differentiation.* Dev Cell, 2008. **15**(6): p. 797-9.
24. Hathaway, J.D. and A. Haque, *Insights into the Role of PAX-3 in the Development of Melanocytes and Melanoma.* Open Cancer J, 2011. **4**: p. 1-6.
25. Yokoyama, S., et al., *A novel recurrent mutation in MITF predisposes to familial and sporadic melanoma.* Nature, 2011. **480**(7375): p. 99-103.
26. Chin, L., L.A. Garraway, and D.E. Fisher, *Malignant melanoma: genetics and therapeutics in the genomic era.* Genes Dev, 2006. **20**(16): p. 2149-82.
27. Davies, H., et al., *Mutations of the BRAF gene in human cancer.* Nature, 2002. **417**(6892): p. 949-54.
28. Rutkowski, P. and C. Blank, *Dabrafenib for the treatment of BRAF V600-positive melanoma: a safety evaluation.* Expert Opin Drug Saf, 2014. **13**(9): p. 1249-58.
29. Liu, F., et al., *Stat3-targeted therapies overcome the acquired resistance to vemurafenib in melanomas.* J Invest Dermatol, 2013. **133**(8): p. 2041-9.
30. Michaloglou, C., et al., *BRAFE600-associated senescence-like cell cycle arrest of human naevi.* Nature, 2005. **436**(7051): p. 720-4.
31. Pollock, P.M., et al., *Melanoma mouse model implicates metabotropic glutamate signaling in melanocytic neoplasia.* Nat Genet, 2003. **34**(1): p. 108-12.
32. Waldmann, A., et al., *Skin cancer screening participation and impact on melanoma incidence in Germany--an observational study on incidence trends in regions with and without population-based screening.* Br J Cancer, 2012. **106**(5): p. 970-4.
33. Tentori, L., P.M. Lacal, and G. Graziani, *Challenging resistance mechanisms to therapies for metastatic melanoma.* Trends Pharmacol Sci, 2013. **34**(12): p. 656-66.
34. Bajetta, E., et al., *Multicenter phase III randomized trial of polychemotherapy (CVD regimen) versus the same chemotherapy (CT) plus subcutaneous interleukin-2 and interferon-alpha2b in metastatic melanoma.* Ann Oncol, 2006. **17**(4): p. 571-7.
35. Atkins, M.B., et al., *Phase III trial comparing concurrent biochemotherapy with cisplatin, vinblastine, dacarbazine, interleukin-2, and interferon alfa-2b with cisplatin, vinblastine, and dacarbazine alone in patients with metastatic malignant melanoma (E3695): a trial coordinated by the Eastern Cooperative Oncology Group.* J Clin Oncol, 2008. **26**(35): p. 5748-54.
36. Garbe, C., et al., *Systematic review of medical treatment in melanoma: current*

status and future prospects. Oncologist, 2011. **16**(1): p. 5-24.
37. Avril, M.F., et al., *Fotemustine compared with dacarbazine in patients with disseminated malignant melanoma: a phase III study.* J Clin Oncol, 2004. **22**(6): p. 1118-25.
38. Bedikian, A.Y., et al., *Bcl-2 antisense (oblimersen sodium) plus dacarbazine in patients with advanced melanoma: the Oblimersen Melanoma Study Group.* J Clin Oncol, 2006. **24**(29): p. 4738-45.
39. Eigentler, T.K., et al., *Palliative therapy of disseminated malignant melanoma: a systematic review of 41 randomised clinical trials.* Lancet Oncol, 2003. **4**(12): p. 748-59.
40. Elvington, M., et al., *Complement-dependent modulation of antitumor immunity following radiation therapy.* Cell Rep, 2014. **8**(3): p. 818-30.
41. Khan, N., et al., *The evolving role of radiation therapy in the management of malignant melanoma.* Int J Radiat Oncol Biol Phys, 2011. **80**(3): p. 645-54.
42. Jenrette, J.M., *Malignant melanoma: the role of radiation therapy revisited.* Semin Oncol, 1996. **23**(6): p. 759-62.
43. Sause, W.T., et al., *Fraction size in external beam radiation therapy in the treatment of melanoma.* Int J Radiat Oncol Biol Phys, 1991. **20**(3): p. 429-32.
44. Temam, S., et al., *Postoperative radiotherapy for primary mucosal melanoma of the head and neck.* Cancer, 2005. **103**(2): p. 313-9.
45. Fenig, E., et al., *Role of radiation therapy in the management of cutaneous malignant melanoma.* Am J Clin Oncol, 1999. **22**(2): p. 184-6.
46. Dudley, M.E., et al., *Adoptive cell transfer therapy following non-myeloablative but lymphodepleting chemotherapy for the treatment of patients with refractory metastatic melanoma.* J Clin Oncol, 2005. **23**(10): p. 2346-57.
47. Antony, P.A., et al., *CD8+ T cell immunity against a tumor/self-antigen is augmented by CD4+ T helper cells and hindered by naturally occurring T regulatory cells.* J Immunol, 2005. **174**(5): p. 2591-601.
48. Finn, L., S.N. Markovic, and R.W. Joseph, *Therapy for metastatic melanoma: the past, present, and future.* BMC Med, 2012. **10**: p. 23.
49. Trunzer, K., et al., *Pharmacodynamic effects and mechanisms of resistance to vemurafenib in patients with metastatic melanoma.* J Clin Oncol, 2013. **31**(14): p. 1767-74.
50. Chapman, P.B., et al., *Improved survival with vemurafenib in melanoma with BRAF V600E mutation.* N Engl J Med, 2011. **364**(26): p. 2507-16.
51. McDermott, J. and A. Jimeno, *Pembrolizumab: PD-1 inhibition as a therapeutic strategy in cancer.* Drugs Today (Barc), 2015. **51**(1): p. 7-20.
52. Poulikakos, P.I. and N. Rosen, *Mutant BRAF melanomas--dependence and resistance.* Cancer Cell, 2011. **19**(1): p. 11-5.
53. Barker, C.A. and M.A. Postow, *Combinations of radiation therapy and immunotherapy for melanoma: a review of clinical outcomes.* Int J Radiat Oncol Biol Phys, 2014. **88**(5): p. 986-97.
54. Punt, C.J., et al., *Chemoimmunotherapy with dacarbazine, cisplatin, interferon-alpha2b and interleukin-2 versus two cycles of dacarbazine followed by*

chemoimmunotherapy in patients with metastatic melanoma: a randomised phase II study of the European Organization for Research and Treatment of Cancer Melanoma Group. Eur J Cancer, 2006. **42**(17): p. 2991-5.
55. Graziani, G., L. Tentori, and P. Navarra, *Ipilimumab: a novel immunostimulatory monoclonal antibody for the treatment of cancer.* Pharmacol Res, 2012. **65**(1): p. 9-22.
56. Barker, C.A., et al., *Concurrent radiotherapy and ipilimumab immunotherapy for patients with melanoma.* Cancer Immunol Res, 2013. **1**(2): p. 92-8.
57. Gerber, N.K., et al., *Ipilimumab and whole brain radiation therapy for melanoma brain metastases.* J Neurooncol, 2015. **121**(1): p. 159-65.
58. Ma, Y.M., et al., *A pilot study on acute inflammation and cancer: a new balance between IFN-gamma and TGF-beta in melanoma.* J Exp Clin Cancer Res, 2009. **28**: p. 23.
59. Zhang, Q.J., et al., *TAP expression reduces IL-10 expressing tumor infiltrating lymphocytes and restores immunosurveillance against melanoma.* Int J Cancer, 2007. **120**(9): p. 1935-41.
60. Kim, S.H., et al., *Repression of TNF-alpha-induced IL-8 expression by the glucocorticoid receptor-beta involves inhibition of histone H4 acetylation.* Exp Mol Med, 2009. **41**(5): p. 297-306.
61. Wang, C.T., et al., *Over-expression of receptor activator of nuclear factor-kappaB ligand (RANKL), inflammatory cytokines, and chemokines in periprosthetic osteolysis of loosened total hip arthroplasty.* Biomaterials, 2010. **31**(1): p. 77-82.
62. Zwirner, N.W. and C.I. Domaica, *Cytokine regulation of natural killer cell effector functions.* Biofactors, 2010. **36**(4): p. 274-88.
63. Hofmann, M.A., et al., *Serum TNF-alpha, B2M and sIL-2R levels are biological correlates of outcome in adjuvant IFN-alpha2b treatment of patients with melanoma.* J Cancer Res Clin Oncol, 2010.
64. Chichiarelli, S., et al., *Role of ERp57 in the signaling and transcriptional activity of STAT3 in a melanoma cell line.* Arch Biochem Biophys, 2010. **494**(2): p. 178-83.
65. Li, L., et al., *The invasive potential of human melanoma cell lines correlates with their ability to alter fibroblast gene expression in vitro and the stromal microenvironment in vivo.* Int J Cancer, 2009. **125**(8): p. 1796-804.
66. Kruger-Krasagakes, S., et al., *Expression of interleukin 10 in human melanoma.* Br J Cancer, 1994. **70**(6): p. 1182-5.
67. Cesana, G.C., et al., *Characterization of CD4+CD25+ regulatory T cells in patients treated with high-dose interleukin-2 for metastatic melanoma or renal cell carcinoma.* J Clin Oncol, 2006. **24**(7): p. 1169-77.
68. Ribatti, D. and A. Vacca, *Novel therapeutic approaches targeting vascular endothelial growth factor and its receptors in haematological malignancies.* Curr Cancer Drug Targets, 2005. **5**(8): p. 573-8.
69. Melnikova, V.O. and M. Bar-Eli, *Inflammation and melanoma metastasis.* Pigment Cell Melanoma Res, 2009. **22**(3): p. 257-67.
70. Sala, R., et al., *The human melanoma associated protein melanotransferrin*

promotes endothelial cell migration and angiogenesis in vivo. Eur J Cell Biol, 2002. **81**(11): p. 599-607.
71. Petreaca, M.L., et al., *Transactivation of vascular endothelial growth factor receptor-2 by interleukin-8 (IL-8/CXCL8) is required for IL-8/CXCL8-induced endothelial permeability.* Mol Biol Cell, 2007. **18**(12): p. 5014-23.
72. Birrane, G., A. Soni, and J.A. Ladias, *Structural basis for DNA recognition by the human PAX3 homeodomain.* Biochemistry, 2009. **48**(6): p. 1148-55.
73. Ria, R., et al., *Angiogenesis and progression in human melanoma.* Dermatol Res Pract, 2010. **2010**: p. 185687.
74. Hofmann, K.W., et al., *Interleukin-6 serum levels in patients with Parkinson's disease.* Neurochem Res, 2009. **34**(8): p. 1401-4.
75. Waugh, D.J. and C. Wilson, *The interleukin-8 pathway in cancer.* Clin Cancer Res, 2008. **14**(21): p. 6735-41.
76. Wang, D. and A. Richmond, *Nuclear factor-kappa B activation by the CXC chemokine melanoma growth-stimulatory activity/growth-regulated protein involves the MEKK1/p38 mitogen-activated protein kinase pathway.* J Biol Chem, 2001. **276**(5): p. 3650-9.
77. Karst, A.M., et al., *Nuclear factor kappa B subunit p50 promotes melanoma angiogenesis by upregulating interleukin-6 expression.* Int J Cancer, 2009. **124**(2): p. 494-501.
78. Liu, G., et al., *Selective induction of interleukin-8 expression in metastatic melanoma cells by transforming growth factor-beta 1.* Cytokine, 2005. **31**(3): p. 241-9.
79. Kondratiev, S., et al., *Expression and prognostic role of MMP2, MMP9, MMP13, and MMP14 matrix metalloproteinases in sinonasal and oral malignant melanomas.* Hum Pathol, 2008. **39**(3): p. 337-43.
80. Bosserhoff, A.K., *Novel biomarkers in malignant melanoma.* Clin Chim Acta, 2006. **367**(1-2): p. 28-35.
81. Beshir, A.B., et al., *Raf kinase inhibitor protein suppresses nuclear factor-kappaB-dependent cancer cell invasion through negative regulation of matrix metalloproteinase expression.* Cancer Lett, 2010.
82. Seftor, R.E., et al., *Cooperative interactions of laminin 5 gamma2 chain, matrix metalloproteinase-2, and membrane type-1-matrix/metalloproteinase are required for mimicry of embryonic vasculogenesis by aggressive melanoma.* Cancer Res, 2001. **61**(17): p. 6322-7.
83. Hofmann, U.B., et al., *Expression and activation of matrix metalloproteinase-2 (MMP-2) and its co-localization with membrane-type 1 matrix metalloproteinase (MT1-MMP) correlate with melanoma progression.* J Pathol, 2000. **191**(3): p. 245-56.
84. Kerkela, E. and U. Saarialho-Kere, *Matrix metalloproteinases in tumor progression: focus on basal and squamous cell skin cancer.* Exp Dermatol, 2003. **12**(2): p. 109-25.
85. Berinstein, N.L., *Strategies to enhance the therapeutic activity of cancer vaccines: using melanoma as a model.* Ann N Y Acad Sci, 2009. **1174**: p. 107-17.

86. Norton, D.L. and A. Haque, *Insights into the Role of GILT in HLA Class II Antigen Processing and Presentation by Melanoma.* J Oncol, 2009. **2009**: p. 142959.
87. Reipert, B.M., et al., *Opportunities and limitations of mouse models humanized for HLA class II antigens.* J Thromb Haemost, 2009. **7 Suppl 1**: p. 92-7.
88. Rocha, N. and J. Neefjes, *MHC class II molecules on the move for successful antigen presentation.* EMBO J, 2008. **27**(1): p. 1-5.
89. Brown, J.H., et al., *Three-dimensional structure of the human class II histocompatibility antigen HLA-DR1.* Nature, 1993. **364**(6432): p. 33-9.
90. Bikoff, E.K., et al., *Defective major histocompatibility complex class II assembly, transport, peptide acquisition, and CD4+ T cell selection in mice lacking invariant chain expression.* J Exp Med, 1993. **177**(6): p. 1699-712.
91. Roche, P.A. and P. Cresswell, *Invariant chain association with HLA-DR molecules inhibits immunogenic peptide binding.* Nature, 1990. **345**(6276): p. 615-8.
92. Rudensky, A. and C. Beers, *Lysosomal cysteine proteases and antigen presentation.* Ernst Schering Res Found Workshop, 2006(56): p. 81-95.
93. Shi, G.P., et al., *Cathepsin S required for normal MHC class II peptide loading and germinal center development.* Immunity, 1999. **10**(2): p. 197-206.
94. Driessen, C., et al., *Cathepsin S controls the trafficking and maturation of MHC class II molecules in dendritic cells.* J Cell Biol, 1999. **147**(4): p. 775-90.
95. Costantino, C.M., et al., *Lysosomal cysteine and aspartic proteases are heterogeneously expressed and act redundantly to initiate human invariant chain degradation.* J Immunol, 2008. **180**(5): p. 2876-85.
96. Moss, C.X., J.A. Villadangos, and C. Watts, *Destructive potential of the aspartyl protease cathepsin D in MHC class II-restricted antigen processing.* Eur J Immunol, 2005. **35**(12): p. 3442-51.
97. Goldstein, O.G., et al., *Gamma-IFN-inducible-lysosomal thiol reductase modulates acidic proteases and HLA class II antigen processing in melanoma.* Cancer Immunol Immunother, 2008. **57**(10): p. 1461-70.
98. Mosyak, L., D.M. Zaller, and D.C. Wiley, *The structure of HLA-DM, the peptide exchange catalyst that loads antigen onto class II MHC molecules during antigen presentation.* Immunity, 1998. **9**(3): p. 377-83.
99. Denzin, L.K., et al., *Assembly and intracellular transport of HLA-DM and correction of the class II antigen-processing defect in T2 cells.* Immunity, 1994. **1**(7): p. 595-606.
100. Rosenberg, S.A., J.C. Yang, and N.P. Restifo, *Cancer immunotherapy: moving beyond current vaccines.* Nat Med, 2004. **10**(9): p. 909-15.
101. Haque, M.A., et al., *Absence of gamma-interferon-inducible lysosomal thiol reductase in melanomas disrupts T cell recognition of select immunodominant epitopes.* J Exp Med, 2002. **195**(10): p. 1267-77.
102. Li, P., M.A. Haque, and J.S. Blum, *Role of disulfide bonds in regulating antigen processing and epitope selection.* J Immunol, 2002. **169**(5): p. 2444-50.
103. Haque, M.A., J.W. Hawes, and J.S. Blum, *Cysteinylation of MHC class II*

ligands: peptide endocytosis and reduction within APC influences T cell recognition. J Immunol, 2001. **166**(7): p. 4543-51.
104. Phan, U.T., R.L. Lackman, and P. Cresswell, *Role of the C-terminal propeptide in the activity and maturation of gamma -interferon-inducible lysosomal thiol reductase (GILT).* Proc Natl Acad Sci U S A, 2002. **99**(19): p. 12298-303.
105. Phan, U.T., B. Arunachalam, and P. Cresswell, *Gamma-interferon-inducible lysosomal thiol reductase (GILT). Maturation, activity, and mechanism of action.* J Biol Chem, 2000. **275**(34): p. 25907-14.
106. Arunachalam, B., et al., *Enzymatic reduction of disulfide bonds in lysosomes: characterization of a gamma-interferon-inducible lysosomal thiol reductase (GILT).* Proc Natl Acad Sci U S A, 2000. **97**(2): p. 745-50.
107. Rausch, M.P. and K.T. Hastings, *GILT modulates CD4+ T-cell tolerance to the melanocyte differentiation antigen tyrosinase-related protein 1.* J Invest Dermatol, 2012. **132**(1): p. 154-62.
108. Maric, M., et al., *Defective antigen processing in GILT-free mice.* Science, 2001. **294**(5545): p. 1361-5.
109. O'Donnell, P.W., et al., *Cutting edge: induction of the antigen-processing enzyme IFN-gamma-inducible lysosomal thiol reductase in melanoma cells Is STAT1-dependent but CIITA-independent.* J Immunol, 2004. **173**(2): p. 731-5.
110. Bosch, J.J., et al., *MHC class II-transduced tumor cells originating in the immune-privileged eye prime and boost CD4(+) T lymphocytes that cross-react with primary and metastatic uveal melanoma cells.* Cancer Res, 2007. **67**(9): p. 4499-506.
111. Seliger, B., M.J. Maeurer, and S. Ferrone, *Antigen-processing machinery breakdown and tumor growth.* Immunol Today, 2000. **21**(9): p. 455-64.
112. Ray, S., et al., *Obstacles to and opportunities for more effective peptide-based therapeutic immunization in human melanoma.* Clin Dermatol, 2009. **27**(6): p. 603-13.
113. Xie, Y., et al., *Naive tumor-specific CD4(+) T cells differentiated in vivo eradicate established melanoma.* J Exp Med. **207**(3): p. 651-67.
114. Quezada, S.A., et al., *Tumor-reactive CD4(+) T cells develop cytotoxic activity and eradicate large established melanoma after transfer into lymphopenic hosts.* J Exp Med. **207**(3): p. 637-50.
115. Bosch, J.J., et al., *Uveal melanoma cell-based vaccines express MHC II molecules that traffic via the endocytic and secretory pathways and activate CD8(+) cytotoxic, tumor-specific T cells.* Cancer Immunol Immunother. **59**(1): p. 103-12.
116. Bioley, G., et al., *Melan-A/MART-1-specific CD4 T cells in melanoma patients: identification of new epitopes and ex vivo visualization of specific T cells by MHC class II tetramers.* J Immunol, 2006. **177**(10): p. 6769-79.
117. Zarour, H.M., et al., *Melan-A/MART-1(51-73) represents an immunogenic HLA-DR4-restricted epitope recognized by melanoma-reactive CD4(+) T cells.* Proc Natl Acad Sci U S A, 2000. **97**(1): p. 400-5.
118. Ebert, L.M., et al., *A long, naturally presented immunodominant epitope from NY-ESO-1 tumor antigen: implications for cancer vaccine design.* Cancer Res, 2009.

69(3): p. 1046-54.
119. Hunder, N.N., et al., *Treatment of metastatic melanoma with autologous CD4+ T cells against NY-ESO-1.* N Engl J Med, 2008. **358**(25): p. 2698-703.
120. Zarour, H.M., et al., *NY-ESO-1 encodes DRB1*0401-restricted epitopes recognized by melanoma-reactive CD4+ T cells.* Cancer Res, 2000. **60**(17): p. 4946-52.
121. Kierstead, L.S., et al., *gp100/pmel17 and tyrosinase encode multiple epitopes recognized by Th1-type CD4+T cells.* Br J Cancer, 2001. **85**(11): p. 1738-45.
122. Enk, C.D., et al., *Molecular detection of MART-1, tyrosinase and MIA in peripheral blood, lymph nodes and metastatic sites of stage III/IV melanoma patients.* Melanoma Res, 2004. **14**(5): p. 361-5.
123. Trepiakas, R., et al., *Vaccination with autologous dendritic cells pulsed with multiple tumor antigens for treatment of patients with malignant melanoma: results from a phase I/II trial.* Cytotherapy.
124. Campillo, J.A., et al., *Natural killer receptors on CD8 T cells and natural killer cells from different HLA-C phenotypes in melanoma patients.* Clin Cancer Res, 2006. **12**(16): p. 4822-31.
125. Frankel, T.L., et al., *Both CD4 and CD8 T cells mediate equally effective in vivo tumor treatment when engineered with a highly avid TCR targeting tyrosinase.* J Immunol. **184**(11): p. 5988-98.
126. Ahmadzadeh, M., et al., *Tumor antigen-specific CD8 T cells infiltrating the tumor express high levels of PD-1 and are functionally impaired.* Blood, 2009. **114**(8): p. 1537-44.
127. Prieto, P.A., et al., *Enrichment of CD8+ cells from melanoma tumor-infiltrating lymphocyte cultures reveals tumor reactivity for use in adoptive cell therapy.* J Immunother. **33**(5): p. 547-56.
128. Zeng, G., et al., *Identification of CD4+ T cell epitopes from NY-ESO-1 presented by HLA-DR molecules.* J Immunol, 2000. **165**(2): p. 1153-9.
129. Phan, U.T., M. Maric, and P. Cresswell, *Disulfide reduction in major histocompatibility complex class II-restricted antigen processing by interferon-gamma-inducible lysosomal thiol reductase.* Methods Enzymol, 2002. **348**: p. 43-8.
130. Haque, A., et al., *Induction of apoptosis and immune response by all-trans retinoic acid plus interferon-gamma in human malignant glioblastoma T98G and U87MG cells.* Cancer Immunol Immunother, 2007. **56**(5): p. 615-25.
131. Wells, A.D., H. Gudmundsdottir, and L.A. Turka, *Following the fate of individual T cells throughout activation and clonal expansion. Signals from T cell receptor and CD28 differentially regulate the induction and duration of a proliferative response.* J Clin Invest, 1997. **100**(12): p. 3173-83.
132. Ndejembi, M.P., et al., *Control of memory CD4 T cell recall by the CD28/B7 costimulatory pathway.* J Immunol, 2006. **177**(11): p. 7698-706.
133. Hsu, K.F., et al., *Cathepsin L mediates resveratrol-induced autophagy and apoptotic cell death in cervical cancer cells.* Autophagy, 2009. **5**(4): p. 451-60.
134. Devetzi, M., et al., *Cathepsin B protein levels in endometrial cancer: Potential*

value as a tumour biomarker. Gynecol Oncol, 2009. **112**(3): p. 531-6.
135. Costantino, C.M., H.L. Ploegh, and D.A. Hafler, *Cathepsin S regulates class II MHC processing in human CD4+ HLA-DR+ T cells.* J Immunol, 2009. **183**(2): p. 945-52.
136. Rhodes, J.M. and A.B. Andersen, *Role of cathepsin D in the degradation of human serum albumin by peritoneal macrophages and veiled cells in antigen presentation.* Immunol Lett, 1993. **37**(2-3): p. 103-10.
137. Pathak, S.S. and J.S. Blum, *Endocytic recycling is required for the presentation of an exogenous peptide via MHC class II molecules.* Traffic, 2000. **1**(7): p. 561-9.
138. Hiraiwa, A., et al., *Structural requirements for recognition of the HLA-Dw14 class II epitope: a key HLA determinant associated with rheumatoid arthritis.* Proc Natl Acad Sci U S A, 1990. **87**(20): p. 8051-5.
139. Radwan, F.F., et al., *Mechanisms regulating enhanced human leukocyte antigen class II-mediated CD4 + T cell recognition of human B-cell lymphoma by resveratrol.* Leuk Lymphoma, 2012. **53**(2): p. 305-14.
140. Zhao, D., et al., *Enhancement of HLA class II-restricted CD4+ T cell recognition of human melanoma cells following treatment with bryostatin-1.* Cell Immunol, 2011. **271**(2): p. 392-400.
141. Radfar, S., Y. Wang, and H.T. Khong, *Activated CD4+ T cells dramatically enhance chemotherapeutic tumor responses in vitro and in vivo.* J Immunol, 2009. **183**(10): p. 6800-7.
142. Hurwitz, A.A., E.D. Kwon, and A. van Elsas, *Costimulatory wars: the tumor menace.* Curr Opin Immunol, 2000. **12**(5): p. 589-96.
143. Greenwald, R.J., G.J. Freeman, and A.H. Sharpe, *The B7 family revisited.* Annu Rev Immunol, 2005. **23**: p. 515-48.
144. Prieto, P.A., et al., *Enrichment of CD8+ cells from melanoma tumor-infiltrating lymphocyte cultures reveals tumor reactivity for use in adoptive cell therapy.* J Immunother, 2010. **33**(5): p. 547-56.
145. Hsing, L.C. and A.Y. Rudensky, *The lysosomal cysteine proteases in MHC class II antigen presentation.* Immunol Rev, 2005. **207**: p. 229-41.
146. Honey, K. and A.Y. Rudensky, *Lysosomal cysteine proteases regulate antigen presentation.* Nat Rev Immunol, 2003. **3**(6): p. 472-82.
147. Marks, M.S., J.S. Blum, and P. Cresswell, *Invariant chain trimers are sequestered in the rough endoplasmic reticulum in the absence of association with HLA class II antigens.* J Cell Biol, 1990. **111**(3): p. 839-55.
148. Cresswell, P., *Assembly, transport, and function of MHC class II molecules.* Annu Rev Immunol, 1994. **12**: p. 259-93.
149. Teyton, L. and P.A. Peterson, *Assembly and transport of MHC class II molecules.* New Biol, 1992. **4**(5): p. 441-7.
150. Stern, L.J., I. Potolicchio, and L. Santambrogio, *MHC class II compartment subtypes: structure and function.* Curr Opin Immunol, 2006. **18**(1): p. 64-9.
151. Sant, A.J., et al., *The relationship between immunodominance, DM editing, and the kinetic stability of MHC class II:peptide complexes.* Immunol Rev, 2005. **207**: p. 261-78.

152. Haile, S.T., et al., *Tumor cell programmed death ligand 1-mediated T cell suppression is overcome by coexpression of CD80.* J Immunol, 2011. **186**(12): p. 6822-9.
153. Li, Y., et al., *MART-1-specific melanoma tumor-infiltrating lymphocytes maintaining CD28 expression have improved survival and expansion capability following antigenic restimulation in vitro.* J Immunol, 2010. **184**(1): p. 452-65.
154. Ostrand-Rosenberg, S., *CD4+ T lymphocytes: a critical component of antitumor immunity.* Cancer Invest, 2005. **23**(5): p. 413-9.
155. Chen, Y.T., et al., *A testicular antigen aberrantly expressed in human cancers detected by autologous antibody screening.* Proc Natl Acad Sci U S A, 1997. **94**(5): p. 1914-8.
156. Kawakami, Y., et al., *Identification of a human melanoma antigen recognized by tumor-infiltrating lymphocytes associated with in vivo tumor rejection.* Proc Natl Acad Sci U S A, 1994. **91**(14): p. 6458-62.
157. Kittlesen, D.J., et al., *Human melanoma patients recognize an HLA-A1-restricted CTL epitope from tyrosinase containing two cysteine residues: implications for tumor vaccine development.* J Immunol, 1998. **160**(5): p. 2099-106.
158. Eccles, M.R., et al., *MITF and PAX3 Play Distinct Roles in Melanoma Cell Migration; Outline of a "Genetic Switch" Theory Involving MITF and PAX3 in Proliferative and Invasive Phenotypes of Melanoma.* Front Oncol, 2013. **3**: p. 229.
159. Hornyak, T.J., et al., *Transcription factors in melanocyte development: distinct roles for Pax-3 and Mitf.* Mech Dev, 2001. **101**(1-2): p. 47-59.
160. Medic, S. and M. Ziman, *PAX3 across the spectrum: from melanoblast to melanoma.* Crit Rev Biochem Mol Biol, 2009. **44**(2-3): p. 85-97.
161. Kubic, J.D., et al., *Pigmentation PAX-ways: the role of Pax3 in melanogenesis, melanocyte stem cell maintenance, and disease.* Pigment Cell Melanoma Res, 2008. **21**(6): p. 627-45.
162. Cao, Y. and C. Wang, *The COOH-terminal transactivation domain plays a key role in regulating the in vitro and in vivo function of Pax3 homeodomain.* J Biol Chem, 2000. **275**(13): p. 9854-62.
163. Blake, J.A. and M.R. Ziman, *Pax3 transcripts in melanoblast development.* Dev Growth Differ, 2005. **47**(9): p. 627-35.
164. Lang, D., et al., *Pax3 functions at a nodal point in melanocyte stem cell differentiation.* Nature, 2005. **433**(7028): p. 884-7.
165. Wang, Q., et al., *Pax genes in embryogenesis and oncogenesis.* J Cell Mol Med, 2008. **12**(6A): p. 2281-94.
166. Kubic, J.D., et al., *GSK-3 promotes cell survival, growth, and PAX3 levels in human melanoma cells.* Mol Cancer Res, 2012. **10**(8): p. 1065-76.
167. Wang, X.D., S.C. Morgan, and M.R. Loeken, *Pax3 stimulates p53 ubiquitination and degradation independent of transcription.* PLoS One, 2011. **6**(12): p. e29379.
168. Waardenburg, P.J., *A new syndrome combining developmental anomalies of the eyelids, eyebrows and nose root with pigmentary defects of the iris and head hair and with congenital deafness.* Am J Hum Genet, 1951. **3**(3): p. 195-253.
169. Wollnik, B., et al., *Homozygous and heterozygous inheritance of PAX3 mutations*

causes different types of Waardenburg syndrome. Am J Med Genet A, 2003. **122A**(1): p. 42-5.
170. Pingault, V., et al., *Review and update of mutations causing Waardenburg syndrome.* Hum Mutat, 2010. **31**(4): p. 391-406.
171. Dye, D.E., et al., *Melanoma biomolecules: independently identified but functionally intertwined.* Front Oncol, 2013. **3**: p. 252.
172. Mollaaghababa, R. and W.J. Pavan, *The importance of having your SOX on: role of SOX10 in the development of neural crest-derived melanocytes and glia.* Oncogene, 2003. **22**(20): p. 3024-34.
173. Ploski, J.E., M.K. Shamsher, and A. Radu, *Paired-type homeodomain transcription factors are imported into the nucleus by karyopherin 13.* Mol Cell Biol, 2004. **24**(11): p. 4824-34.
174. Mingot, J.M., et al., *Importin 13: a novel mediator of nuclear import and export.* EMBO J, 2001. **20**(14): p. 3685-94.
175. Takeda, K., et al., *Induction of melanocyte-specific microphthalmia-associated transcription factor by Wnt-3a.* J Biol Chem, 2000. **275**(19): p. 14013-6.
176. Pani, L., M. Horal, and M.R. Loeken, *Rescue of neural tube defects in Pax-3-deficient embryos by p53 loss of function: implications for Pax-3- dependent development and tumorigenesis.* Genes Dev, 2002. **16**(6): p. 676-80.
177. Blake, J.A., et al., *Perplexing Pax: from puzzle to paradigm.* Dev Dyn, 2008. **237**(10): p. 2791-803.
178. Li, H.G., et al., *PAX3 and PAX3-FKHR promote rhabdomyosarcoma cell survival through downregulation of PTEN.* Cancer Lett, 2007. **253**(2): p. 215-23.
179. Margue, C.M., et al., *Transcriptional modulation of the anti-apoptotic protein BCL-XL by the paired box transcription factors PAX3 and PAX3/FKHR.* Oncogene, 2000. **19**(25): p. 2921-9.
180. McGill, G.G., et al., *Bcl2 regulation by the melanocyte master regulator Mitf modulates lineage survival and melanoma cell viability.* Cell, 2002. **109**(6): p. 707-18.
181. Miller, P.J. and A.D. Hollenbach, *The oncogenic fusion protein Pax3-FKHR has a greater post-translational stability relative to Pax3 during early myogenesis.* Biochim Biophys Acta, 2007. **1770**(10): p. 1450-8.
182. Boutet, S.C., et al., *Regulation of Pax3 by proteasomal degradation of monoubiquitinated protein in skeletal muscle progenitors.* Cell, 2007. **130**(2): p. 349-62.
183. Zimmerer, J.M., et al., *STAT1-dependent and STAT1-independent gene expression in murine immune cells following stimulation with interferon-alpha.* Cancer Immunol Immunother, 2007. **56**(11): p. 1845-52.
184. Morozov, V.M., et al., *Regulation of c-met expression by transcription repressor Daxx.* Oncogene, 2008. **27**(15): p. 2177-86.
185. Dong, L., et al., *FGF2 regulates melanocytes viability through the STAT3-transactivated PAX3 transcription.* Cell Death Differ, 2012. **19**(4): p. 616-22.
186. Hartsough, E.J. and A.E. Aplin, *A STATement on vemurafenib-resistant melanoma.* J Invest Dermatol, 2013. **133**(8): p. 1928-9.

187. Shirakata, Y., *Regulation of epidermal keratinocytes by growth factors.* J Dermatol Sci, 2010.
188. Fuxe, J., T. Vincent, and A.G. de Herreros, *Transcriptional crosstalk between TGFbeta and stem cell pathways in tumor cell invasion: Role of EMT promoting Smad complexes.* Cell Cycle, 2010. **9**(12).
189. ten Dijke, P. and C.S. Hill, *New insights into TGF-beta-Smad signalling.* Trends Biochem Sci, 2004. **29**(5): p. 265-73.
190. Chen, D., et al., *SKI knockdown inhibits human melanoma tumor growth in vivo.* Pigment Cell Melanoma Res, 2009. **22**(6): p. 761-72.
191. Pardali, K. and A. Moustakas, *Actions of TGF-beta as tumor suppressor and pro-metastatic factor in human cancer.* Biochim Biophys Acta, 2007. **1775**(1): p. 21-62.
192. Zhao, W., et al., *TGF-beta1 attenuates mediator release and de novo Kit expression by human skin mast cells through a Smad-dependent pathway.* J Immunol, 2008. **181**(10): p. 7263-72.
193. Moustakas, A. and C.H. Heldin, *Dynamic control of TGF-beta signaling and its links to the cytoskeleton.* FEBS Lett, 2008. **582**(14): p. 2051-65.
194. Siegel, P.M. and J. Massague, *Cytostatic and apoptotic actions of TGF-beta in homeostasis and cancer.* Nat Rev Cancer, 2003. **3**(11): p. 807-21.
195. Stavroulaki, M., et al., *Exposure of normal human melanocytes to a tumor promoting phorbol ester reverses growth suppression by transforming growth factor beta.* J Cell Physiol, 2008. **214**(2): p. 363-70.
196. Yang, G., et al., *Inhibition of PAX3 by TGF-beta modulates melanocyte viability.* Mol Cell, 2008. **32**(4): p. 554-63.
197. Quan, T., et al., *Solar ultraviolet irradiation reduces collagen in photoaged human skin by blocking transforming growth factor-beta type II receptor/Smad signaling.* Am J Pathol, 2004. **165**(3): p. 741-51.
198. Choi, C.P., et al., *The effect of narrowband ultraviolet B on the expression of matrix metalloproteinase-1, transforming growth factor-beta1 and type I collagen in human skin fibroblasts.* Clin Exp Dermatol, 2007. **32**(2): p. 180-5.
199. Cui, R., et al., *Central role of p53 in the suntan response and pathologic hyperpigmentation.* Cell, 2007. **128**(5): p. 853-64.
200. Gambichler, T., et al., *Significant downregulation of transforming growth factor-beta signal transducers in human skin following ultraviolet-A1 irradiation.* Br J Dermatol, 2007. **156**(5): p. 951-6.
201. Sommers, J.A., et al., *p53 modulates RPA-dependent and RPA-independent WRN helicase activity.* Cancer Res, 2005. **65**(4): p. 1223-33.
202. Carreira, S., et al., *Mitf regulation of Dia1 controls melanoma proliferation and invasiveness.* Genes Dev, 2006. **20**(24): p. 3426-39.
203. Kubic, J.D., et al., *PAX3 and ETS1 synergistically activate MET expression in melanoma cells.* Oncogene, 2014.
204. Mascarenhas, J.B., et al., *PAX3 and SOX10 activate MET receptor expression in melanoma.* Pigment Cell Melanoma Res, 2010. **23**(2): p. 225-37.
205. Schepsky, A., et al., *The microphthalmia-associated transcription factor Mitf*

interacts with beta-catenin to determine target gene expression. Mol Cell Biol, 2006. **26**(23): p. 8914-27.
206. Scholl, F.A., et al., *PAX3 is expressed in human melanomas and contributes to tumor cell survival.* Cancer Res, 2001. **61**(3): p. 823-6.
207. Iyengar, A.S., et al., *Phosphorylation of PAX3 contributes to melanoma phenotypes by affecting proliferation, invasion, and transformation.* Pigment Cell Melanoma Res, 2014. **27**(5): p. 846-8.
208. Medic, S. and M. Ziman, *PAX3 expression in normal skin melanocytes and melanocytic lesions (naevi and melanomas).* PLoS One, 2010. **5**(4): p. e9977.
209. Muratovska, A., et al., *Paired-Box genes are frequently expressed in cancer and often required for cancer cell survival.* Oncogene, 2003. **22**(39): p. 7989-97.
210. Plummer, R.S., et al., *PAX3 expression in primary melanomas and nevi.* Mod Pathol, 2008. **21**(5): p. 525-30.
211. Koyanagi, K., et al., *Multimarker quantitative real-time PCR detection of circulating melanoma cells in peripheral blood: relation to disease stage in melanoma patients.* Clin Chem, 2005. **51**(6): p. 981-8.
212. Kiyohara, E., et al., *Circulating tumor cells as prognostic biomarkers in cutaneous melanoma patients.* Methods Mol Biol, 2014. **1102**: p. 513-22.
213. Rodeberg, D.A., et al., *Generation of tumoricidal PAX3 peptide antigen specific cytotoxic T lymphocytes.* Int J Cancer, 2006. **119**(1): p. 126-32.
214. Himoudi, N., et al., *Development of anti-PAX3 immune responses; a target for cancer immunotherapy.* Cancer Immunol Immunother, 2007. **56**(9): p. 1381-95.
215. Hastings, K.T. and P. Cresswell, *Disulfide reduction in the endocytic pathway: immunological functions of gamma-interferon-inducible lysosomal thiol reductase.* Antioxid Redox Signal, 2011. **15**(3): p. 657-68.
216. Chiang, H.S. and M. Maric, *Lysosomal thiol reductase negatively regulates autophagy by altering glutathione synthesis and oxidation.* Free Radic Biol Med, 2011. **51**(3): p. 688-99.
217. Mizushima, N., et al., *Autophagy fights disease through cellular self-digestion.* Nature, 2008. **451**(7182): p. 1069-75.
218. Scherz-Shouval, R., E. Shvets, and Z. Elazar, *Oxidation as a post-translational modification that regulates autophagy.* Autophagy, 2007. **3**(4): p. 371-3.
219. He, S.J., et al., *Transfection of melanoma cells with antisense PAX3 oligonucleotides additively complements cisplatin-induced cytotoxicity.* Mol Cancer Ther, 2005. **4**(6): p. 996-1003.
220. Koyanagi, K., et al., *Serial monitoring of circulating tumor cells predicts outcome of induction biochemotherapy plus maintenance biotherapy for metastatic melanoma.* Clin Cancer Res, 2010. **16**(8): p. 2402-8.
221. Yuen, J.W. and M.D. Gohel, *Anticancer effects of Ganoderma lucidum: a review of scientific evidence.* Nutr Cancer, 2005. **53**(1): p. 11-7.
222. Sliva, D., *Ganoderma lucidum (Reishi) in cancer treatment.* Integr Cancer Ther, 2003. **2**(4): p. 358-64.
223. Xu, Z., et al., *Ganoderma lucidum polysaccharides: immunomodulation and potential anti-tumor activities.* Am J Chin Med, 2011. **39**(1): p. 15-27.

224. Boh, B., et al., *Ganoderma lucidum and its pharmaceutically active compounds.* Biotechnol Annu Rev, 2007. **13**: p. 265-301.
225. Zhu, M., et al., *Triterpene antioxidants from ganoderma lucidum.* Phytother Res, 1999. **13**(6): p. 529-31.
226. Miyamoto, I., et al., *Regulation of osteoclastogenesis by ganoderic acid DM isolated from Ganoderma lucidum.* Eur J Pharmacol, 2009. **602**(1): p. 1-7.
227. Wang, P.H., et al., *Human nonmetastatic clone 23 type 1 gene suppresses migration of cervical cancer cells and enhances the migration inhibition of fungal immunomodulatory protein from Ganoderma tsugae.* Reprod Sci, 2007. **14**(5): p. 475-85.
228. Hsu, S.C., et al., *Ganoderma tsugae extracts inhibit colorectal cancer cell growth via G(2)/M cell cycle arrest.* J Ethnopharmacol, 2008. **120**(3): p. 394-401.
229. Li, C., et al., *Ganoderic acid Sz, a new lanostanoid from the mushroom Ganoderma lucidum.* Nat Prod Res, 2005. **19**(5): p. 461-5.
230. Liu, J., et al., *Ganoderic acids from Ganoderma lucidum: inhibitory activity of osteoclastic differentiation and structural criteria.* Planta Med, 2010. **76**(2): p. 137-9.
231. Liu, Y.W., et al., *Evaluation of antiproliferative activities and action mechanisms of extracts from two species of Ganoderma on tumor cell lines.* J Agric Food Chem, 2009. **57**(8): p. 3087-93.
232. Wu, G., et al., *Ganoderma lucidum extract induces G1 cell cycle arrest, and apoptosis in human breast cancer cells.* Am J Chin Med, 2012. **40**(3): p. 631-42.
233. Lin, S.B., et al., *Triterpene-enriched extracts from Ganoderma lucidum inhibit growth of hepatoma cells via suppressing protein kinase C, activating mitogen-activated protein kinases and G2-phase cell cycle arrest.* Life Sci, 2003. **72**(21): p. 2381-90.
234. Jiang, J., et al., *Ganoderma lucidum suppresses growth of breast cancer cells through the inhibition of Akt/NF-kappaB signaling.* Nutr Cancer, 2004. **49**(2): p. 209-16.
235. Liu, J., et al., *Target proteins of ganoderic acid DM provides clues to various pharmacological mechanisms.* Sci Rep, 2012. **2**: p. 905.
236. Yue, Q.X., et al., *Proteomics characterization of the cytotoxicity mechanism of ganoderic acid D and computer-automated estimation of the possible drug target network.* Mol Cell Proteomics, 2008. **7**(5): p. 949-61.
237. Tang, W., et al., *Ganoderic acid T from Ganoderma lucidum mycelia induces mitochondria mediated apoptosis in lung cancer cells.* Life Sci, 2006. **80**(3): p. 205-11.
238. Chen, N.H., J.W. Liu, and J.J. Zhong, *Ganoderic acid Me inhibits tumor invasion through down-regulating matrix metalloproteinases 2/9 gene expression.* J Pharmacol Sci, 2008. **108**(2): p. 212-6.
239. Hossain, A., et al., *A possible cross-talk between autophagy and apoptosis in generating an immune response in melanoma.* Apoptosis, 2012. **17**(10): p. 1066-78.
240. Lim, J.Y., et al., *Type I interferons induced by radiation therapy mediate*

recruitment and effector function of CD8(+) T cells. Cancer Immunol Immunother, 2014. **63**(3): p. 259-71.
241. Picaud, S., et al., *Enhanced tumor development in mice lacking a functional type I interferon receptor.* J Interferon Cytokine Res, 2002. **22**(4): p. 457-62.
242. Lugade, A.A., et al., *Local radiation therapy of B16 melanoma tumors increases the generation of tumor antigen-specific effector cells that traffic to the tumor.* J Immunol, 2005. **174**(12): p. 7516-23.
243. Ugen, K.E., et al., *Regression of subcutaneous B16 melanoma tumors after intratumoral delivery of an IL-15-expressing plasmid followed by in vivo electroporation.* Cancer Gene Ther, 2006. **13**(10): p. 969-74.
244. Radwan, F.F., et al., *Reduction of myeloid-derived suppressor cells and lymphoma growth by a natural triterpenoid.* J Cell Biochem, 2015. **116**(1): p. 102-14.
245. Boyle, G.M., *Therapy for metastatic melanoma: an overview and update.* Expert Rev Anticancer Ther, 2011. **11**(5): p. 725-37.

Biography

Jessica Hathaway-Schrader graduated with high honors in May 2009 with a B.S. in Biology from the University of Saint Francis in Fort Wayne, Indiana. In August 2009, Jessica matriculated into the Microbiology and Immunology Master's program at MUSC. In January 2010, Jessica began her project, in the lab of Dr. Azizul Haque, PhD, involving the role of GILT and PAX3 in melanoma. She completed her Master's degree in April 2011. During this time, Jessica also published a journal article and co-authored a book chapter on melanoma. In August 2011, Jessica matriculated into the Ph.D. program to delve more deeply into her project on GILT and PAX3. She has three journal articles currently submitted, based on her graduate research. Jessica also has presented her research work at the Perry V. Halushka Student Research Day (2010, 2013), Children's Research Day (2011), Hollings Cancer Center Research Retreat (2012), Biology seminar series at her alma mater (2013), and the Cancer Immunology Program Retreat (2014). After graduation, Jessica will continue on as the Program Coordinator for the MUSC Post-baccalaureate Research Education Program, with plans for a career in biomedical education.